The application of metabolomics by high field nuclear magnetic resonance to study thyroid signalisation pathologies in mice

Houda Boumaza

Numéro National de Thèse : **2019LYSEN003**

THESE de DOCTORAT DE L'UNIVERSITE DE LYON
Opérée par
L'Ecole Normale Supérieure de Lyon

Ecole Doctorale N° 340
Biologie Moléculaire, Intégrative et Cellulaire (BMIC)

Spécialité de doctorat : Biologie

Soutenue publiquement le 08/03/2019, par:

Houda BOUMAZA

Etude métabolomique par résonance magnétique nucléaire de pathologies associées à la signalisation thyroïdienne chez la souris

---

Devant le jury composé de :

SAVARIN, Philippe Professeur des universités, Université de Paris 13 - Rapporteur

DAMBLON, Christian Professeur des universités, Université de Liège - Rapporteur

SHINTU, Laetitia Maître de conférence, Aix-Marseille Université - Examinatrice

RODIEN, Patrice Professeur des universités - praticien hospitalier, CHU-Angers - Examinateur

FLAMANT, Frédéric Directeur de recherche, INRA, ENS de Lyon - Directeur de thèse

ELENA-HERRMANN, Bénédicte Chargée de recherche, CNRS, Université Grenoble Alpes - Co-directrice de thèse

Acknowledgements

Je souhaiterais remercier le Professeur Philippe Savarin et le Professeur Christian Damblon pour avoir accepté d'évaluer ce travail de thèse, ainsi que le Docteur Laetitia Shintu et le Docteur Patrice Rodien pour avoir accepté d'être membres du jury.

Ce manuscrit de thèse est l'aboutissement de trois années de travail et de nombreux défis. Je souhaiterais donc remercier les personnes talentueuses avec lesquelles j'ai pu interagir avant et tout au long de ma thèse.

Je remercie mes directeurs de thèses : Docteur Frédéric Flamant et Docteur Bénédicte Elena-Herrmann de m'avoir fait confiance et de m'avoir donné l'opportunité d'effectuer cette thèse dans des conditions favorables. Je les remercie pour leur encadrement et leur disponibilité permanente. Merci de m'avoir permis de développer une autonomie et une indépendance dans ce travail.

Je remercie le Docteur Elodie Jobard de m'avoir formée en métabolomique, d'avoir été toujours présente pour répondre à des questions techniques, d'avoir partagé avec moi ses expériences et son parcours.

Je remercie le Docteur Gilles Rautureau d'avoir été toujours disponible pour répondre à mes questions sur le projet et sur mon parcours professionnel.

Je remercie Suzy Markossian de m'avoir formée et beaucoup aidée pour effectuer les expériences biologiques à l'IGFL. Merci pour sa disponibilité et sa bonne humeur contagieuse.

Je remercie le Docteur Karine Gauthier pour son aide précieuse dans ce projet de thèse.

J’ai eu la chance d’effectuer ma thèse en même temps que mon amie rencontrée au laboratoire Manhal Mili. Je la remercie sincèrement pour ses encouragements, sa bienveillance et sa bonne humeur.

Je remercie les anciens membres de l’équipe de métabolomique avec qui il a été très agréable de travailler et d’échanger : Docteur Tony Palama, Docteur Aurélien Scalabre et Sylvie Guibert.

Je remercie également tous les membres du CRMN anciens et nouveaux arrivants pour l’ambiance chaleureuse : Anne, Guido, Diane, Olivier, James, Tanguy, Pierrick, Cécile, Dorothea, Audrey, David, Baptiste et tous les autres.

Je remercie aussi les membres de l’IGFL de m’avoir accueillie. Merci à Romain, Sabine et Denise.

Je remercie l’Agence Nationale de Recherche pour le financement de cette thèse.

Pour finir, je remercie mes proches qui ont également contribué par leur présence et leur soutien à l’accomplissement de ce doctorat.

Merci à ma mère Samia, mon frère Bader et mes sœurs Rym et Maroua, ma belle-sœur Marine, mon petit neveu Taqqyeddine, mon beau-frère Driss et mon beau-père Kamel, pour leur soutien constant, et les agréables moments passés en famille toujours ressourçant. Un grand merci à ma maman à qui je dois tant. Merci à ma grand-mère, qui nous a quittés aujourd’hui, de m’avoir toujours encouragée à faire des études et aller le plus loin possible.

Merci à ma deuxième famille, mes amis. Merci à Inès, à Sophiana, à Anaïs, à Linda, à Coralie, à Sabrina, à Myriam, à Mehdi et bien d’autres. Merci à tous ceux que j’ai rencontrés dans le milieu associatif qui ont su enrichir mon âme.

Enfin, je remercie toutes les personnes qui ont contribué de près ou de loin à l’aboutissement de ce travail qui est ci-important à mes yeux.

Résumé

La métabolomique par résonance magnétique nucléaire (RMN) permet d'étudier la réponse métabolique globale d'un système biologique à un stimulus ou un événement physiopathologique (maladie, manipulation génétique, etc.). Cette discipline connaît un essor important dans la recherche clinique et biologique, et constitue ainsi un outil à fort potentiel pour la découverte de biomarqueurs de maladies, et l'étude de la fonction des gènes.

Cette thèse est dédiée à l'application de la métabolomique par RMN à hauts champs pour l'étude des pathologies associées à la signalisation thyroïdienne chez la souris. L'objectif global est d'identifier des biomarqueurs spécifiques liés aux différentes maladies hormonales : l'hypothyroïdie et la maladie génétique émergente résistance à l'hormone thyroïdienne due à une mutation au niveau du récepteur TRα1 (RTHα). Cette dernière est particulièrement difficile à diagnostiquer à cause du manque de marqueurs biochimiques et de symptômes spécifiques à cette maladie. De plus, elle présente des similitudes avec l'hypothyroïdie au niveau symptomatique. Des modèles murins de RTHα et de l'hypothyroïdie ont été analysés, et l'investigation a été menée sur l'urine et le plasma sanguin dans le but de différencier métaboliquement ces maladies et d'identifier des biomarqueurs spécifiques à RTHα. Des signatures métaboliques liées à chaque maladie ont été identifiées dans l'urine et le plasma sanguin. Cinq métabolites qui varient de façon significative ont été identifiés dans l'urine comme étant liés à la maladie RTHα : trimethylamine, dimethylamine, isovalerylglycine, N-acetylglucosamine et la choline. Dans le sang, ce sont les lipides insaturés qui varient de façon significative chez les souris mimant la maladie RTHα.

L'impact des hormones thyroïdiennes (HT) et le récepteur TRβ sur le métabolisme hépatique a été également étudié dans ce présent manuscrit. Un modèle murin présentant une inactivation du récepteur TRβ au niveau des hépatocytes (LTRβ-KO) a été généré pour étudier cette question. Pour comprendre la fonction des HT médiée par le récepteur TRβ, les réponses métaboliques hépatiques à HT, obtenues sur des extraits hépatiques aqueux et tissus hépatiques intacts, des souris TRβ-KO et des souris sauvages ont été comparées. Les résultats obtenus suggèrent la présence d'un effet direct (par le récepteur TRβ) et un effet indirect des hormones thyroïdiennes sur le métabolisme hépatique.

Abstract

Metabolomics by nuclear magnetic resonance (NMR) allows studying the metabolic response of a global biological system to a stimuli or a physiopathological even (diseases, genetic modifications, etc.). This discipline is growing especially in the clinical and biological fields, and represents a strong potential tool to identify biomarkers related to diseases, and study the function of genes.

This thesis is dedicated to the application of metabolomics by high field NMR to study thyroid signalisation pathologies in mice. The main goal is to identify biomarkers related to the emerging genetic disease called resistance to thyroid hormone due to a mutation in thyroid hormone receptor TRα1 (RTHα). This disease is particularly difficult to diagnose because of the lack of biochemical markers and specific symptoms. In addition, it presents common features with hypothyroidism in term of symptoms. Mice models of RTHα and hypothyroidism were analysed, and the investigation were driven on urine and blood plasma in order to differentiate metabolically theses diseases and identify biomarkers related to RTHα. Metabolic fingerprints related to each disease were identified in both urine and blood plasma. Five metabolites vary significantly in the urine of RTHα mice: trimethylamine, dimethylamine, isovalerylglycine, N-acetylglucosamine and choline. Unsaturated lipids vary significantly in the blood plasma of RTHα mice.

The impact of thyroid hormones (TH) and the thyroid hormone receptor TRβ on the liver metabolism were also studied in the present manuscript through NMR-based metabolomics. A mouse model, with a specific knock-out of TRβ gene in hepatocytes (LTRβ-

KO), were used to study this question. To understand the function of TH mediated by TRβ, the liver metabolic response to TH, obtained from liver aqueous extracts and intact liver tissues, TRβKO and wild-type mice were compared. The results suggest the presence of direct and indirect effects of thyroid hormones on the liver metabolism.

Table of contents

Acknowledgements	2
Résumé	4
Abstract	6
Table of contents	8
Table of abbreviations	11
Introduction	13
Chapter 1 – Metabolomics: from fundamentals to clinical applications	17
1.1 Metabolomics approach	17
1.1.1 Metabolomics and metabonomics	17
1.1.2 From genomics to metabolomics	18
1.1.3 Platforms for metabolomics	19
1.2 Nuclear magnetic resonance	20
1.2.1 The principle of NMR	20
1.2.2 NMR parameters	22
1.2.3 NMR methods	25
1.3 NMR-based metabolomics for the investigation of biological samples	27
1.3.1 Biological samples explored by metabolomics	27
1.3.2 Targeted and untargeted analyses	28
1.4 Metabolomics and biomarkers	28
1.4.1 Metabolomics to study pathologies	28
1.4.2 Metabolomics and genetic diseases	29
1.5 Conclusion	29
Chapter 2 - Thyroid hormones system and alterations	30
2.1 Thyroid hormone system	30
2.1.1 Thyroid hormones function	30
2.1.2 Thyroid hormones receptors	31
2.1.3 Mechanism of actions	33
2.1.4 Regulation	34
2.1.5 Alterations in thyroid hormone system	34
2.2 Resistance to thyroid hormone α	35
2.2.1 The first cases	36
2.2.2 RTHα is different from RTHβ	36
2.2.3 A high variability in clinical features	37
2.2.4 Molecular aspect	38
2.2.5 Relation between genotype and phenotype?	39
2.2.6 Mouse models to study RTHα	40
Chapter 3 – Materials and methods	43
3.1 Introduction	43
3.2 Biological samples preparation	45

3.2.1 Collection and storage	45
3.2.2 Preparation and handling	46
3.3 NMR-based metabolomics	47
3.3.1 Data acquisition	47
3.3.2 Data processing	49
3.3.3 Multivariate analysis of metabolic profiles	52
3.3.4 Metabolite identification	55
Chapter 4: ^{1}H NMR-based metabolomics for the study of the impact of the excess and the privation of thyroid hormones on murine metabolism	56
4.1 Introduction	56
4.2 Study design	58
4.3 Results	60
4.3.1 Quality of ^{1}H NMR data	60
4.3.2 Discrimination according to mice phenotype in urine	61
4.3.3 Impact of thyroid hormones on the metabolism	61
4.3.4 Determination of a metabolomic signature associated with hypothyroidism	64
4.3.5 Determination of a metabolic signature associated with TH treatment	65
4.4 Conclusion	69
Chapter 5: NMR as a putative diagnostic tool for the presence of thyroid hormone receptor alpha 1 mutations	70
5.1 Introduction	70
5.2 Study design	72
5.3 results	74
5.3.1 Quality of ^{1}H NMR data	74
5.3.2 Discrimination between group of mutants and wild-type group	74
5.3.3 Discrimination between each mutant group and wild-type group	75
5.3.4 Metabolomic analysis segregates two types of frameshift mutations	77
5.3.5 Discrimination between Thra$^{S/+}$ mice with human-like mutations and wild-type mice	79
5.3.6 Determination of metabolic signature of Thra mutation in urine and blood plasma	81
5.3.7 RTHα signature is different from hypothyroidism signature	83
5.4 Discussion	84
Chapter 6: Functional genomics by metabonomics to study thyroid hormone receptor β	87
6.1 Introduction	88
6.2 Study design	89
6.3 Results	89
6.3.1 Untargeted NMR Metabolomics analysis of the liver response to thyroid hormone	89
6.3.2 Impact of TH nuclear receptor on liver metabolism	91
6.3.3 Impact of TRβ on liver metabolism	92

6.3.4 Summary	94
6.4 Conclusion	96
Conclusion and perspectives	98
References	101
Appendices	111
Appendix 1: Clinical features of RTHα patients	111
Appendix 2: Metabolites identified from 1D and 2D NMR profiles of mice urine	117
Appendix 3: Metabolites identified from 1D and 2D NMR profiles of mice plasma	120
Appendix 4: Metabolites identified from 1D and 2D NMR profiles of mice liver aqueous extracts	122

Table of abbreviations

ANOVA: Analysis Of Variance

CPMG: Carr-Purcell-Meiboom-Gill

DA: Discriminant Analysis

DBD: DNA-Binding Domain

FHCTD: Thyroid Hormone Cell Transport Defects

FID: Free Induction Decays

FT4: Free T4

GC: Gas Chromatography

HCA: Hierarchical Clustering Analysis

HDL: High Density Lipoproteins

HMDB: Human Metabolome Database

HPT axis: Hypothalamus/Pituitary/Thyroid axis

HP: High Pressure

HR-MAS: High Resolution-Magic Angle Spinning

HSQC: Heteronuclear Single Quantum Correlation

KI: Knocking In

KO: Knocking Out

LBD: Ligand-Binding Domain

LC: Liquid Chromatography

MCT: Monocarboxylate Transporter

MMMDB: Mouse Multiple tissue Metabolome Database

MS: Mass Spectrometry

NMR: Nuclear Magnetic Resonance

NOESY: Nuclear Overhauser Effect

OPLS: Orthogonal Partial Least Squares

PCA: Principal Component Analysis

PLS: Projection to Latent Structures

PQN: Probabilistic Quotient Normalization

PTU: Propylthiouracil

QC: Quality Control

RTH: Resistance to Thyroid Hormone

RTHα: Resistance to Thyroid Hormone due a mutation in thyroid hormone receptor α

RTHβ: Resistance to Thyroid Hormone due a mutation in thyroid hormone receptor β

SRV: Statistical Recoupling of Variables

TH: Thyroid Hormone

THCTD: Thyroid Hormone Cell Transport Defects

THMD: Thyroid Hormone Metabolism Defect

TOCSY: TOtal Correlation SpectroscopY

TSP: 3-Trimethylsilylpropionic acid

TRα: Thyroid hormone Receptor α

TRβ: Thyroid hormone Receptor β

TRH: Thyrotropin-Releasing Hormone

TRs: Thyroid Receptors

TSH: Thyroid-Stimulating Hormone

T3: 3, 5, 3'-triiodothyronine

T4: Thyroxine

RXR: Retinoid X Receptor

UP: Ultra Performance

UV: Unit Variance

Introduction

The relation between the variation in the composition and the aspect of biofluids or tissues and pathologies was identified hundreds of years back[1]. This concept exists from the Middle age, in a "urine charts", the colors, smells and tastes were related to specific medical conditions (Figure 1). These variations come, of course, from the metabolism, which is influenced by certain conditions. Nowadays, modern-day metabolomics uses the same principle to analyze biological samples, but with modern techniques.

Figure 1: **"Urine charts".**

Ulrich Pinder published this illustration in 1506, in his book "Epiphanie Medicorum". This chart connects colors, smells and tastes of urine to diseases.

The big challenge in biological and clinical studies is to discover biological markers, which lead to diagnose easily and at early stage of a disease to improve human health. The goal is to take care of patients as soon as possible to curb the disease. Biomarkers are

"biological characteristics that are measured and evaluated as indicators of normal or pathological processes, and pharmacologic responses to a therapeutic intervention"[2]. A good biomarker must be easily measurable, and help for the diagnosis. High throughput "-omics" methods (genomics, transcriptomics, proteomics, metabolomics, etc.) lead to a new diagnostic approach and to targeted therapies.

In practical terms, metabolomics consists in the measurement of the small molecules, named metabolites, involved in biochemical processes present in a biological system (tissue, cells, biofluids, etc.). Metabolites are the final products of interactions between genes, proteins and the impact of environment. Thus, each individual has his own metabolic state at a specific time, which is also defined by the metabotype[3]. Analyzing metabolites provides information that cannot be obtained only from the genome or the proteome. With this approach, the overall response of a biological system to a physiological or pathological event (disease, genetic manipulation, drugs, nutrition, lifestyle, etc.) can be defined.

Metabolomics was applied to different biological and clinical conditions like cancers, cardiovascular diseases, diabetes, inborn errors of metabolism, etc[4-12]. Metabolomics studies in this field aim to understand the impact of diseases on the organism, and to discover biomarkers that predict disease incidence, severity, and progression and detect abnormalities. In addition to its application in the discovery of biomarkers, metabolomics is often used to understand biological processes of diseases and genetic mutations[3,10,13-15]. Metabolomics is now developing as an important functional genomics tool to evaluate the impact of gene change[16].

This thesis is dedicated to the application of NMR-based metabolomics for the investigation of thyroid signalisation pathologies in mice. We prospectively explored urine and blood plasma of murine models to obtain metabolic fingerprints of hypothyroidism, excess of thyroid hormone and the emerging genetic disease called resistance to thyroid hormone due to a mutation in thyroid hormone receptor TRα1 (RTHα). RTHα is particularly difficult to diagnose because of the lack of biochemical markers and specific symptoms. Nowadays, only few researchers were carried out to understand this disease, and try to identify biomarkers to facilitate its diagnosis. RTHα patients present common features with hypothyroid patients with near normal thyroid function tests. The study of hypothyroidism here serves as a base to understand RTHα. We investigate in the end the impact of thyroid

hormones and the role of thyroid hormone nuclear receptor β in the liver, by using liver samples.

The first chapter presents the metabolomics approach and its application as a diagnostic tool in the medical field. We set then in the second chapter the background of the present study. We describe thyroid hormone functions, molecular actions, their receptors and the different hormonal diseases. Materials and methods are detailed in the chapter 3. The different steps of our metabolomics studies are described.

The fourth chapter is dedicated to the investigation by using non-targeted ^{1}H-NMR-based metabolomics of two biofluids (urine and blood plasma) issue from mice to identify non-hormonal biomarkers related to hypothyroidism. It was crucial for us to study this disease at first to understand then the specific metabolic changes caused by RTHα. Here, murine models for hypothyroidism were compared to a control group to obtain metabolic fingerprints related to each disease in both urine and plasma. Clear discriminations between murine model for hypothyroidism and the control group were observed and specific metabolic signatures of the hypothyroid condition were identified.

The fifth chapter concerns the study of the new emerging genetic disease called resistance to thyroid hormone due to a mutation in thyroid hormone receptor TRα (RTHα), which its symptoms are close to those of hypothyroidism. Patients present a high variability in clinical features (skeletal dysplasia, growth retardation, intellectual disability, etc.), and the absence of reliable biochemical markers make the diagnosis of this disease difficult. The main goal of the study is to find, by the use of NMR based-metabolomics approach, a metabolic signature related to RTHα in mice, identify specific biomarkers and differentiate it from hypothyroidism. Five mice models carrying a mutation in Thra gene were studied, and the investigation were driven on urine and blood. Five metabolites vary significantly in the urine of RTHα mice: trimethylamine, dimethylamine, isovalerylglycine, N-acetylglucosamine and choline. Unsaturated lipids vary significantly in RTHα mice blood plasma.

In the sixth chapter, the impact of thyroid hormones (TH) and the thyroid hormone receptor TRβ on the liver metabolism were studied through NMR-based metabolomics. A mouse model, with a specific knockout of TRβ gene in hepatocytes (LTRβ-KO), was generated to study this question. To understand the function of TH mediated by TRβ, the liver

metabolic response to TH, obtained from liver aqueous extracts and intact liver tissues, LTRβ-KO and wild-type mice were compared. The results suggest the presence of direct and indirect effects of thyroid hormones on the liver metabolism.

1. Metabolomics: from fundamentals to clinical applications

1.1. Metabolomics approach

1.1.1. Definitions

Metabolites are low molecular weights molecules (less than 1.5kDa) that are involved in metabolic pathways. They are the reactants, intermediates and end products of complex multiple cascade, which is initiated by the genome followed by the transcriptome and proteome. They can be endogenous (from the organism) or exogenous (i.e. nutrition, medication, microbiota, etc.). They include polysaccharides, lipids, steroids, organic acids, amino acids, ketones and peptides, or else. They fulfill diverse functions, ranging from signal transduction to energy fuels[17,18]. Each type of biological sample (fluid, tissue, cells, organism) or each subtype (type of cell, type of fluid, etc.) has his own characteristic set of metabolites[3].

The Metabolome represents the entire set of metabolites present in a biological system[19]. The human metabolome is estimated to contain about 150 000 metabolites (endogenous and exogenous) or more[20]. Environmental factors (diet, gut microbial activity, disease, medication, stress level, physical activity, etc.) have an effect on the metabolism, which lead to changes in the concentrations of metabolites, and thus in the metabolome.

Metabolomics[19,21] corresponds to the quantification and identification as many as possible of the metabolites present in a biological system (biological fluid, cell, tissue, organism, etc.). Analyzing metabolites in a biological system provides information on the metabolic phenotype or metabotype of individuals or populations[3]. Thanks to technological advances in the identification, quantification and analysis of metabolites, metabolomics has grown significantly in different fields[1,22]. Metabolomic analyses are often built as case-control studies, which aim to compare two groups of samples coming from two different

physio-pathological states. By the use of bioinformatics and biostatistics tools, the difference between the two groups in term of molecules can be identified[23].

The application of metabolomics in different fields has increased strongly over the past years (Figure 1.1.1).

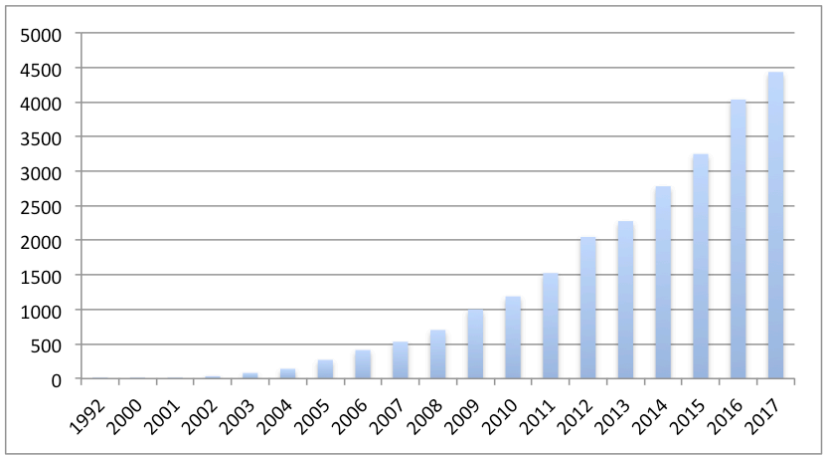

Figure 1.1.1: **Number of metabolomics publications per year.**
The research was performed in the Web of science (WOS) database, using metabolomics or metabonomics as keywords. The data was collected up to 2017.

1.1.2. From genomics to metabolomics

Omics strategies represent an important step in sciences area, and they are widely used nowadays. The principle of these approaches is to identify and quantify the entire set of biomolecules (genes, transcripts, proteins, metabolites, etc.) present in a given biological matrix (tissues, cells, organisms, biofluids), and to determine the relationship between their variations and specific pathophysiological states or external perturbations. Studying only genes, transcripts or proteins is insufficient to understand the complete phenotypic changes induced by these factors[24]. The number of metabolites is smaller than the estimated number of genes (25.000), transcripts (100.000) and proteins (1.000.000) found in humans[10]. Metabolites represent a more sensitive level[25] than the other biomolecules, and they are the result of the interaction between theses biomolecules and the environment. In addition to the interactions

between metabolites and the other biomolecules, metabolites are also the building blocks of proteins (amino-acids), genes and transcripts (nucleotides). Metabolic pathways reflect the genome and proteome states with up to 10.000-fold increase in metabolite concentration resulting from a single amino acid change in a protein or base change in a gene[22,26]. Metabolic changes are detectable within minutes of a biological event and thus provide an almost 'real-time' feedback[22].

Now, metabolomics is considered as a strong phenotyping tool, which provides molecular information that complement data obtained from genomics, transcriptomics and proteomics (Figure 1.1.2).

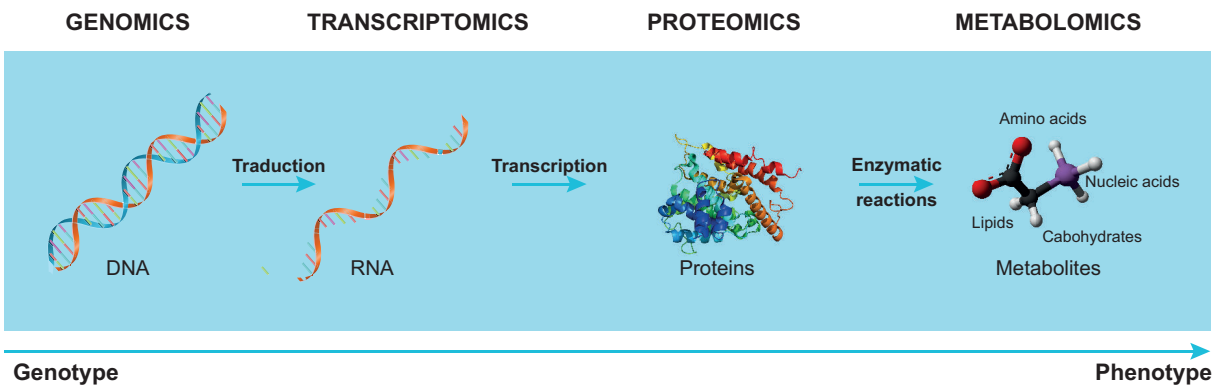

Figure 1.1.2: **Correlation between omics sciences.**

Omics strategies (Genomics, Transcriptomics, Proteomics and Metabolomics) aim at identifying all the biomolecules present in biological system (genes, RNA, proteins, metabolites).

1.1.3. Platforms for metabolomics

The two main technologies that are amply employed in metabolomics studies are NMR spectroscopy and mass spectrometry[24,27,28]. NMR spectroscopy is used in metabolomics studies to detect hydrogen atoms in metabolites, and identify compounds with identical masses[8]. Each metabolite, with concentrations above the detection limit, gives a ^{1}H NMR spectrum. Thus, a ^{1}H NMR spectrum of a complex mixture (biofluids, cells/tissue extracts) corresponds to the superposition of the spectra of all the present metabolites, which means

that NMR provides a direct fingerprint of all observable metabolites in a short time. NMR has several advantages like a minimal sample preparation, low cost per sample, excellent data acquisition and reproducibility[29,30]. However, NMR has a low sensitivity and limited detection range (micromolar) compared to MS (nanomolar). NMR is not destructive; samples can be reused for other analyses, and has also the ability to analyze intact tissues like biopsies.

In the other hand, MS[31] is highly sensitive and has the capability to detect a broader range of metabolites. But samples are usually separated before analysis using chromatography (gas chromatography (GC), liquid chromatography (LC), ultraperformance (UP), high pressure (HP)) or electrophoresis (capillary electrophoresis/electrospray ionization).

NMR and MS are thus highly complementary[17,18], and their use is often necessary for full molecular characterization[32].

Whatever the technique used, the result of the detection and quantification of metabolites is called a spectrum.

1.2 Nuclear magnetic resonance

NMR was first described in 1938, and become rapidly a powerful and interdisciplinary method[33]. Demonstration of the use of protons (^{1}H) NMR and the development of Fourier Transformation (FT) were developed in the followed few years[32]. The first use of ^{1}H NMR for metabolic studies was described in 1977[34], where some metabolites were identified in a suspension of red blood cells. From here, ^{1}H NMR was recognized to have a promising role in the investigation of diseases, especially since the development of modern spectrometers and software.

1.2.1 The principle of NMR

Atom is composed of a nucleus and electrons. The nucleus, itself, is composed of protons and neutrons. All these particles possess an intrinsic property called spin. NMR is a nuclei specific spectroscopy, which detects only nuclei with a non-zero nuclear spin because they act as elementary magnet contrary to nuclei with zero nuclear spin. The isotopes of particular interest and use to organic chemists are: ^{1}H, ^{13}C, ^{15}N, ^{19}F and ^{31}P. ^{1}H NMR remain the best described and the most used in metabolomics, because approximately all the metabolites present in a biological sample contain hydrogens[26,27].

In practical terms, when the sample is placed in a strong magnetic field, an electromagnetic radiation (radiofrequency pulses) is used to excite the hydrogens. After their excitation, the protons returns to equilibrium, and the energy is recorded as an oscillating electromagnetic signal, named the free induction decay (FID). A mathematical algorithm, Fourier transformation (FT), is applied to the FID to produce ^{1}H NMR spectra of intensity versus chemical shift (δ) using the computer. The magnitude or intensity of NMR resonance signals is displayed along the vertical axis of a spectrum, and is proportional to the molar concentration of the different metabolites present in the sample. NMR can calculate metabolites concentration by using an internal or external standard with a known concentration.

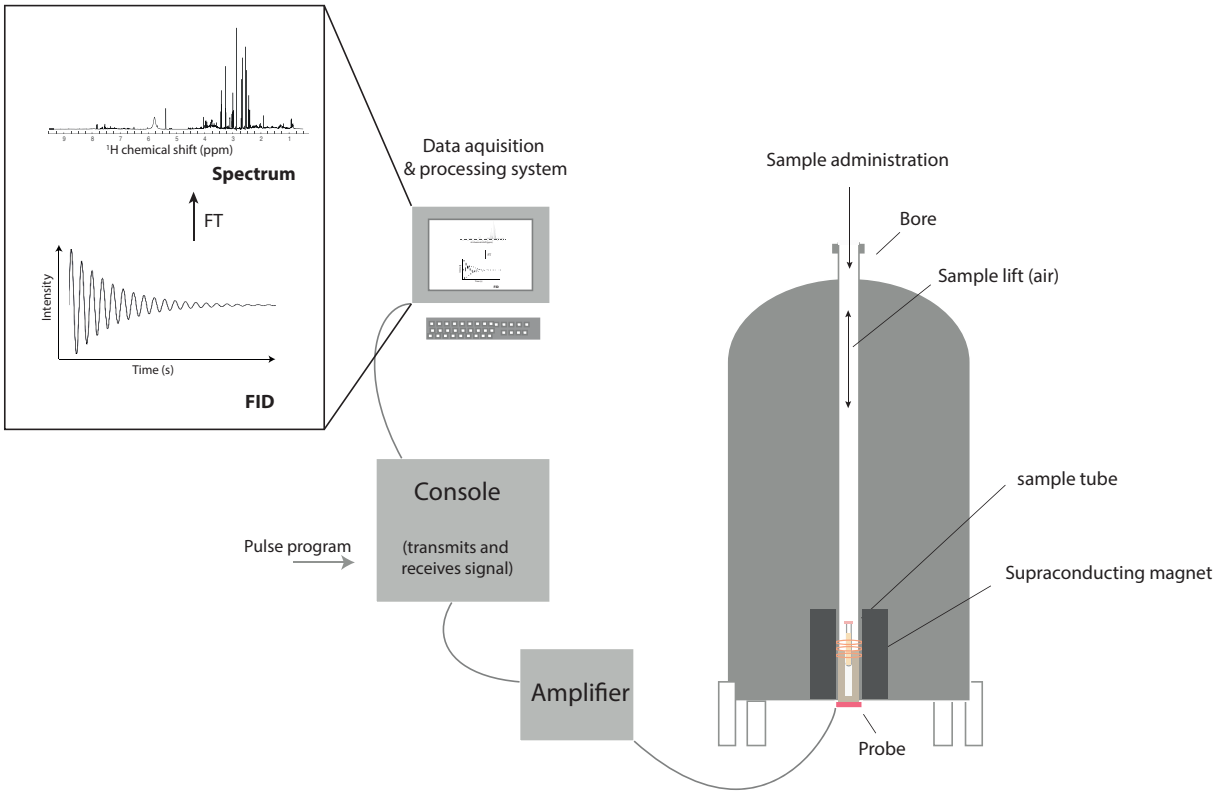

Figure 1.2.1: **Diagram of NMR spectrometer.**

A supraconducting magnet is present in the heart of the spectrometer. 5 mm glass tube is oriented between the poles of a powerful magnet. Radio frequency (RF) radiation of appropriate energy is broadcast into the sample from an antenna coil. A receiver coil surrounds the sample tube, and dedicated electronic devices and a computer monitor emission of absorbed RF energy. A free induction decay (FID) is acquired and then converted to NMR spectrum by Fourier transformation (FT) algorithm.

1.2.2 NMR Parameters

Each signal in a ^{1}H NMR spectrum may be split into one or more peaks, which is named signal multiplicity (1 peak = singlet, 2 peaks = doublet, 3 peaks = triplet, 4 peaks = quartet, and several peaks = multiplet). The multiplicity tells us how many neighbouring hydrogen atoms are present around the hydrogens producing a specific peak. The chemical shift δ (expressed in ppm) and the multiplicity are central to provide information about the structure of the molecule, and then facilitate its identification. Coupling constant J (expressed

in Hz) corresponds to the measure of the interaction between a pair of protons is also often used in the identification of metabolites.

In order to standardize the NMR scale it is necessary so set a 0 reference point to which all protons can then be compared. This association with the reference signal is called the chemical shift. This shift is measured in parts per million (ppm).

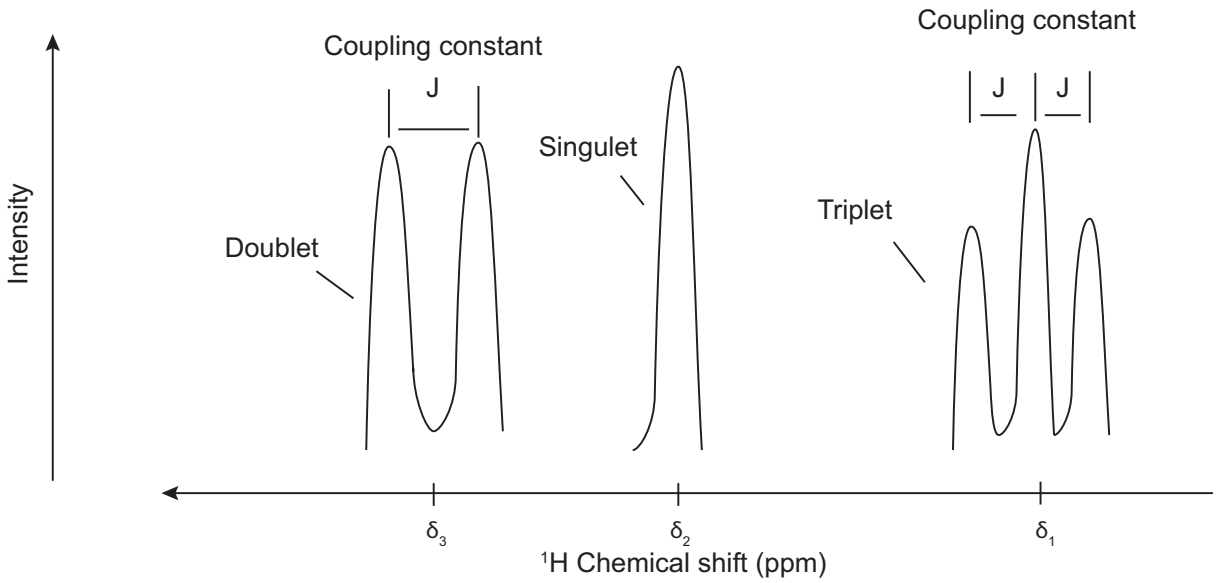

Figure 1.2.2: **Schematic representation of NMR parameters.**

The spectrum of a complex mixture like biological samples, which contain hundreds of metabolites, corresponds to the sum of individual metabolites spectra (Figure 1.2.2).

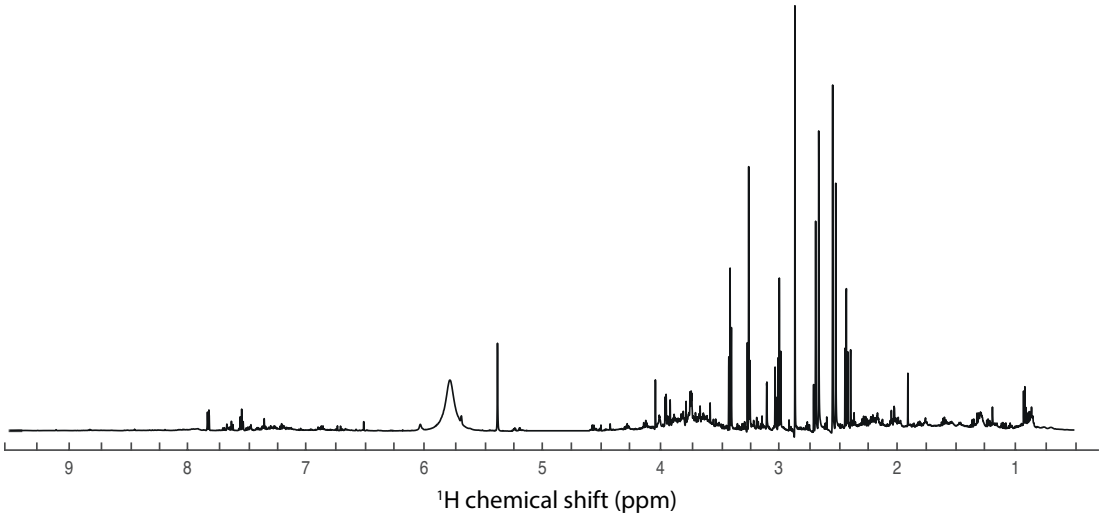

Figure 1.2.3: **Example of a 600 MHz ^{1}H-NMR urine spectrum.**

1.2.3 NMR methods

Biofluids and tissue or cell extracts are considered as homogenous liquids. All the molecules present inside are in a homogeneous chemical environment. They are thus analyzed by liquid state NMR experiments in metabolomics. The obtained spectra are well resolved and the resonances are well defined. A minimal sample preparation by the addition of specific buffer to the samples is needed here.

Other biological samples like cells, biopsies or small organisms (*Caenorhabditis elegans*, *Daphnia*, etc.) are used to understand the cellular metabolisms of physiological and pathological processes. This kind of sample is considered as semi-solid samples. They are heterogeneous, and a different NMR technique is used in this case. The use of liquid NMR state experiments here gives spectra with very poor resolution.
The development of a technique called high-resolution ^{1}H magic angle spinning (MAS) NMR spectroscopy has enabled to acquire high-resolution NMR data on small pieces of intact tissues with no pretreatment[35-38]. The sample heterogeneity causes line broadening. This method is based on the fact that the sample is spinning at an angle (so-called *magic angle*) of 54.7°, which reduces the loss of information caused by line broadening effect[39].

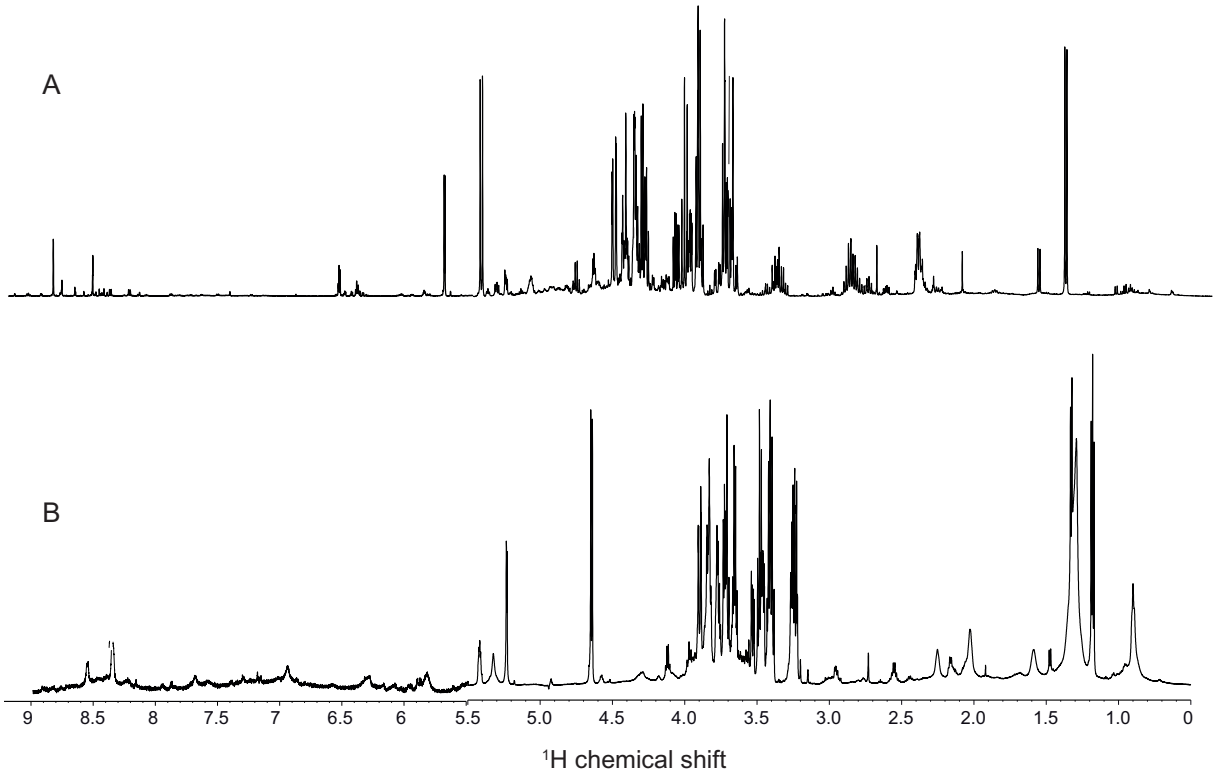

Figure 1.2.4: **Typical NMR spectra.**

(A) Typical spectrum of liver extract acquired at 700MHz. (B) Typical spectrum of intact liver tissue acquired at 700MHz with HR-MAS technique.

The limited of the 1D spectra is the presence of overlapped signals; a given pic can hide two different metabolites. To facilitate metabolite identification, two-dimensional (2D) ^{1}H NMR spectra are highly recommended to provide additional information about metabolite content. Total Correlation SpectroscopY (TOCSY)[40] and J-resolved[41] experiments reveal molecular connectivities and the multiplicity of resonances, respectively. ^{1}H-^{13}C HSQC (Heteronuclear Single Quantum Correlation), which investigate heteronuclear coupling, is also used. 2D NMR spectroscopy is useful for increasing signal dispersion and to clarify the connectivities between signals. They help to identify metabolites.

1.3 NMR-based metabolomics for the investigation of biological samples

1.3.1 Biological samples explored by metabolomics

Different sample types can be used in metabolomics studies: biofluids (whole blood, plasma, serum, urine, saliva, amniotic fluid, faecal water, etc.), intact cells and tissues (cardiac, liver, kidney, etc.). To answer to a specific biological or clinical issue, it is primordial to choose the more appropriate type of sample. In clinical studies, the priority is given to biofluids because there is a real need to non-invasive methods to understand and diagnose diseases. For biological studies, tissues and cells in addition to biofluids are used to understand mechanisms in a specific organ. In this case, animal models are investigated because it is ethically non acceptable to take biopsies from healthy individuals.

Biofluids are easily obtained, and non-invasive compared to biopsies[17,18,24]. Urine, one of the most widely studied biofluids in metabolomics, reflects a more short-term state of the organism. Urine contains endogenous and exogenous (like drugs, food) metabolites, which made it very interesting in disease biomarker discovery[2] and toxicology[29].
About 3000 urine metabolites were identified[18]. For metabolomics studies, it is important to collect the first morning voids, which are following by an overnight fast to reduce the impact of food or mediation[42]. Fasting plasma and serum changes reflect more chronic and long-term snapshots of the system[43]. However, it is very important to consider external factors related to ethnicity, diet, diurnal rhythm, etc., for human samples before drawing conclusions. Analyzing cerebrospinal fluid (CSF) offers great understanding of neurological disorders. Saliva is a good source of biomarkers related to pathologies[44]. Sweat and breast milk is used in metabolomics to improve the infants nutrition.

Metabolomic study on the whole organism does not provide information about a specific cell type or organ. Investigate specific cells and organs is more appropriate to understand the local mechanisms. These two approaches can be combined to provide complementary information.

Standardization of protocols has enabled to work in the same conditions and make the data comparable[45,46].

1.3.2 Targeted and untargeted analyses

A targeted metabolomics consists in looking for specific metabolites in a biological system. In practical terms, it is the quantification (concentrations are determined) or semi-quantification (intensities are determined) of a set of metabolites that might be associated to the common classes, to study specific metabolic pathways for example. Lipidomics[9], a subtype of metabolomics, which aim to study only lipids, can be considered as targeted metabolomics. This discipline can be also considered as untargeted metabolomics because there are different types of lipids. An extraction step for wanted metabolites is often needed in this approach.

In the other hand, untargeted metabolomics is the quantification or semi-quantification of all the detectable metabolites present in a biological sample. Sample preparation is usually minimal.

1.4 Metabolomics and biomarkers

1.4.1 Metabolomics to study pathologies

Clinical metabolomics is nowadays an area of intense investigation. This use was born from the need to diagnose diseases, understand their mechanisms, identify new drugs targets, and monitor therapeutic outcomes. Specific investigations are carried to identify potential biomarkers related to pathologies[10,13,47]. Metabolic changes as a disease symptom have already been recognized in ancient medicine[1]. The challenge of biological and clinical researches is to develop fast and reliable methods for diagnosing the disease non-invasively.
Since the start of metabolomics, the number of studies in biological and clinical researches has grown quickly. The study design consists often in the comparison between control (healthy) and case subjects, and the same thing in terms of cells, tissues and biofluids, in human and/or animal models. We can find also epidemiologic studies, which aim to determine the causes of diseases outcomes.

Several pathologies were highly investigated through metabolomics especially cancer including lung, colorectal, breast, prostate, bladder, gastric and thyroid[28,38,48-55]. It was discovered that blood acetate is associated with biliary tract cancer[54], urine taurine are associated to bladder cancer[48]. Investigation of cerebrospinal fluid revels a deregulation in cholesterol and phospholipids metabolisms in brain cancer[56].

For Cardiovascular diseases, amino-acid metabolism were found altered, and an increase of methylated arginine species and lipids (specially fatty acids) were noticed[6,7,57].. In neurological field, Alzheimer and depression are highly studied[20,58]. Other diseases like infectious diseases[59,60] and diabetes[12] and others were also investigated.

1.4.2 Metabolomics and genetic diseases

The association of genetic variation with metabolite levels is well documented[61,62]. A number of studies have highlighted the influence of genetics on the metabolites levels [63,64]. It was discovered more than 150 genetic loci that associate with blood levels of more than 300 distinct metabolites[65,66]. For example, metabolomics approach was used to explore several genetic diseases like Inborn errors metabolism, which is actually implemented in clinical routines[67]. Mitochondrial diseases, a group of disorders that can result from abnormalities in the mitochondrial and nuclear genomes, could be also recognized by metabolomics[68].

1.5 Conclusion

The application of metabolomic approach in medical research is a dynamic field, and has a high potential in disease diagnosis. These discoveries make metabolomics a promising diagnostic tool, with has the advantage to be non-invasive and highly reproducible. Metabolomic technologies offer a sensitive means to search human biofluids for metabolite profiles potentially usable as biomarkers for diseases. In this thesis, we will use a ^{1}H NMR based metabolomics to investigate murine models for thyroid hormone pathologies.

2 Thyroid hormone system and diseases

2.1 Thyroid hormone system

2.1.1 Thyroid hormone functions

Thyroid hormones (TH), thyroxine (T4) and 3,5,3'-triiodothyronine (T3), the main secretion products of the thyroid gland, are essential for normal growth, development and metabolism regulation[69-71]. T4 is more abundant in the blood, T3 is considered as the major active hormone due to its high affinity for nuclear receptors and intracellularly generated from T4.

TH play significant roles during embryogenesis and childhood. They are involved in nearly all tissues, with major effects on the basal metabolic rate and oxygen consumption[72,73]. TH are known to maintain heart rate, myocardial contractility and vascular function[74]. They are also key regulators of thermogenesis, which allows the maintenance of body internal temperature[75,76]. They are involved in body weight regulation, in the development and maintenance of adult bone mass and strength[77]. It is well established that changes in TH level, compared to the reference range, is associated with body weight change in both men and women[78]. Skeletal muscle is an important TH target for contractile function and regeneration[79]. TH regulate lipids metabolism such as: cholesterol synthesis and efflux, bile acid synthesis, fatty acid metabolism. Carbohydrates are also regulated by thyroid hormones (Figure 2.1.1).

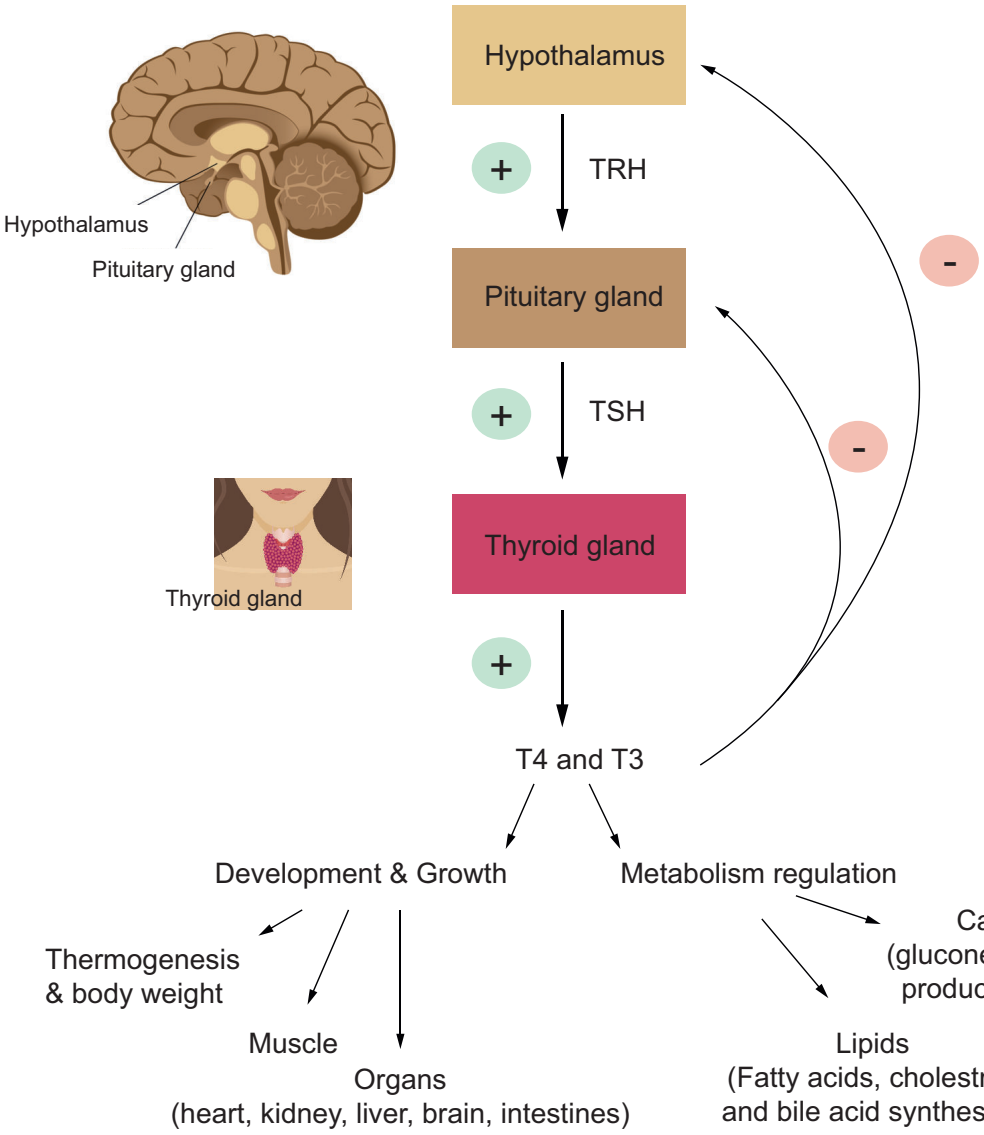

Figure 2.1.1: **The hypothalamus-pituitary-thyroid (HPT) axis and thyroid hormones (TH) actions.**

HPT axis regulates and maintains thyroid hormones homeostasis. Hypothalamus secretes TRH in response to low concentration of circulating T4/T3. This secretion stimulates the pituitary gland, which secretes TSH in turn. This leads to T4/T3 release in the blood. T3 negative feedback on TRH and TSH levels keeps the T3/T4 ration constant in circulation. Thyroid hormones have a central role in development, growth and metabolism regulation.

2.1.2 Thyroid hormones receptors

Thyroid hormones exert their effects via thyroid hormone receptors (TRs), member of the superfamily of hormone-responsive nuclear transcription factors. These receptors share a similar structure and mechanism of action[80]. THRA and THRB encode the two major TR isoforms: TRα1 and TRβ (β1 and β2), which are distributed differentially in tissues. TRα1 is predominantly expressed in brain (central nervous system), heart (myocardium), skeletal muscle, adipose tissue and gastrointestinal tract. TRα2 and TRα3 are variants of TRs, which are non TH-binding proteins, and their function is not understood[81]. TRβ is expressed in the sensory tissue (the inner ear and retina), the kidney, the liver and cardiac ventricles[82].

As described in figure 2.1.2, all these receptors contain three conserved domains: a N-terminal domain, a DNA-binding domain (DBD) and a ligand-binding domain (LBD). The α and β receptors have a similar DBD and LBD, but differ in their N-terminal domain. The three receptors (TRα1, TRβ1, TRβ2) bind the same ligand due to these structural homologies[69].

TRs are considered as transcription factors because they regulate target gene expression directly through DNA response element (TRE)[83].
Non-genomic actions of thyroid hormone were also reported and are little studied [84]. They have extranuclear actions, which are not TRE-mediated.

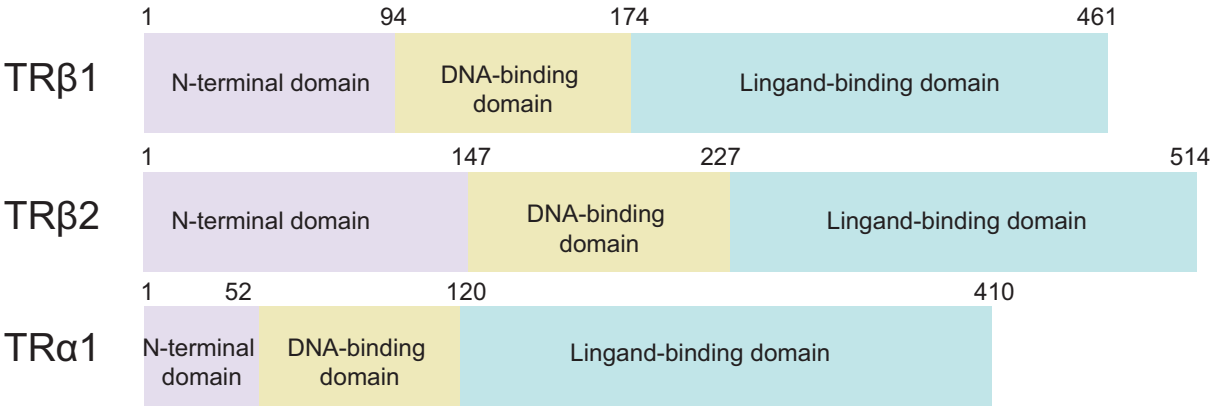

Figure 2.1.2: **Schematic alignment of thyroid hormone receptors: TRβ1, TRβ2 and TRα1.**
TH receptors are composed of three domains: N-terminal domain (activation function), DNA-binding domain (DBD) and Ligand-binding domain (LBD). DBD and LBD are highly conserved domains between the three TH receptors, contrary to the N-terminal domain.

2.1.3 Mechanisms of action

The thyroid gland secretes T4 and T3 hormones, which are transported into the cells by membrane transporters like the monocarboxylate transporter (MCT) family[85], and more precisely MCT8. T3 is secreted by the thyroid gland, but also converted from T4 under the action of type 1 or type 2 of 5' deiodinase, which are tissue-dependent. Unliganded TR in the nucleus forms a heterodimer with the retinoid X receptor (RXR), which then binds the thyroid hormone response element (TRE) in the regulatory sequences of TH-responsive gene. This results in the activation or repression of TH target genes transcription.

In the absence of T3, corepressor proteins are associated to the TR-RXR complex and prevent genes transcription[86]. However, in the presence of T3, corepressor proteins leave the complex, and coactivator proteins are recruited, which lead to target genes transcription[87] (Figure 2.1.3).

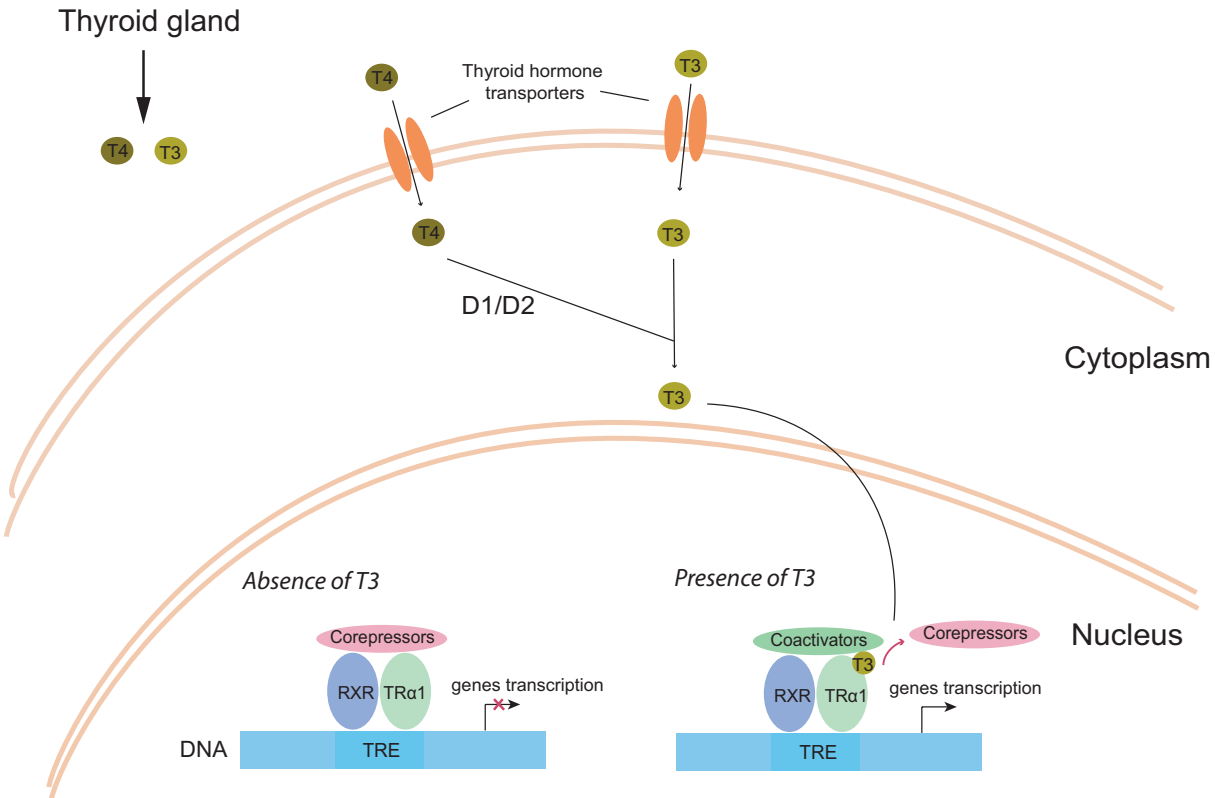

Figure 2.1.3: **Mechanisms of action of thyroid hormones.**

Membrane transporters transport T4 and T3, after their secretion by thyroid gland, into the cell. A part of T4 is converted to T3 under the action of type 1 and 2 5' deiodinase (D1 and D2). Unliganded TR heterodimerizes with RXR, and then the complex recognizes TRE. In the absence of T3, corepressor proteins bind the complex to repress target gene expression. In the presence of T3, corepressor proteins are dropped and coactivator proteins are recruited, which lead to target gene transcription.

2.1.4 Regulation

TH regulates a large amount of genes, which are involved in growth, metabolic balance and thermogenesis[88]. TH synthesis and secretion are regulated by a negative-feedback system that involves the hypothalamus, pituitary, and thyroid gland (hypothalamic/pituitary/thyroid (HPT) axis)[89]. Hypothalamus secretes TRH. Thyrotropes, endocrine cells from pituitary, secrete then Thyroid-Stimulating hormone (TSH). TSH acts on the thyroid gland to induce thyroxine (T4) and 3,5,3'-triiodothronine (T3) hormones production, which then act on body growth and development and metabolism regulation. High levels of T4 and T3 in turn feed back lead to TSH level secretion diminution in the pituitary, which then regulate T4 and T3 levels.

2.1.5 Alterations in thyroid hormone system

TH action requires (i) the availability of TH (production/secretion, conversion of T4 to T3) (ii) intact and adapted membrane transport (iii) cytosolic and nuclear processing (iv) association with intact receptors (v) interaction with co-regulators (co-activator or co-repressor proteins). Alteration in one of these steps can lead to a heavy metabolic disorder[90].

Associated diseases are the most common endocrine disorders worldwide[91]. In addition to clinical symptoms, biochemical tests like determination of TSH and free T4 levels in blood are used to suspect thyroid disorder. Hypothyroidism and hyperthyroidism lead to alterations in metabolism (lipids, carbohydrates), growth and energy homeostasis[92]. Hypothyroidism,

results from low levels of TH, presents a low metabolic rate, and leads to cardiovascular diseases, whereas hyperthyroidism, which is a catabolic syndrome, is associated with a high metabolic rate, and leads to tachycardia and loss of body mass. These diseases are related to the secretion and production of the thyroid hormones by the organism.

Other diseases are known to lead to hypothyroid or hyperthyroid phenotypes, without alteration in TH production, but caused by genetic mutations. Thyroid hormone cell transport defects (THCTD) caused by a mutation in MCT8 gene lead to production of defective cell-transport proteins, which reduce hormone transport and causes reduced levels of intracellular TH[90]. Thyroid hormone metabolism defect (THMD) is caused by a mutation in selenocysteine-binding protein 2, which interferes with conversion of T4 to T3, resulting in a low T3 and high T4[93].

Other diseases known under the name of resistance to thyroid hormone (RTH)[94] were discovered. The first described cause was a mutation in TRβ gene in 1989, which is characterized by high serum concentration of free T4 and T3, and normal or slightly elevated TSH concentration. This disease is called RTHβ. Twenty-four years later, the first mutation in TRα gene was discovered, and the disease has been named RTHα.

2.2 Resistance to thyroid hormones α

Resistance to thyroid hormone (RTH) was first described as a clinical entity in 1967[95]. Patients are hyposensitive to TH and they present reduced clinical and biochemical manifestations of TH action relative to the circulating hormone levels. The molecular explication of this syndrome was determined in 1989 when the first case of RTH caused by a mutation in the THRB gene was discovered. This disorder was named resistance to thyroid hormone due to a mutation in the thyroid hormone receptor β, abbreviated by RTHβ[96,97].

RTHβ is characterized by the impairment of the HPT axis: elevated levels of thyroid hormone, normal or elevated levels of TSH. Patients present with different degree of goiter, hearing abnormalities, tachycardia, mental retardation, attention-deficit, and delayed bone growth and maturation[94,97,98]. They present features of hypothyroidism and hyperthyroidism,

which is explained by variable resistance in different tissues. The incidence of RTHβ is actually estimated to be 1 in 40.000 with 160 different mutations approximately[99,100]. Patients with RTHβ are currently found in more than 400 families[101]. This syndrome can be suspected in patients with these features and can easily be recognized by physicians.

2.2.1 The first cases

Patients with mutations in *THRA* were not identified until 2012. The first case of RTHα was discovered, after a whole-exome sequencing, in a little 6-year-old girl, which presents classical features of hypothyroidism (e.g. growth retardation, developmental retardation, skeletal dysplasia, low heart rate, and severe constipation) and nearly normal thyroid function biochemical tests[102].

Other cases, female and male of different ages, were discovered with different mutations in TRα1[100,103-112]. The phenotype of the identified patients consists of varying degrees of growth impairment, mental and motor development, delayed bone, constipation, and near-normal thyroid function tests. Some cases have specific health issues like autism[106], chronic anaemia[104,110,113], epilepsy[114], etc. (Appendix 1).

2.2.2 RTHα is different from RTHβ

RTHα is clinically distinct from RTHβ. TRα and TRβ, are differentially expressed during development and are differentially distributed in adult tissues, which explains the difference between the two diseases. TRβ has an important role in inner ear, cerebellar, and retinal development, TSH regulation, and mediating the metabolic actions of T3 in the liver[71]. TRα has specific roles in the heart, brain, intestine and in mediating adaptive thermogenesis in brown adipose tissue (BAT)[71,115]. RTHα is thus characterized by a tissue-selective hypothyroidism (e.g. skeleton, gastrointestinal tract, myocardium, etc.) and near-normal thyroid function biochemical tests. In figure 3.2.1, organs that present a dominance of TRα (bones, heart, intestine, brain and particularly the central nervous system, and muscles) are resistant to TH. While, liver that presents more than 80% of TRβ is resistant to TH. The pituitary-thyroid axis in RTHα is not dysregulated as noticed in RTHβ patients.

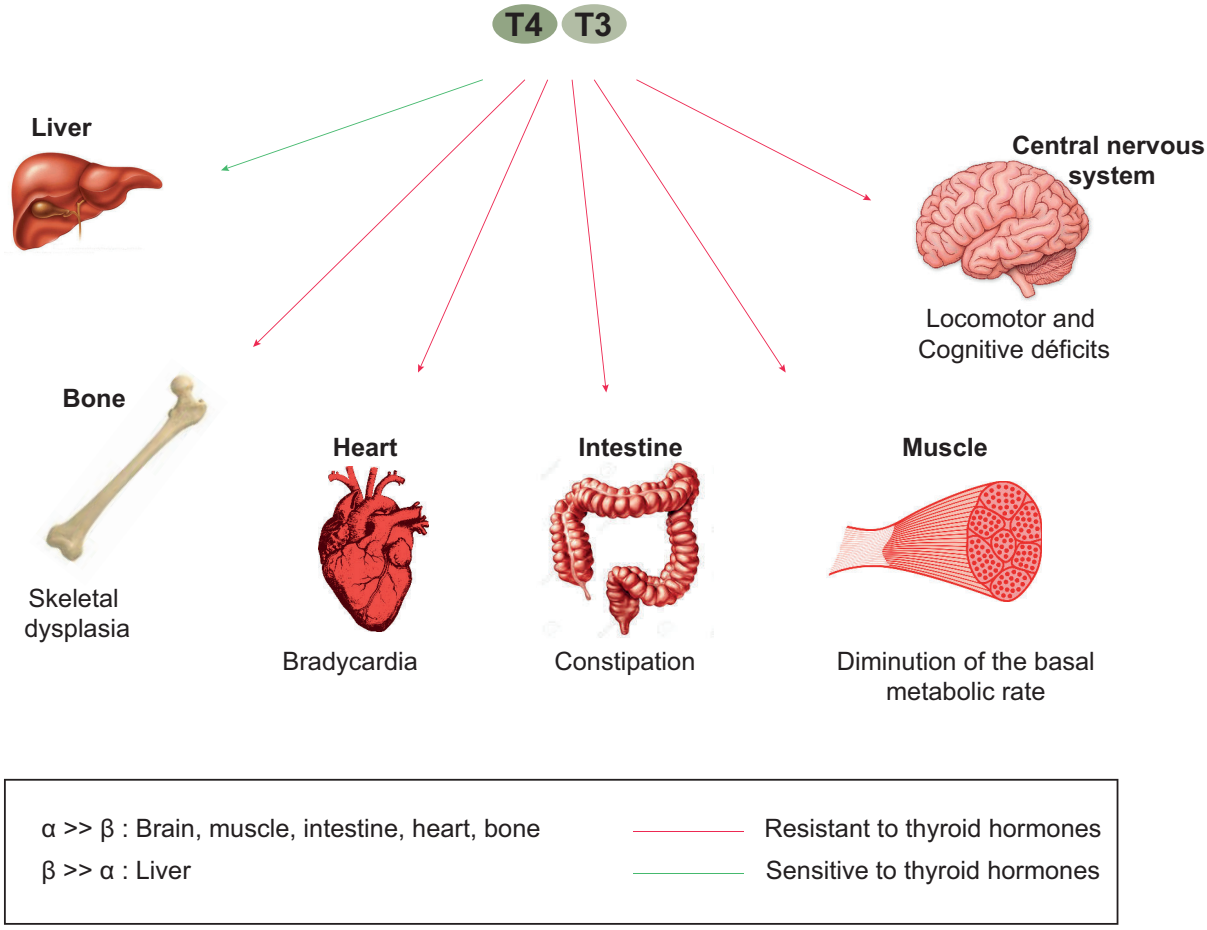

Figure 2.2.1: **The sensitivity of organs to thyroid hormones depends on the type of thyroid receptor present.**

2.2.3 A high variability in the clinical features

The high variability of clinical features and the absence of specific traits and reliable biochemical markers make the diagnosis of this disease difficult. In addition, identified RTHα patients present some common features with hypothyroid patients, which may delay the diagnosis in some cases. Since its first description, 45 cases of RTHα have been reported worldwide, corresponding to 25 different mutations of TRα1. In 2015, the sequence of 60 000 anonymous exomes were released by the Exac database (http://exac.broadinstitute.org), revealing the existence of 68 *THRA* missense or frameshift, which almost certainly alter TRα1 function. It is thus thought that the incidence of RTHα may be similar to RTHβ incidence.

The inability to quickly recognize patients with RTHα is regrettable because the developmental consequences of the disease can be greatly reduced by an early therapeutic intervention. Motor skills and body growth have been restored in a young patient treated with an excess of thyroxine to overcome tissue resistance[108,109]. Two adult patients with normal adult stature received thyroxine treatment during childhood by chance[105]. Authors suggest here that the neurocognitive abnormalities are may be less severe because of this treatment[105]. Another study on a murine model (Arg384cys) showed also that increased concentrations of thyroid hormones can reverse neurological abnormalities[116].

It is thus primordial to find a reliable way to identify these patients, and to manage them at early stage to minimize the consequences of this disease.

2.2.4 Molecular aspect

All the identified patients are heterozygous for *THRA* mutation, which generate a mutant receptor that inhibits wild-type receptor function in a dominant negative manner[106,108,112]. All the known mutations are present in the carboxyterminus, the ligand-binding domain (LBD) of the receptor (Figure 3.2.2), to which the helix 12 belongs. These mutations lead to the destabilization of this helix[102].

Two types of mutations were identified in RTHα patients: frameshift [103,104,107,114] and missense mutations[102,105-108].
Amino acid substitutions (D211G, H361Q, R384H, A263V) reduce the affinity of TRα1 for T3. While, c-terminal substitutions (P398R and E403K), truncations (C392X and E403X), and frameshift mutations (C380fs387X, A382PfsX7, F397fs406X, and F401S) alter ligand binding, by modifying or eliminating the helix 12, and prevent thus coactivator recruitment[117]. This kind of mutation is more deleterious and present severe loss of function.

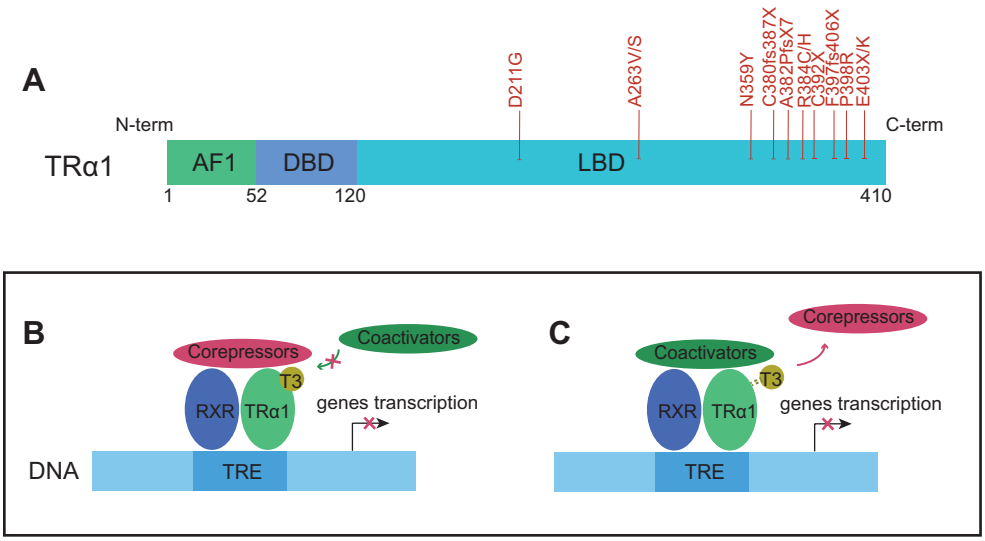

Figure 2.2.2**: *THRA* mutations consequences.**

Thyroid hormones regulate target genes transcription via nuclear receptors TRα and TRβ. These receptors are composed of 3 distinct regions: N-terminal domain, DNA binding domain (DBD) and ligand binding domain (LBD). All the known RTHα mutations are located in the LBD (A). Mutations in TRα1 disturb target gene transcriptional regulation. Two functional alterations were observed in the presence of T3: the dissociation of corepressor proteins is prevented (B), or affinity between TRα1 and T3 is reduced (C).

2.2.5 Relation between genotype and phenotype?

There are thus different mutations with different degrees of severity of the disease. Two patients (6-year-old and 15-year-old girls), which were found with the same mutation (E403X)[102,118] present similar features. Two other patients were found with TRα1 mutation in the same position (A263V and A263S), but, as noticed, the original amino acid alanine was substituted by valine in the first case and by serine in the other case. The functional analysis of the A263V mutant indicates a greater defect in transcriptional activity of TRα1 than that induced by the A263S mutation. It was also noticed that a more up-stream mutation lead to a more severe phenotype, like the mutation C392X[118].

All these observations suggest that the variability in the symptoms is maybe related to the type of the mutation and its position. The relationship between genotype and phenotype need to be further discerned. To understand this relationship and to study the impact of RTHα disease on the whole organism, different murine models were developed.

2.2.6 Mouse models to study RTHα

Mouse *Thra* and human *THRA* genes present sequence similarities. The two TRα1 amino acid sequences differ at three positions only (AA34, 37, and 170), which makes mouse lines with *Thra* mutations highly relevant animal models for RTHα disease. Prior to the identification of human RTHα cases, several researchers were done using TRα knockout and knockin mouse models to predict the phenotype of human disorder[99,115,119-124]. The first mouse model of RTHα was a knockout of *Thra* gene, in which TRα1 and TRα2 isoforms were inactivated[124]. Mice failed to survive 5 weeks after birth, and features of hypothyroidism and serious delayed maturation in the small intestine and bones were observed in these mice[124]. It was reported also in another study that a mutation in TRα1 exhibit several distinct neurological abnormalities: extreme anxiety, reduced recognition memory, and locomotor dysfunction[116]. Another model was developed before its discovery in a human patient[107,121]. Other researchers showed the significant implication of TRα1 on metabolic homeostasis[119]. The phenotype of mice models is often close to the clinical features of RTHα patients.

These models allowed the good understanding of the function of *THRA* gene and the TRα receptor, and facilitate the comprehension of RTHα disease and its impact on the organism.

For the metabolomic study presented in this thesis, we have used mouse models that were previously generated by Markossian et al[117] to understand the relationship between specific *THRA* mutations and phenotype. Five novel germline mutations (four frameshift: E395fs401X, E395fs485X, E395fs406X, and K389fs479X; and one missense N359Y), which are closely modeling the mutations found in RTHα patients, were introduced in mouse *Thra* gene. Markossian et al have investigated skeleton, blood, heart, cerebellum and intestinal epithelium. They concluded that like human patients, mutant mice displayed a hypothyroid-

like phenotype, with altered development. Phenotype severity varied between the different mouse models[117].

From a global literature screening, about a hundred of research studies have been conducted to study the thyroid system by metabolomics approaches. About 50% of these studies address about thyroid cancer, which is explained by its increased incidence worldwide. The main medical treatment in the case of thyroid cancer is the total thyroidectomy (removal of the thyroid), even if the tumour is benign. A number of studies, with different methods, were performed to distinguish between cancer patients and healthy individuals, and between benign and malignant thyroid nodules[55,125] to improve thyroid cancer diagnosis. Several toxicological studies, which highlight the harmful impact of certain chemicals (mainly glyphosphate-based herbicide and decabromodiphenyl) on the thyroid hormone system[126,127]. A few studies, also aimed providing deeper understanding of thyroid disease mechanism, such Graves' disease[14], hypothyroidism[128], hyperthyroidism[129], depression, low T3 syndrome, type 2 diabetes[12] and selenium deficiency. Others correspond to population-based studies seeking for linear relationship between either TSH or free T4 (FT4) and metabolite levels[55,129]. Other works focused on the direct effect of thyroid hormones status on the brain[130] or hepatic lipids, to provide deeper understanding of the mechanism behind the biological phenomenon.

At this point, metabolomics investigations of genetic diseases that disturb thyroid system such as RTH (α and β) or THCTD or THMD, have never been reported in the literature.

We notice overall that the thyroid system has little been explored by metabolomics approaches, and more precisely genetic diseases. A number of studies have highlighted the influence of genetics on the metabolites levels [63,64]. The association of genetic variation with metabolite levels is well documented[61]. For example, metabolomics approach was used to explore several genetic diseases like Inborn errors metabolism, which is actually implemented in clinical routines[67]. Mitochondrial diseases, a group of disorders that can result from abnormalities in the mitochondrial and nuclear genomes, could be also recognized by metabolomics[68].

In the work described in the following chapters of this thesis, we study different pathologies related to the thyroid hormone system. We exploit the metabolic fingerprint of hypothyroidism. We investigate the same series of mouse models of RTHα used by Markossian et al. [117] to assess the capacity of ^{1}H NMR analysis of body fluids to recognize the presence of *Thra* mutations. And in the end, we study the impact of thyroid hormone on the hepatic metabolism and the specific role of the thyroid hormone receptor β in this mediation.

3 Materials, methods and analytical workflow

3.1 Introduction

The NMR metabolomic global workflow contains several steps: sample preparation, NMR data acquisition, data processing, statistical analysis, metabolite identification, and interpretation. Two different approaches can be used: untargeted approach (with no *a priori* hypothesis) and targeted approach (applied on a predefined set of metabolites). The different steps are detailed in the following section (Figure 3.1).

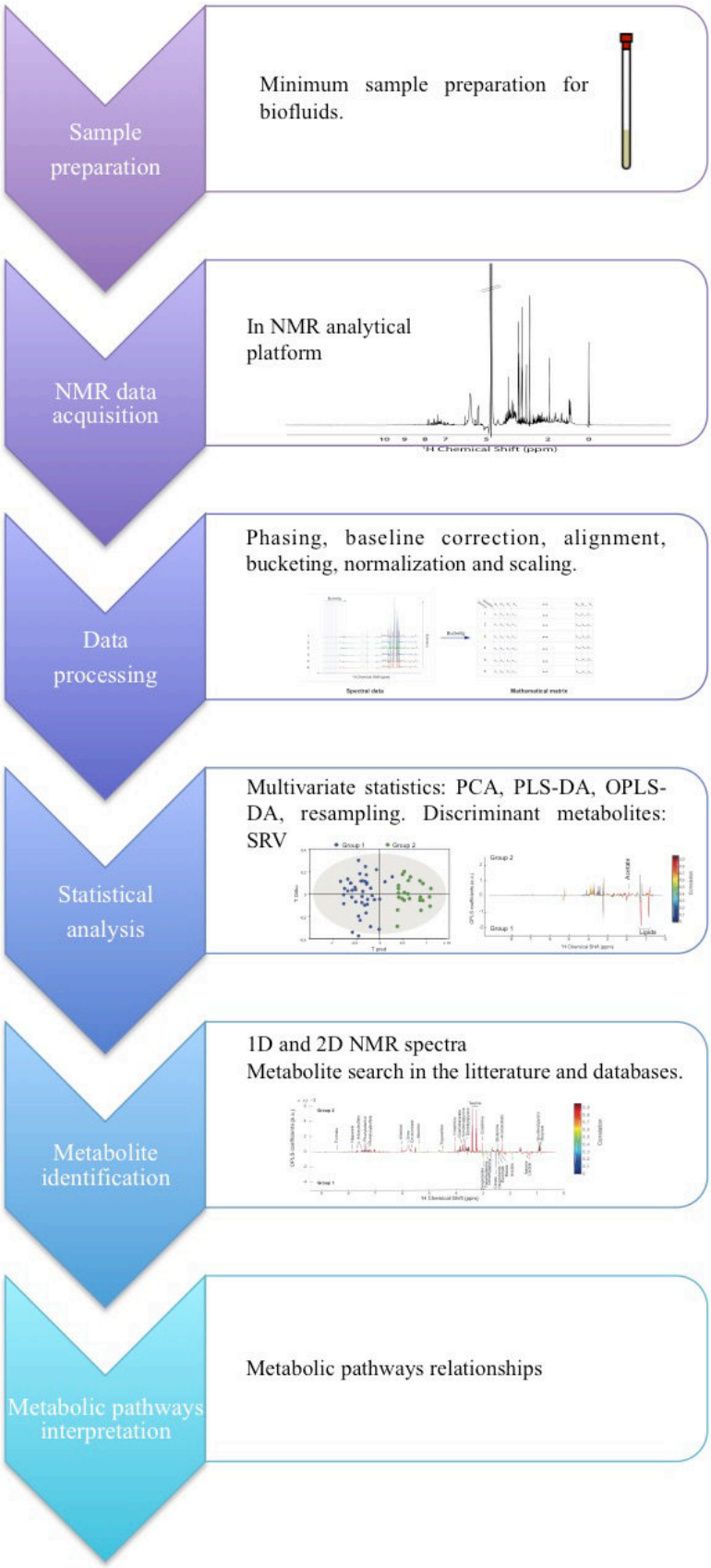

Figure 3.1: **Analytical workflow for NMR-based metabolomics studies**

3.2 Biological samples preparation

3.2.1 Collection and storage

NMR liquid samples preparation is straightforward and the protocols[46] are standardized and highly reproducible. This step can be automated by using a robotic liquid handling technology. It is very important to collect the biofluids with the same manner, and to handle properly the samples. Because, in some cases, errors related to samples handling (time of collection, contaminations) can introduce variations in signal intensity that are not from metabolism.

- Urine

Time of collection for urine samples can make a quantitative and qualitative difference in the urine metabolome. The first morning void is the preferred type, because it is collected after several hours of fasting, which minimizes the impact of food or medication on the urine metabolome. It is important to respect the same time of collection between subjects, and between time points in the case of longitudinal studies. For human subjects, urine collection is easy contrary to animals. Animal houses need to be clean before their first urine, which are around 7 am for the majority. In addition, in some cases, we find urine and feces in the same place, which can alter considerably the composition of urine. The volume of mouse urine needed for classical metabolomics studies is 200µl. This quantity is sometimes not reached, and we need to wait for a second sample, in fasting condition also, to obtain the needed volume. Urine is then quickly stored at -80°C after collection, before NMR analysis.

- Blood

The main difference between blood serum and plasma is the presence or absence of clotting. For plasma, the whole blood is collected into tubes with anti-coagulant and then a centrifugation step lead to separate the liquid state from blood cells. For serum, whole blood is collected into tubes and is allowed to clot for a specified time and temperature before centrifugation to pellet the clot and cells. Different studies showed that there is not a difference between these two types in term of metabolite composition. In our study, we

collected mice blood from the abdominal aortic, and we investigated the plasma. The timing of blood collection is also important. The volume collected from mice is also limited given the quantity of their whole blood, which is around 1ml. After the coagulation step, we obtain about 200-300 µl of plasma from each mouse. Samples are stored at -80°C after their collection.

- Liver biopsies

Tissues are metabolically active and therefore require rapid metabolic quenching when they have been collected. Liver used for the work described in chapter 6 of this thesis, were flash-frozen in liquid nitrogen just after their collection, and then stored at -80°C. We collected about 100-150mg of liver for each sample, which provides good coverage of the tissue metabolome[131].

3.2.2 Preparation and handling

- Urine

The samples were prepared according to standard protocol (Bruker Biospin GmbH, Rheinstetten, Germany). Urine samples were thawed at room temperature, and then centrifuged for 5 min at 6000 rpm. 200 µl of the supernatant were mixed with 300 µl of water and 50 µl of buffer solution (1.5M KH_2PO_4, 2mM sodium azide (NaN_3), 0.1% trimethylsilyl propionate (TSP) pH7.4 in D2O).

Variations in chemical shift of the same metabolite signals can be observed due to small differences in pH between samples. It is crucial to homogenise the PH in the samples, where the use of a buffer solution here. NaN_3 is used to prevent microbial contamination, and TSP as an internal standard. 550 µl of the mixture were then transferred into 5mm NMR tubes.

- Plasma

Plasma sample were thawed at room temperature, coagulated particles were removed by centrifugation at 6000 rpm during 5 minutes. It was difficult to have 300µl of plasma from all mice. We decided thus to dilute the samples and then normalize data before statistical analysis performing. The liquid phase (200µl) was mixed with 100µl of water and 300µl of

buffer (0.142M Na2HPO4, 0.1%NaN3, 0.1% TSP pH7.4 in 20% D2O). Samples were kept at 4°C until analysis.

- Liver tissue

30µL disposable Kel-F® inserts with sealing caps for 4 mm NMR rotors were filled with intact liver fragments and 5µL of D2O. Inserts were stored at -80 °C before high-resolution magic angle spinning nuclear magnetic resonance (^{1}H HR-MAS NMR) analyses.

Extractions of polar and lipophilic metabolites was performed as described in Beckonert protocol[46]. A liver fragment (0.3 g) was homogenized in 1.2 mL 80% methanol at 4°C. The homogenates were sonicated twice in an ice-cold water bath for 10 s. Homogenates were then transferred into a glass tube and 3 mL of chloroform were added. Tubes were vortexed again and diluted adding by adding 1.2 mL of chloroform and 1.2 mL of water. Tubes were vortexed, kept on ice for 15 min, and the phases were separated by centrifugation (1500 g, 20 min, 4°C). Each phase (aqueous / lipophilic) was collected and vacuum. The dry residue was dissolved in 600 µL of deuterated phosphate buffer (pH = 7.2, 100 % D2O)[46].

An additional series of quality control (QC) samples for each type of samples was included to evaluate the quality and the reproducibility of the NMR data acquisition.

3.3 NMR-based metabolomics

3.3.1 Data acquisition

- Urine

All NMR experiments were performed on a Bruker Avance III spectrometer operating at 600.55 MHz (proton resonance frequency), with a 5mm standard TCI cryoprobe, and an automated sample changer with sample cooling (4°C). The temperature was controlled at 300K for urine. Standard one-dimensional ^{1}H NMR spectra were acquired with the 'noesygppr1d' pulse sequence for each sample. A total of 128 transient free induction decays (FID) were collected for each experiment with a spectral width of 20 ppm. The acquisition

time was set to 1.5s with relaxation delay of 2s. The noesy mixing time was set to 10ms. All FIDs were multiplied by an exponential function corresponding to a 0.3Hz line-broadening factor, prior Fourier transformation.

- Plasma

All NMR experiments were performed on a Bruker Avance III spectrometer operating at 600.55 MHz (proton resonance frequency), with a 5mm standard TCI cryoprobe, and an automated sample changer with sample cooling (4°C). The temperature was controlled at 310K for plasma samples. Standard one-dimensional ^{1}H NMR spectra were acquired with the 'noesygppr1d' and 'cpmgpr1d.be' pulse sequences for each sample. A total of 128 transient free induction decays (FID) were collected for each experiment with a spectral width of 20 ppm. The acquisition time was set to 1.5s with relaxation delay of 2 s. The noesy mixing time was set to 10ms. All FIDs were multiplied by an exponential function corresponding to a 0.3Hz line-broadening factor, prior Fourier transformation.

- Liver extracts

Experiments were carried out on a Bruker Avance III spectrometer, operating at 600.55 MHz (^{1}H resonance frequency), equipped with a TCI cryoprobe and an automated sample changer with cooling capacity. The experiment temperature was controlled at 300°K. 1D ^{1}H NOESY NMR experiments with water presaturation and gradients were performed on each aqueous extract sample to derive metabolic profiles. 256 FIDs were co-added, with a 20 ppm spectral width and an acquisition time of 1.36 s, corresponding to 32 k data points, with a relaxation delay of 2 s, for a total experimental time of 15 minutes per spectrum. The NOESY mixing time was set to 10 ms and the delay for gradient recovery was set to 200 μs. The ^{1}H 90° hard pulse length was automatically calibrated at around 13 μs for each sample. 2D NMR experiments, including ^{1}H-^{1}H TOCSY and ^{1}H-^{13}C HSQC experiments, were carried out on a subset of selected samples to characterize structural connectivity between nuclei and refine metabolite identification. A simple 1D Bloch decay ^{1}H NMR experiment was performed on each lipid extract sample.

- Intact liver tissue

Experiments were carried out on a Bruker Avance II spectrometer, operating at 700.09 MHz (^{1}H resonance frequency), equipped with a 4 mm HR-MAS double resonance (^{1}H-^{13}C) probe. Temperature was controlled at 10°C throughout the experiments and the magic-angle

spinning frequency was set to 3.5 kHz. 1D ^{1}H NOESY NMR experiments with water presaturation were performed on each sample to derive metabolic profiles. 256 free induction decays (FIDs) were co-added, with a 12 ppm spectral width and an acquisition time of 1.36 s, corresponding to 22856 data points, with a relaxation delay of 2 s, for a total experimental time of 15 minutes per spectrum. The NOESY mixing time was set to 100 ms. The ^{1}H 90° hard pulse length was calibrated at 6.5µs.

2D NMR experiments (^{1}H-^{13}C HSQC, ^{1}H-^{1}H TOCSY and J-Resolved) were recorded on a subset of samples (urine, plasma and liver aqueous extracts) to achieve structural assignment of the metabolic signals.

3.3.2 NMR data processing

- Baseline correction and spectra calibration

NMR spectra are processed by baseline and phase corrections, and then calibrated. The calibration is performed on a metabolite signals with stable chemical shift (uninfluenced by PH) like α-glucose anomeric proton (δ = 5.23 ppm) for blood plasma, and with an internal standard like TSP (3-trimethylsilylpropionic acid) introduced in samples for urine. HR-MAS spectra were calibrated on the CH3 alanine doublet at δ = 1.48 ppm and spectra of aqueous extracts were referenced to the anomeric glucose doublet at δ = 5.23 ppm.

- Bucketing

Before performing statistical analysis, spectral data are converted to a mathematical matrix (X matrix) by a simple binning approach (Figure 3.2.1). Each row corresponds to a spectrum (a sample) and each column corresponds to regions of individual NMR spectra denoted NMR buckets. After a bucketing with a resolution of 0.001 ppm and a spectral width between 0 and 10 ppm, 10 000 variables are generated for each spectrum. These variables reflect spectral peak intensities or metabolite concentrations at a given point of the spectra.
Biological samples contain a large amount of water, and its residual signal is important. The residual water signal is excluded in this step. Other signals can be excluded like molecules coming from contaminations (e.g. ethanol used to decontaminate animals) or solvents used

during extraction. Regions of the spectrum containing only noise (in the beginning and the end of the spectrum) can be removed.

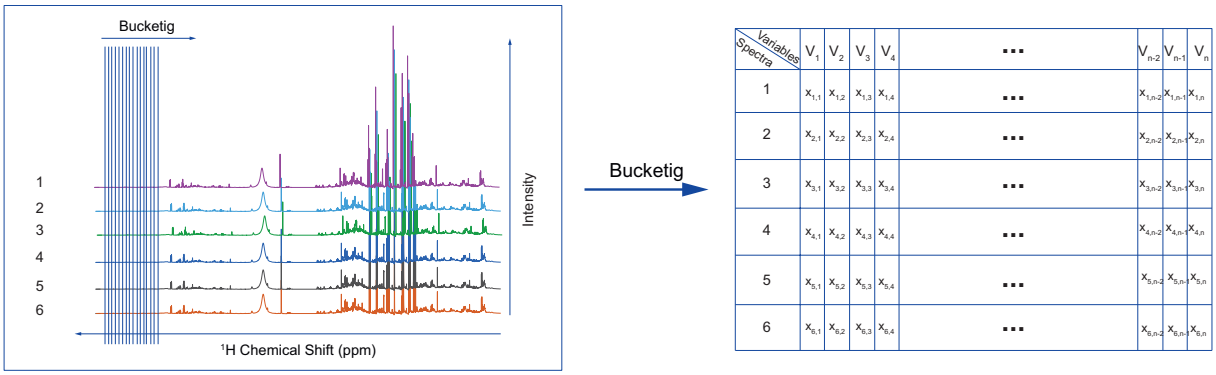

Figure 3.2.1: **Bucketing step.**

Spectral data are converted to a mathematical matrix, where each row relates to a given sample and each column corresponds to a single measurement in that experiment.

- Alignment

Some variations in the chemical shift of certain peaks signals can be noticed, and this is mainly due to differences in pH or osmolarity between samples. Spectra need to be perfectly stackable to ensure that each column of the X matrix corresponds to the same metabolite before statistical analysis. Icoshift[132] is a very effective tool for the alignment of NMR spectra. This method was employed as described in figure 3.2.2. Other alignment tool exist[29,30].

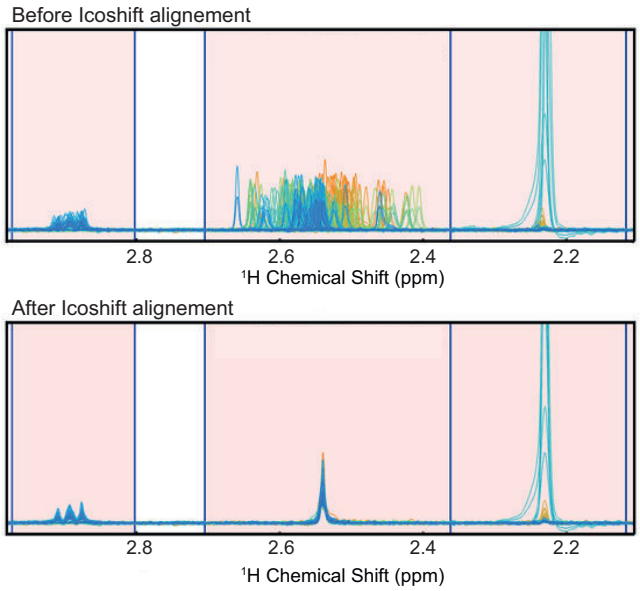

Figure 3.2.2: **Overview of the Icoshift algorithm results.**

- Normalization

NMR samples preparation is straightforward and the protocols are standardized and highly reproducible. However, sample handling and dilution can introduce variations in signal intensities, which are not related to the metabolism. These variations can interfere with multivariate statistical analysis. The goal of normalization[133] is thus to remove or minimize these variations to make the data from all samples directly comparable with each other.

Normalization is essential for urine samples because urine concentration is highly related to the amount of ingested water, drugs, toxins and treatments. The most appropriate normalization in this case is PQN (Probabilistic Quotient Normalization)[134], which looks for the most probable coefficient of dilution between each spectrum and a reference spectrum to normalize spectra.

For blood plasma, metabolite concentrations are highly regulated by homeostasis, and changes caused by a physiological situation are generally small but significant. It is not necessary to normalize in this case, unless the volume differs slightly from one sample to another. Normalization on total intensity, where each bucket is divided by the total intensity of the spectrum, is used in this case to eliminate the effects of variable concentration.

- Scaling

Variables (metabolite concentrations) often have different numerical ranges. A variable with a large range has a large variance, whereas a variable with a small range has a small variance. The scaling methods aim to adjust the variance of the different metabolites[135]. There is several ways to scale the data. The most known is *Auto scaling* or *Unit Variance (UV),* data are mean-centered and then each value is divided by the standard deviation. *Pareto scaling* is also widely used, it aims to reduce the relative importance of large values, and keep data structure partially intact. Here, data are mean-centered, and then divided by the square root of the standard deviation. Both methods make the metabolites equally important.

3.3.3 Multivariate analysis of metabolic profiles

In biological studies, several variables (intensities at a specific NMR chemical shift, age, height, weight, sex…) are used to characterize samples (observations). These data can be arranged in a table, where each row represents an observation and the columns represent the different variables.

The high number of variables generated in metabolomics studies makes the analyses difficult. It is complicated to overview and summarizes the data. The development of chemometrical tools constitutes an important step in sciences, which help to extract information out of data. This discipline is defined as " the chemical discipline that uses mathematical, statistical, and other methods employing formal logic, to design or select optimal measurement procedures and experiments, and to provide maximum relevant chemical information by analyzing chemical data"[136]. Contrary to statistics, Chemometrics is based on computing intensive methods. They are in general multivariate. The main objective of NMR-based metabolomics is to classify a spectrum based on its chemical composition, and then identify which spectrum areas or metabolites are responsible for this classification. With other words, the goal is to interpret chemical and biological changes related to class differences.

Multivariate statistical analyses based on projection methods can be classified in two complementary approaches for modeling data: unsupervised and supervised statistical approaches. Unsupervised analysis like principal component analysis (PCA), which is considered as the basis of for other multivariate analysis, is widely used in metabolomics

studies as an exploratory tool in the beginning of any analysis [137]. Peaks intensities in the spectra are used as coordinates in multidimensional plots of metabolic activity. PCA helps to detect trends, identify outlier samples (resulting from error in sampling, preparation or spectrum acquisition), and delineate classes. This approach is only based on the spectra and no information about samples is provided. Other unsupervised methods can be used like Hierarchical Clustering Analysis (HCA)[138] and self-organizing maps.

In supervised analyses, samples are characterized in classes and they are associated to an outcome y_i value. Projection to latent structures (PLS) [139,140]and its extension orthogonal partial least squares (OPLS) are based on linear regression method, which aim to find a relationship between a descriptor matrix X (areas from the spectra) and a response matrix Y (e.g. a specific disease). PLS and OPLS can be used for discrimination in the form of PLS-DA[141] and OPLS-DA[142]. Discrimination means the separation between two classes and then find the cause (e.g. biomarkers related to a specific disease) of this separation. OPLS-DA, contrary to PLS-DA, has the ability to separate predictive from non-predictive (orthogonal) variation, which facilitate the interpretation. It is actually the method of choice for discrimination and classification. Data can be visualized as score plot, which each point represents a sample, and as loading plot, which shows the contribution of variables (metabolite) involved in the discrimination (Figure 3.2.3).

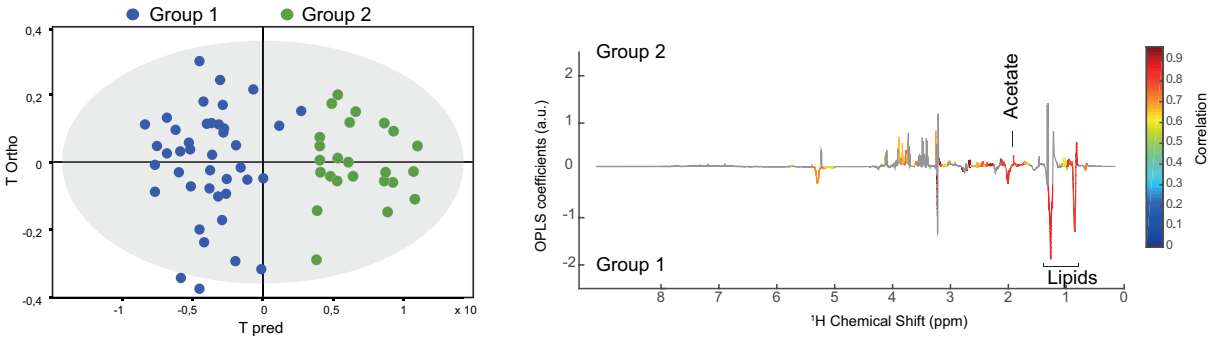

Figure 3.2.3: **Visualization of data from an OPLS-DA analysis**.

5A) This score plot shows a clear discrimination between the group 1 and the group 2. Each point represents a sample. 5B) This loading plot shows the contribution of each metabolite involved in the difference between the two groups. Here, we see that acetate is associated with group 2 and lipids with group 1.

After multivariate analysis, univariate analyses are performed to identify significant changes in metabolite concentrations. Statistical recoupling of variables (SRV)[49] is a homemade tool, which aims to extract the significant differences in metabolite levels between groups defining a metabolic signature.

- Models validation

Several methods are used to ensure the robustness, to validate the performance of the discrimination. R^2 and Q^2 parameters correspond to the explained variance and the predictive power of the model. They aim to assess the quality of the model. To validate PLS and OPLS models, CV-ANOVA[143] and permutation test[144] are generally used. The values in Y matrix are randomly permuted a thousand of times, and for each Y matrix permuted, R^2 and Q^2 are calculated and compared to the original values. If the original values are higher than the new calculated values, this indicates the good quality of the model by rejecting the null hypothesis (Figure 3.2.4).

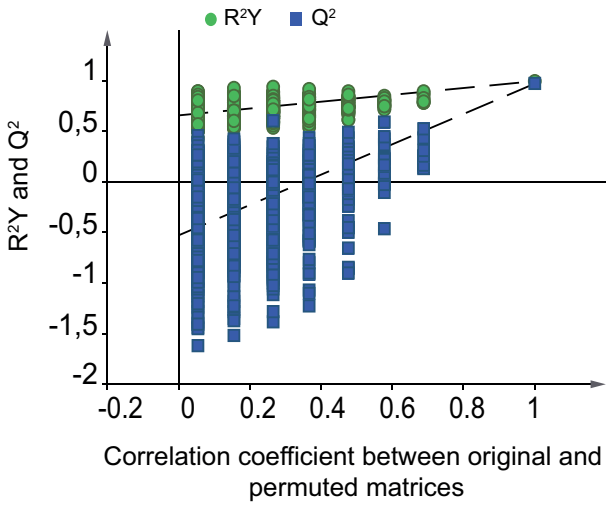

Figure 3.2.4: **Resampling under the null hypothesis to check model robustness.**

3.3.4 Metabolite identification

In addition, 1D ^{1}H-NMR and 2D NMR experiments (^{1}H–^{13}C HSQC, ^{1}H–^{1}H TOCSY and ^{1}H J-resolved experiments) were recorded on a subset of samples to achieve structural assignment of the metabolite signals. Metabolite identification was performed using academic spectral databases (HMDB[145] and MMMDB[146,147]), as well as proprietary databases (NMR Suite v. 7.1, Chenomx Inc., Edmonton, Canada; AMIX SpectraBase v. 1.1.2, Bruker GmbH).

4. ^{1}H NMR-based metabolomics for the study of the impact of the excess and the privation of thyroid hormones on murine metabolism

4.1 Introduction

Hypothyroidism is due to a defective thyroid gland or thyroid hormone biosynthetic dysfunction[148,149]. The most common form of hypothyroidism is due to a problem in the thyroid gland, itself, and presents low levels of circulating thyroid hormones and raised levels of thyrotropin at birth[150]. Central hypothyroidism, another form of hypothyroidism, is caused by impaired Thyroid-Stimulating hormone (TSH)-mediated stimulation of the thyroid gland. Delayed treatment of neonatal hypothyroidism may result in profound neurodevelopmental delay[150]. As described in the previous sections, RTHα patients present some common features with hypothyroid patients. This chapter is dedicated to the study of metabolic changes caused by hypothyroidism, in order to distinguish them from those caused by THRA mutations.

In the present study, we carried out a metabolomic study investigating urine and blood plasma to obtain a reference metabolic signature of hypothyroidism to study RTHα disease. Different anti-thyroid drugs and techniques (thyroidectomy), with their advantages and disadvantages, exist to control TH synthesis[128,151]. Propylthiouracil (PTU) is often used to induce hypothyroidism in mice and rats models to study this disease[128,152]. The inconvenience is that this treatment was associated with liver toxicity[151,153]. The prevalence of this toxicity is extremely low, but should be suspected in research studies. For this metabolomic study, we used PTU-induced hypothyroidism mice models to find biomarkers related to hypothyroidism. The metabolic signature of this condition reflects thus the metabolic changes caused by the hypothyroid condition, and probably the presence of a toxic effect of the PTU treatment. To distinguish between hypothyroid effects from PTU toxic effect, we used another group, treated with PTU followed by T3 treatment during 4 days. The goal is to assess the

reversibility of PTU-induced hypothyroidism. A quick reversibility could reflect a direct effect of TH and the absence of secondary effects of PTU. For this group, a longitudinal study was performed to characterize the kinetic of the metabolic changes. Here we will call this group of mice “TH treated” group.

4.2 Study design

In this study, 30 adult male mice divided in 3 different groups of 10 mice each one were used. The first group is a control group without any treatment. A hypothyroid phenotype was induced in mice by two weeks propylthiouracil (PTU) treatment containing diet[154]. PTU inhibits the enzyme thyroperoxidase, which has an action in thyroid hormone synthesis[155].

In the third group, mice were treated during 14 days with PTU, and underwent three injections of T3 the last 4 days. This group has an excess of thyroid hormones compared to control group (Figure 4.2.1). Urine was collected at different time points: at D_{11} and D_{14} for control and hypothyroid groups, and from D_{11} to D_{14} for TH treated group. Mice from hypothyroid group and TH treated group have the same status at D_{11}. D_{12}, D_{13} and D_{14} correspond to 1 day, 2 days and 3 days after the beginning of T3 injection in TH treated group. At D_{14}, urine was collected from the 3 groups, and mice were then anesthetized in order to collect blood. Mice were killed after this step because the blood volume taken is important and can be lethal. After blood collection, we proceeded to plasma preparation. Urine and plasma samples were then stored at -80°C until NMR analysis.

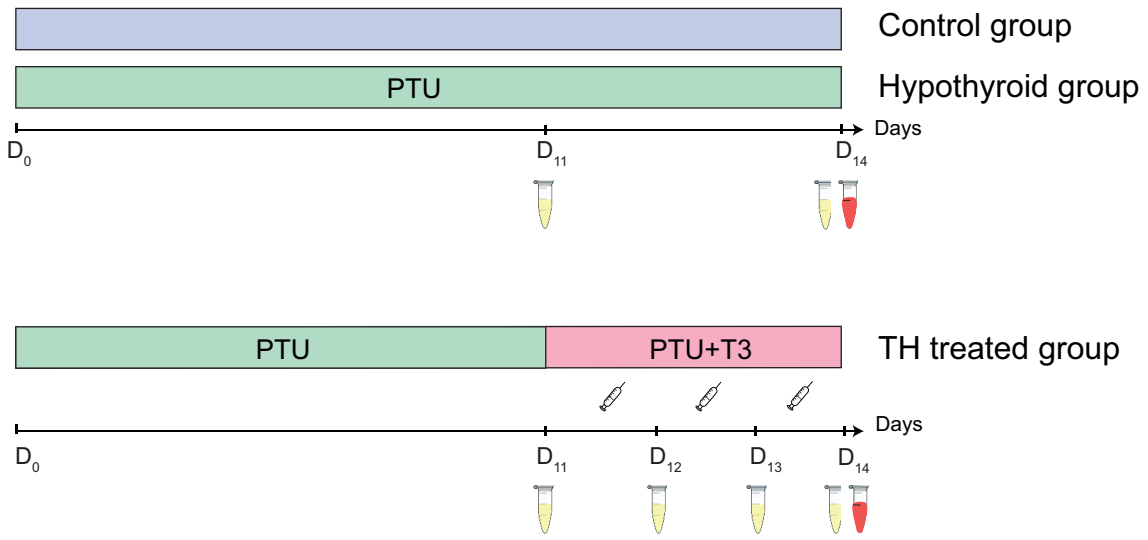

Figure 4.2.1: **Study design.**

Wild-type mice underwent 14 days of PTU treatment to obtain hypothyroid phenotype. For the control and the hypothyroid groups, urine was collected at D_{11} and D_{14}, and blood was collected at D_{14}. To study the response of hypothyroid group to TH, wild-type mice underwent 14 days of PTU

treatment, and three injections of T3 (at D_{11}, D_{12} and D_{13}). Urine was collected at D_{11} (before the first T3 injection), D_{12}, D_{13} and D14. Blood was collected at D_{14}.

Forty-five metabolites were identified in urine and 33 in blood plasma (Figure 4.2.2 and appendices 2 and 3).

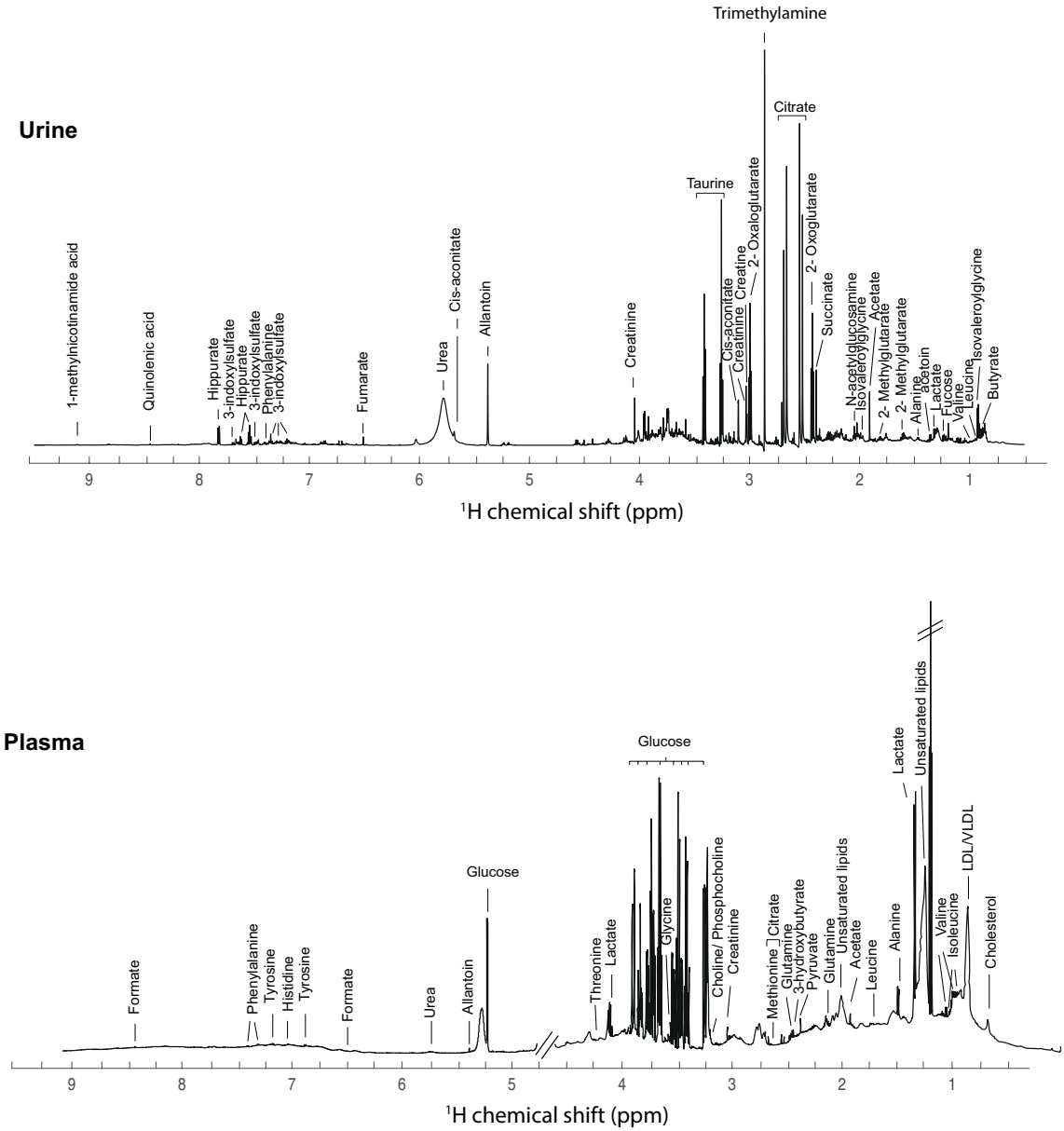

Figure 4.2.2: **Mean 600MHz ^{1}H NMR spectra from mice urine (A) and plasma (B), with metabolites annotations.**

4.3 Results

4.3.1 Quality of the ^{1}H NMR data

A principal component analysis (PCA) was performed for urine and plasma samples separately. The goal is to assess the quality and the reproducibility of the ^{1}H NMR data sets in on the hand, and clean the data sets by identifying and then removing outliers, on the other hand. We can also identify trends in this step.

Here, the good stability and reproducibility is proven by the clustering of the QC samples in both urine and plasma data sets (Figure 4.3.1). In urine PCA, 4 samples are identified as outliers (Figure 4.3.1.A). Three of them are issue from the same mice. These samples were removed from the data set. No outliers were identified in plasma PCA.
The two PCA show a clear separation between the different groups, which mean that they have a different chemical composition. It is so strong that we see it in this unsupervised statistical analysis.

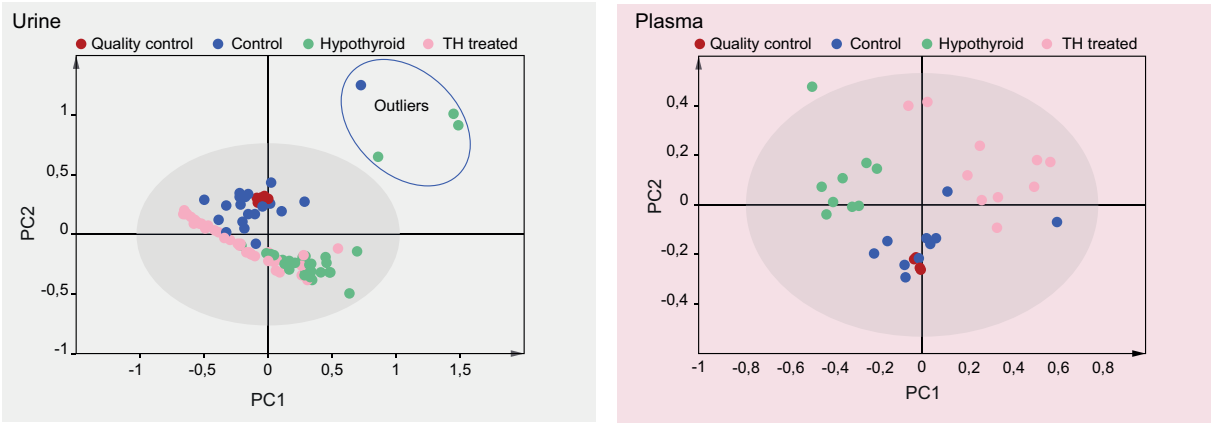

Figure 4.3.1: **Quality of the model and outliers identification in urine and plasma samples.**
(A) Principal component analysis (score plot) based on ^{1}H NMR spectra of QC samples and all urine samples from all times points. A= 12, N= 96, R^2X= 0.851 (B) PCA score plot based on ^{1}H NMR spectra of QC samples and all plasma samples from all time points. A= 9, N= 33, R^2X= 0.959. The QC samples clustering (in red) show the good stability and reproducibility of the experiments.

4.3.2 Discrimination according to mice phenotype in urine

Hypothyroid and TH treated groups had received the same PTU treatment at D_{11}. Thus, mice from these two groups are hypothyroid at this point. The principal component analysis of samples collected at D_{11} shows a clear discrimination between control group and hypothyroid group, which mean that they are chemically different (Figure 4.3.2.A). At D_{14}, after 3 injections of thyroid hormone T3 to TH treated group, which was usually hypothyroid, we see a separation between hypothyroid and TH treated groups (Figure 4.3.2.B). Samples were clearly separated into three distinct groups, indicating that the controls, TH treated group and hypothyroid group had different metabolic profiles.

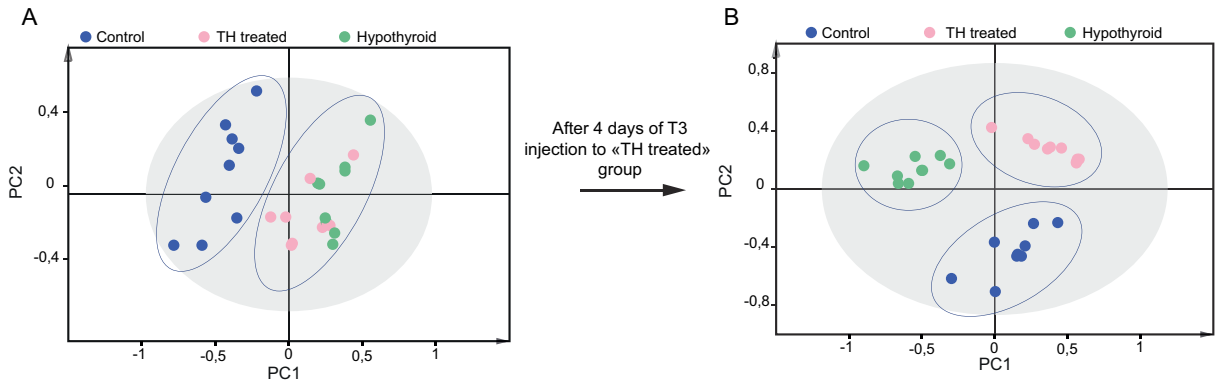

Figure 4.3.2: **Discrimination between control, hypothyroid and TH treated groups at D_{11} and D_{14} in urine.**

At D_{11}, hypothyroid and TH treated groups had received the same PTU treatment. (A) PCA score plot of urine samples at D_{11} shows a clear separation between control group and hypothyroid-TH treated group. A= 4, N= 27, R^2X= 0.68 (B) PCA score plot of urine samples at D_{14} shows a clear separation between control, hypothyroid and TH treated groups. A= 2, N= 28, R^2X= 0.68.

4.3.3 Determination of a metabolic signature associated with hypothyroidism

- Determination of a metabolic signature associated with hypothyroidism in urine

The PCA and the OPLS-DA analyses score plots (Figure 4.3.3.A and B) show a clear discrimination between hypothyroid and control populations. The metabolic signature associated with hypothyroidism (Figure 4.3.3.D) shows a decrease of alanine, lactate, acetate, malate, succinate, oxoglutarate, dimethylamine, trimethylamine, oxoglutarate; and an increase in formate, hippurate, indoxylsulfate, phenylalanine, allantoin, urea, cis-aconitate, trigonelline, creatinine, guanidoacetate, isovalerylglycine, dimethylamine, taurine, glutamine, acetoacetate and butyrate.

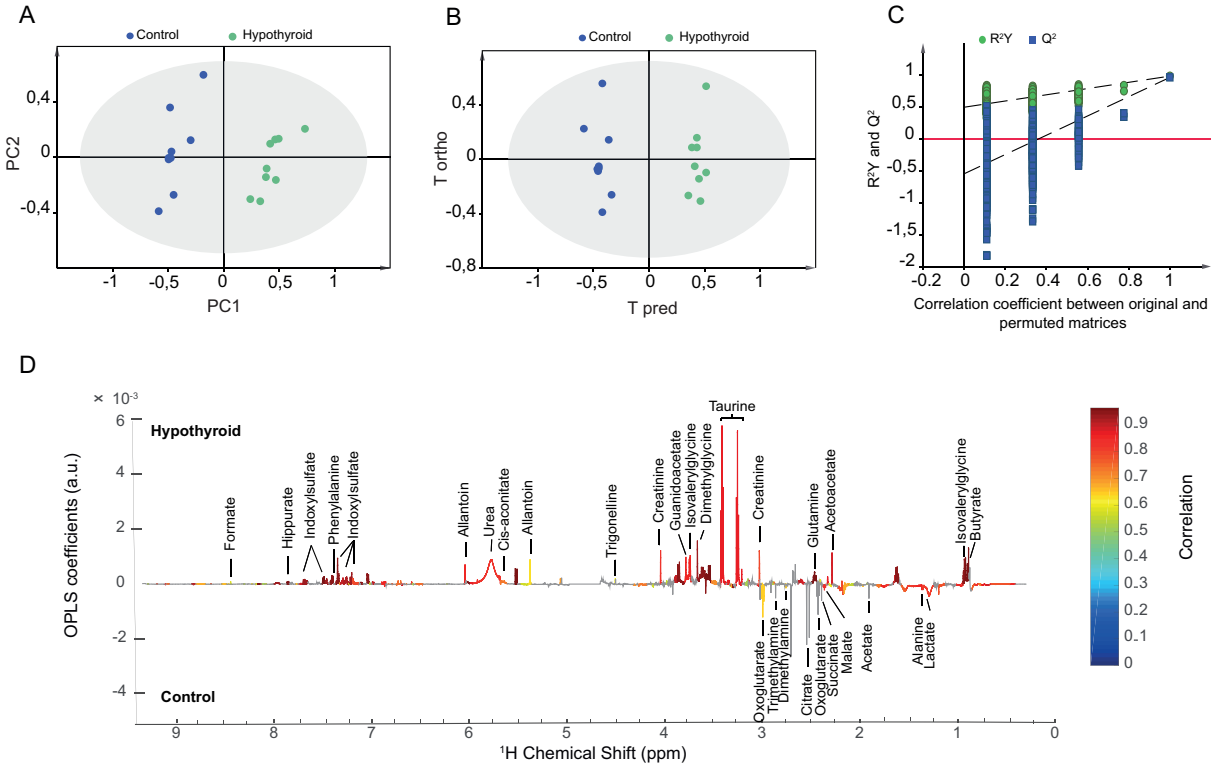

Figure 4.3.3: **Discrimination between hypothyroid phenotype and control groups in urine.**
(A) PCA score plot. A= 2, N= 18, R^2X= 0.65. (B) OPLS-DA score plot. A= 1+1, N= 18, R^2Y= 0.98, Q^2= 0.96, p-value=$4.76.10^{-9}$. (C) OPLS-DA model validation by resampling 1000 times under the null hypothesis. (D) OPLS-DA multivariate metabolic signature discriminating control group from hypothyroid phenotype group.

- Determination of a metabolic signature associated with hypothyroidism in plasma

The PCA and the OPLS-DA analyses score plots (Figure 4.3.4.A and B) show a clear discrimination between hypothyroid and control populations. The metabolic signature associated with hypothyroidism (Figure 4.3.4.D) shows an increase of lipids and a decrease in the high-density lipoprotein (HDL), some amino-acids (leucine, isoleucine, valine, alanine), sugars (glucose and mannose), hydroxybutyrate, citrate, lactate, acetoacetate, pyruvate, choline, phosphocholine, creatine and allantoin.

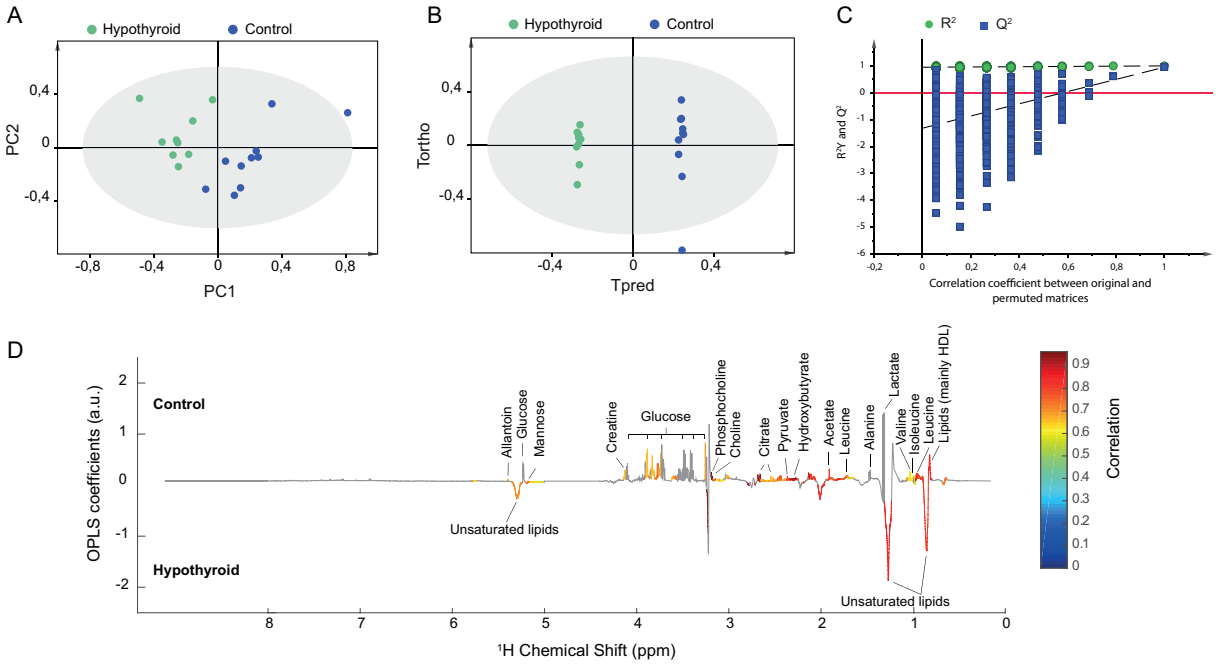

Figure 4.3.4: **Discrimination between hypothyroid phenotype and control groups in plasma.**
(A) PCA score plot. A= 5, N= 19, R^2X= 0.9. (B) OPLS-DA score plot. A= 1+7, N= 19, R^2Y= 0.99, Q^2= 0.56, p-value= 0.0015. (C) OPLS-DA model validation by resampling 1000 times under the null hypothesis. (D) OPLS-DA multivariate metabolic signature discriminating control group from hypothyroid phenotype group.

NMR investigation of urine and plasma allowed also distinguishing between hypothyroid and control groups. A metabolic signature associated with this disease was identified in each biofluid. Hypothyroidism is characterized by a hypo-metabolic state leading to reduced energy expenditure, increased cholesterol levels, reduced lipolysis and gluconeogenesis. This explains the increased level of lipids, and decreased levels of glucose.

It was reported that HDL levels are normal, elevated or in some cases decreased in hypothyroidism[156]. Here we notice a significant decrease of these lipoproteins in the plasma.

The high level of urinary creatinine in hypothyroid group could be explained by renal abnormalities that occur because of the deficiency of thyroid TH reduces the cardiac output leading to generalize hypo-dynamic state of the circulatory system. The vital substances of Krebs cycle like succinate, oxoglutarate and citrate decrease in hypothyroid mice compared to control mice. This can be explained by the reduced biogenesis and respiratory capacity in free mitochondria and neuronal oxygen consumption in the cerebral cortex in developing rats induced by hypothyroidism[157]. Our results are quite agreed with the results of previous studies about thyroid disorder[152,157]. Metabolites related to gut microbiota (hippurate and indoxylsulfate) are present in high concentrations compared to the control group, suggesting probably a modification in the intestine. Variation in the urinary concentration of phenylalanine suggests a perturbation in phenylalanine metabolism. Wu et al. found showed that some metabolites related to phenylalanine metabolism vary in hypothyroid rats.

4.3.4 Impact of thyroid hormones on the metabolism

Unsupervised and supervised multivariate analyses were performed in order to study the evolution of TH treated group over time. Supervised analysis OPLS-DA was applied to remove information unrelated to T3 treatment. A clear separation between samples at different time points is noticed in both PCA and OPLS-DA (Figure 4.3.5 A and B). The OPLS-DA model shows a strong discrimination of the 4 classes, reflected by the explained variance (R^2Y= 0.8), the prediction power (Q^2= 0.55), CV-ANOVA *p*-value (*p*-value= $1.5.10^{-5}$). In addition, the robustness of the OPLS-DA model was validated using permutations (1000) under the null hypothesis (Figure 4.3.5.C).

We noticed an important evolution of samples metabolome from D_{11} to D_{12}, and from D_{12} to D_{13}, compared to D_{13} to D_{14}, which reflect the rate of reaction of the metabolism in

response to TH over time (Figure 4.3.5 B). This suggests that changes related to TH administration are important in the beginning, and then the metabolome stagnates gradually.

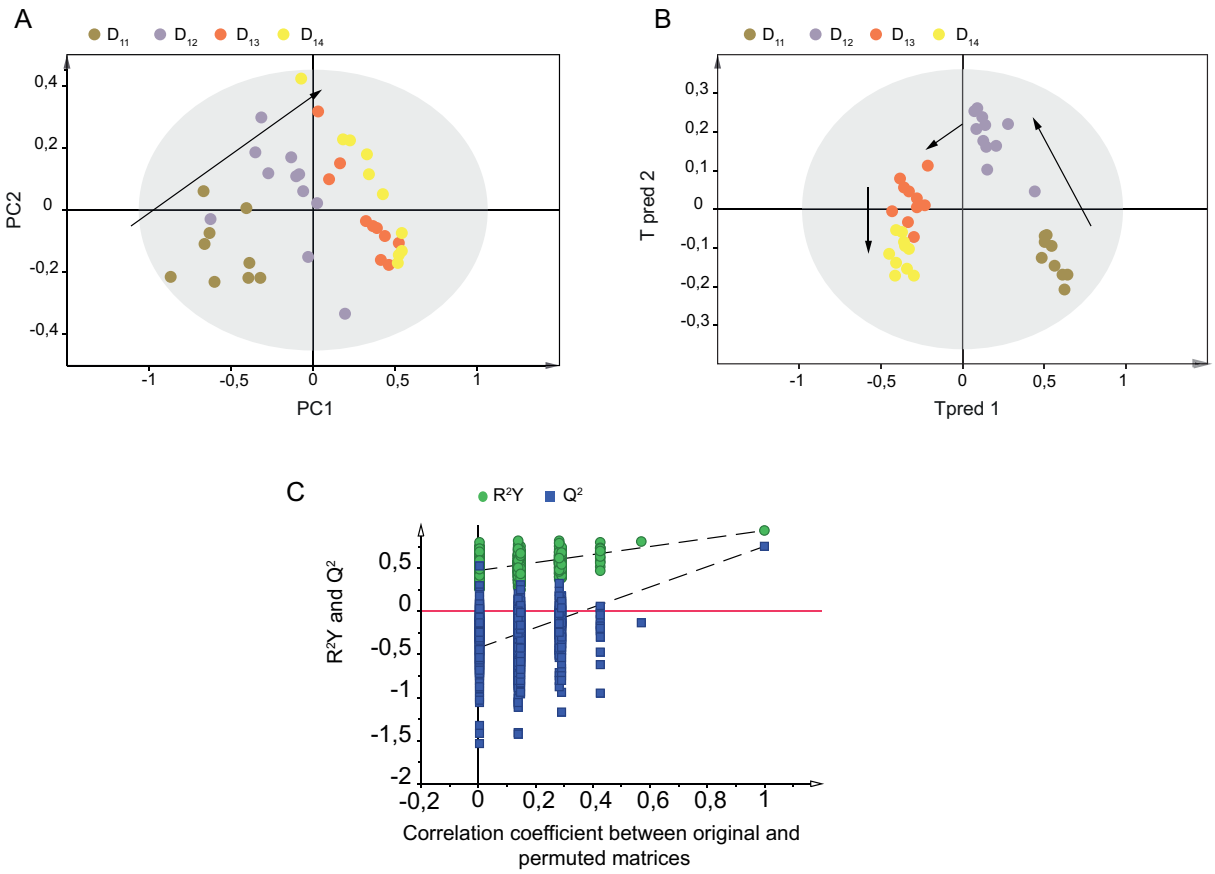

Figure 4.3.5: **Metabolomic urine profiles showing the evolution of hyperthyroid phenotype group over time.**

(A) PCA score plot. A= 5, N= 40, R2X= 0.74. (B) OPLS-DA score plot. A= 3+2, N= 40, R^2Y= 0.8, Q^2= 0.55, p-value= 1.5.10^{-5}. (C) OPLS-DA model validation by resampling 1000 times under the null hypothesis.

4.3.5 Determination of a metabolic signature associated with TH treatment

To understand the metabolic changes caused by TH treatment, unsupervised and supervised analyses were performed in data sets generated from urine and plasma NMR analysis.

- Determination of a metabolic signature associated with TH treatment in urine

Unsupervised and supervised analyses were done to identify variations in the urine dataset related to TH treatment. Both methods, PCA and OPLS-DA, show a clear separation between control and TH treated groups. A strong discrimination of the two classes is noticed, with R^2Y= 0.995, Q^2= 0.97, *p*-value=$1.9.10^{-8}$ (Figure 4.3.6.A and B). The model is well validated after resampling (Figure 4.3.6.C).

The metabolites with a key role on the OPLS model were evaluated by analyzing the loadings plots color-coded based on the correlation coefficients. The metabolic signature associated with TH response (Figure 4.3.6.D) shows a decrease of trimethylamine, creatine, taurine, isovalerylglycine and indoxylsulfate, and an increase of alanine, lactate, acetate, glutamine, succinate, oxoglutarate, dimethylamine, dimethylglycine, creatinine, guanidoacetate, and allantoin.

Here, we were able to distinguish between control and TH treated populations using ^{1}H NMR metabolomic profile for urine samples.

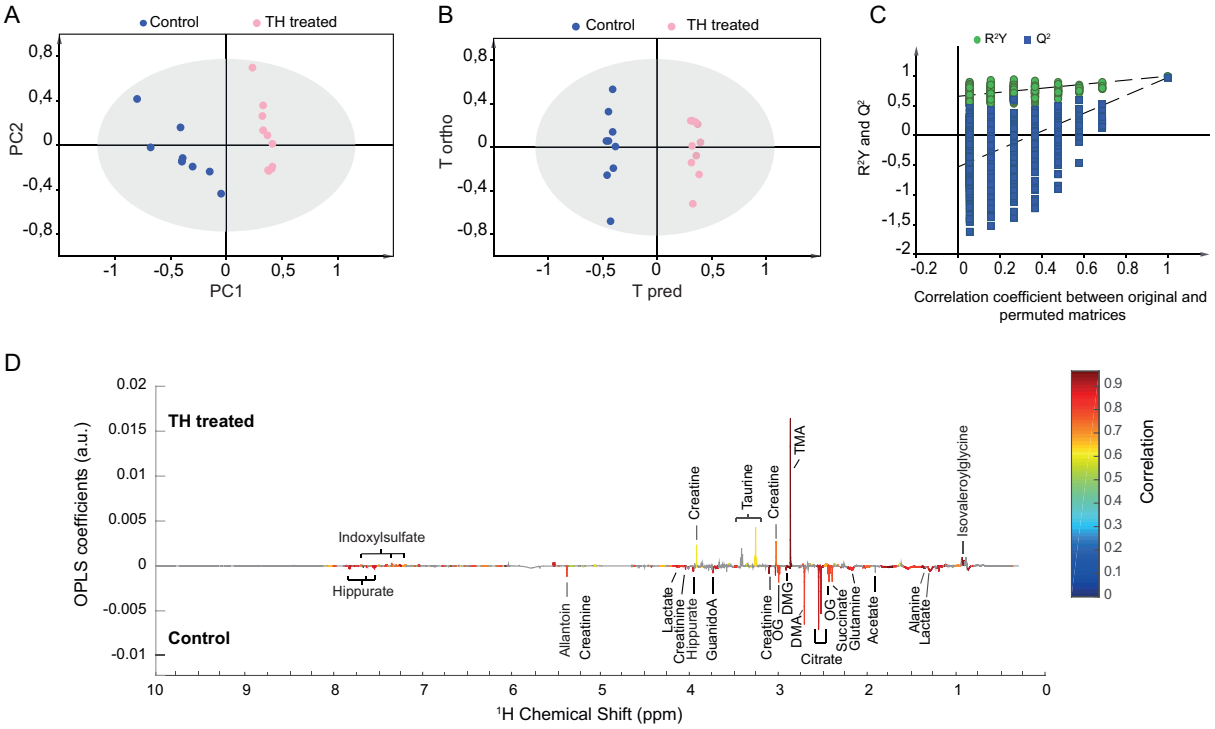

Figure 4.3.5: **Discrimination between control and TH treated groups in urine.**

(A) PCA score plot. A= 2, N= 19, R^2X= 0.72. (B) OPLS-DA score plot. A= 1+2, N= 19, R^2Y= 0.995, Q^2= 0.97, p-value= $1.9.10^{-8}$. (C) OPLS-DA model validation by resampling 1000 times under the null hypothesis. (D) OPLS-DA multivariate metabolic signature discriminating control group from TH treated group. The signature is colored according to the correlation between NMR variables and case-control status after significance to univariate ANOVA testing followed by Benjamini-Hochberg multiple corrections. NMR variables that do not achieve the FDR threshold of 0.05 are represented in grey. DMA (dimethylamine), DMG (dimethylglycine), OG (oxoglutarate), TMA (trimethylamine).

- Determination of a metabolic signature associated with TH treatment in plasma

The PCA unsupervised model and OPLS-DA supervised model show a good discrimination between control and TH treated groups in plasma (Figure 4.3.6.A and B). The explained variance is 0.88, the predictive power is 0.8, and the *p*-value is $8.7.10^{-5}$.The statistical model is also well validated (Figure 4.3.6.C). The metabolic signature related to TH treatment in plasma is represented with a relative increase in glucose, glutamine, lactate, succinate and alanine, and a decrease in lipids level. Among these metabolites, glutamine and lipids vary significantly (Figure 4.3.6.D).

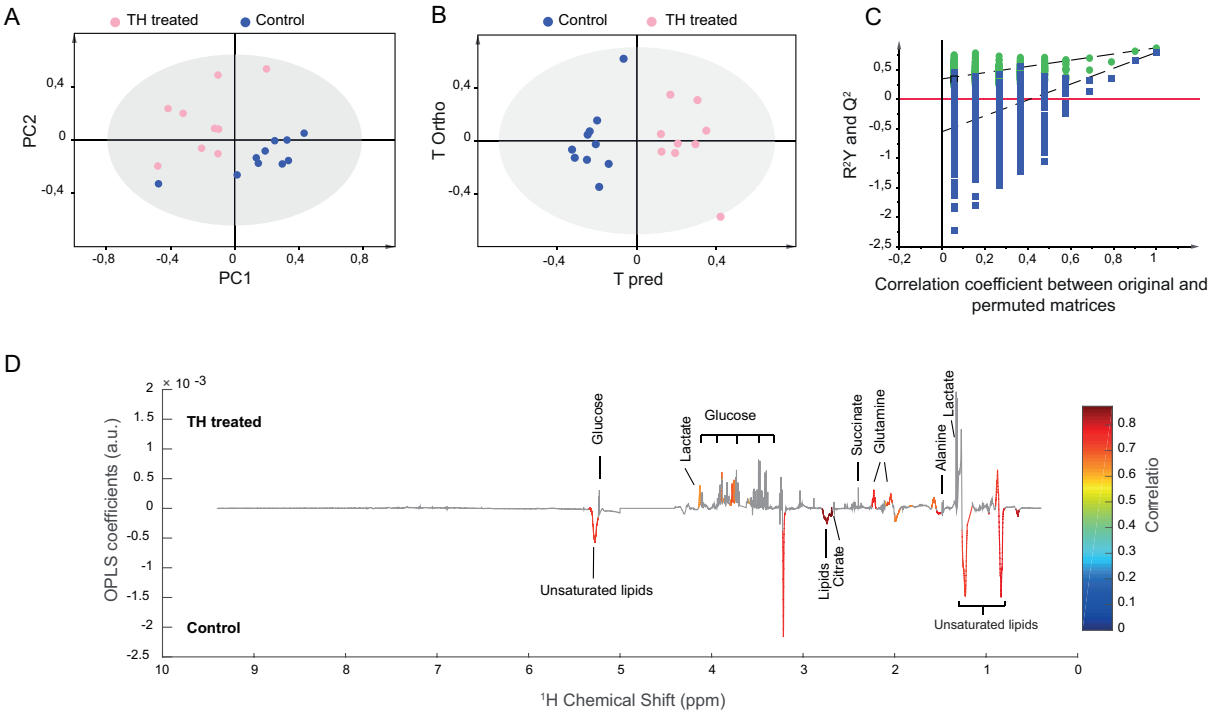

Figure 4.3.6: **Discrimination between TH treated and control groups in plasma.**

(A) PCA score plot. A= 9, N= 19, R^2X= 0.97. (B) OPLS-DA score plot. A= 1+1, N= 19, R^2Y= 0.88, Q^2= 0.8, p-value= $8.7.10^{-5}$. (C) OPLS-DA model validation by resampling 1000 times under the null hypothesis. (D) OPLS-DA multivariate metabolic signature discriminating control group from TH treated group.

NMR investigation of urine and plasma here allowed distinguishing between TH treated and control populations. A metabolic signature associated with TH response in the organism was identified in each biofluid. TH seems to modify rapidly the metabolism. This point was also noticed in a metabolomics study performed by Pietzner et al.[158]. The metabolic signature of TH treated mice is close to the hyperthyroidism-induced metabolic changes described in the literature. Alanine level increases in both urine and plasma of TH treated mice. It is known that hyperthyroidism is associated with elevated alanine amino-transferase, which increases serum alanine concentration, and this reflects a deregulation in liver metabolism[159]. The increased levels of glucose and decreased level of lipids in TH treated mice blood reflect a hyper-metabolic state. Hyperthyroidism is characterized by increased resting energy expenditure, reduced cholesterol levels, increased lipolysis and gluconeogenesis[160,161]. Indoxylsulfate and hippurate, which are produced from the tryptophan, depend on the gut microbiota activity[162]. Their variation reflects a perturbation in the

tryptophan metabolism, which is probably related to a modification in the intestine. A relation between these metabolites and the TH status was already reported in a mass spectrometry-based metabolomics study[152].

The metabolic signature related to TH treatment is different from that related to PTU-induced hypothyroidism, which suggests that TH reversed quickly the impact of PTU on the metabolism.

4.4 Conclusion

The present study, using a ^{1}H NMR-based approach, shows that the metabolomics profile is deeply influenced by the TH levels. The three different groups (euthyroid, hypothyroid and "TH treated") present different metabolic profiles. A global urine and blood metabolomic analysis based on ^{1}H NMR was applied to provide comprehensive and complementary insights into hypothyroidism and the impact of TH at the metabolic level. Specific metabolic signatures were identified for each condition in each biofluid.

Determination of TSH and free thyroxine (FT4) levels represent the gold standard in evaluation of thyroid function. Despite the huge amount of publications studying the action of thyroid hormones on metabolism, so far only the tip of the iceberg have been discovered, with an unexplored "metabolic world" under the surface. The need to a new method for the discovery of new markers of thyroid function and to detect novel pathways of thyroid hormone action is important. Through this study, we showed that NMR-based metabolomics could be an important tool to investigate hypothyroidism, and eventually hyperthyroidism.

The hypothyroid signature described in this chapter in urine and plasma is further exploited in the chapter 5 to evaluate the specificity of metabolic markers for the emerging genetic disease resistance to thyroid hormone α (RTHα).

5. NMR as a putative diagnostic tool for the presence of thyroid hormone receptor alpha 1 mutations

5.1 Introduction

Resistance to thyroid hormone (RTHα) is an emerging genetic disease due to mutations in the *THRA* gene, which encodes thyroid hormone receptor alpha (TRα1). Since its first description in 2012, 45 cases of RTHα have been reported worldwide, corresponding to 25 different mutations of TRα1[100,105,109,110,112,163]. The high variability of clinical features and the absence of reliable biochemical markers make the diagnosis of this disease difficult. In addition, identified RTHα patients present some common features with hypothyroid patients, which may delay the diagnosis in some cases[108]. Some of these mutations have been recently modelled in mice. In our study, we used five germline mutations (four frameshift and the N359Y missense mutation) in the mouse Thra gene, closely modelling the mutations found in RTHα patients[117]. Two of the four frameshift mutations are very close to human mutations, while the two others do not exist in human patients. N359Y missense mutation used here was found in a French patient, with very different symptoms compared to RTHα patients. This patient suffers from extreme skeletal malformations, macrocytic anaemia, chronic diarrhea, and hypercalcemia[110].

We characterized the metabolic phenotypes of urine and plasma samples collected from the five animal models using an untargeted Nuclear Magnetic Resonance (NMR)-based metabolomics approach. Multivariate statistical analysis of the metabolomic profiles shows that biofluids of mouse models that carry human-like mutations can be discriminated from controls. Metabolic signatures associated with *Thra* mutations in urine and plasma are stable over time and clearly differ from the metabolic fingerprint of hypothyroidism in the mouse.

Our results provide a proof-of-principle that easily accessible NMR metabolic fingerprints of biofluids could be used to diagnose RTHα in humans. This chapter describes in details results that were submitted recently for publication[164].

.

.

5.2 Study design

The research project was approved by a local ethic committee and subsequently authorized by the French Ministry of Research (licence #6711), and carried out in accordance with the European Community Council Directives of September 22, 2010 (2010/63/EU) regarding the protection of animals. Mice with *Thra* were all with a major contribution of the C57Bl/6 genetic background. We studied 5 mutations of *Thra*, which introduce a translation frameshift, eliminating the C-terminal helix, which normally interacts with transcription coactivators. E395fs401X and E395fs406X mutations are +1 frameshifts, introducing stop codons few nucleotides downstream to the mutated codon, and shortening the protein ($Thra^{S1/+}$ and $Thra^{S2/+}$ mice; S for small) as in some severe cases of RTHα found in patients. This results in a complete loss of transactivation capacity and a marked dominant-negative activity in heterozygous mice, leading to altered development. The two other mutations, E395fs485X and K389fs479X are +2 frameshifts, which have no known equivalent in human patients, and result in the production of an amphigoric protein of high molecular weight ($Thra^{L1/+}$ and $Thra^{L2/+}$ mice; L for large) which has little dominant-negative activity. Regarding N359Y mutation, there is no frameshift in this model. Therefore, apart from the N359Y amino acid substitution, the C- terminal part of TRα1, including helix 12, is intact. The N359Y amino acid substitution reduces the affinity of TRα1 for T3, but does not alter the interface required for coactivator or corepressor recruitment (Figure 5.2.1).

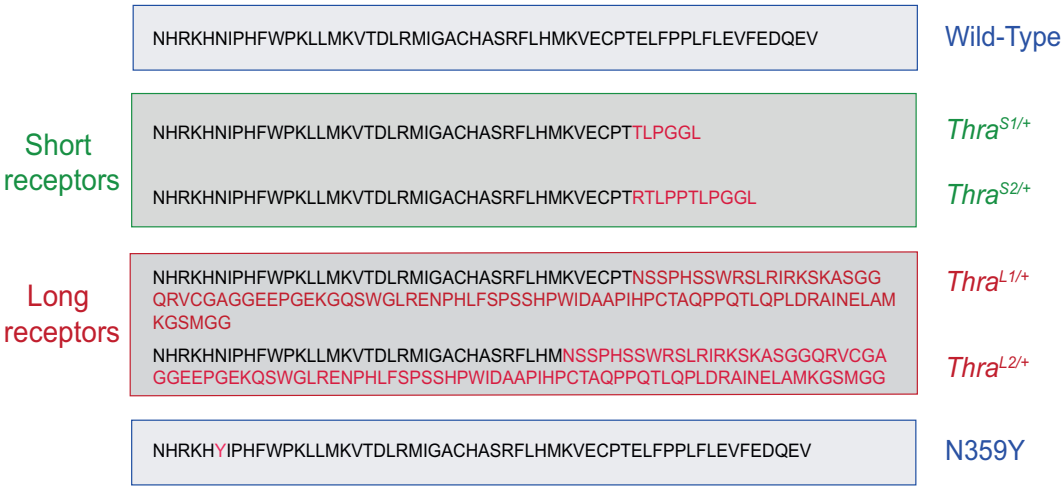

Figure 5.2.1: **Mice models**

Four mice models for RTHα were generated in order to understand their impact on the metabolism. Thra^{S1} and Thra^{S2} mutations are short receptors and are closed to mutations found in human patients, and Thra^{L1} and Thra^{L2} are long receptors and are different from those found in human patients.

95 mice (12 *Thra$^{S1/+}$, 10 Thra$^{2/+}$, 10 Thra$^{L1/+}$, 12 Thra$^{L2/+}$*, 7 N359Y and 44 wild-type*)* were followed during 6 months for this study. Littermates without mutation were used as controls. Urine and plasma samples were collected at two time points: urine samples were collected at 3 and 6 months of age in order to study the RTHα fingerprint stability over time, and plasma samples were collected in anti-coagulant tubes at 6 months (Figure 5.2.2).

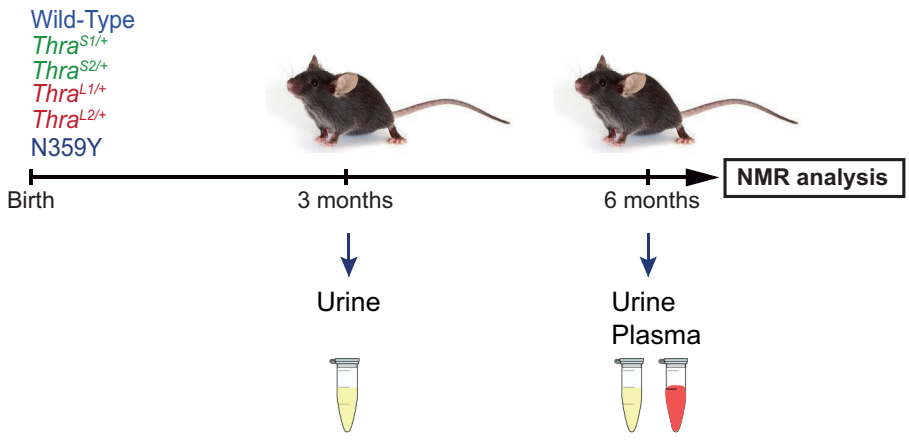

Figure 5.2.2**: Study design.**

Mutants and wild-type mice were followed during 6 months. Urine samples were collected from different mice groups at 3 and 6 months old and blood at 6 months old. NMR analysis was performed for all urine and blood plasma samples.

The steps of metabolomic analyses and multivariate statistical analysis were described in the chapter 3.

5.3 Results

5.3.1 Quality of the ^{1}H NMR data

A principal component analysis (PCA) was performed for each set of samples, urine and blood plasma, to assess the reproducibility of the ^{1}H NMR data sets. Here, the good stability and reproducibility is proven by the clustering of the QC samples in each models (Figure 5.3.1).

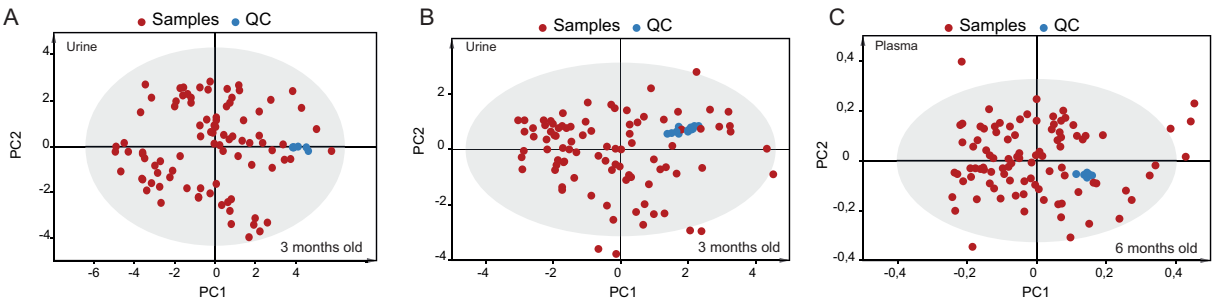

Figure 5.3.1: **PCA based on ^{1}H NMR spectra of QC and samples (urine or plasma)**.
The good stability of the NMR setup and reproducibility of the experiment is attested by the grouped set of QC samples on the PCA score plots. (A) PCA based on urine samples of 3 months old mice (A= 9, N= 95, R^2= 0,792). (B) PCA based on urine samples of 6 months old mice (A= 13, N= 101, R^2= 0,811). (C) PCA based on plasma samples of 6 months old mice (A= 29, N= 102, R^2= 0,985).

5.3.2 Discrimination between the group of mutants and wild-type group

We considered the different groups of mice models as a single group, with the hypothesis that these mutations have the same impact on the metabolome. A PCA and an OPLS-DA of the metabolic profiles were performed to compare mutants mice group to wild-type group, in both urine and blood plasma. No discrimination between the two groups was noticed in both biofluids (Figure 5.3.2).

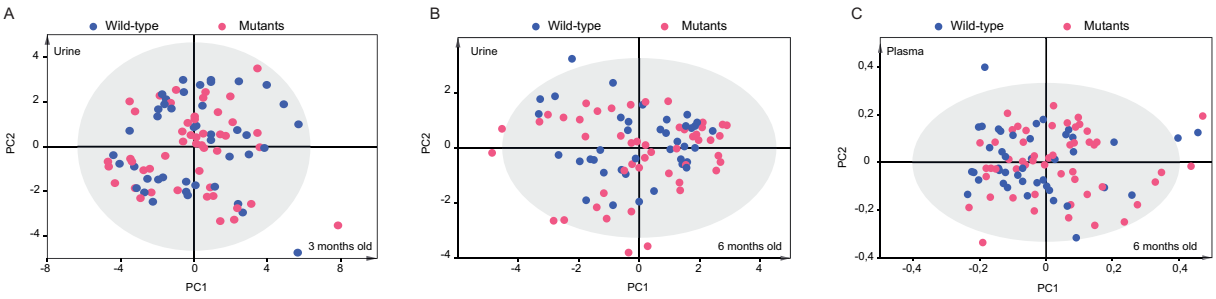

Figure 5.3.2: **Discrimination between wild-type and mutants groups.**
(A) PCA score plot for 3 months old mice urine (A= 14, N= 91, R^2= 0.86). (B) PCA score plot for 6 months old mice urine (A= 15, N= 88, R^2= 0.84). (C) PCA score plot for 6 months old mice plasma (A= 18, N= 95, R^2= 0.97).

5.3.3 Discrimination between each mutant group and wild-type group

We then asked whether each mutant group could be discriminated from wild-type group. The goal was to understand the specific impact of each mutation on the metabolism. We performed an OPLS-DA for each comparison (mutant vs. wild-type), in urine (at different ages) and plasma. As described in Tables 5.1 and table 5.2, in urine, only *Thra*$^{S1/+}$ group can be discriminated from wild-type group. We notice also here that there is a conservation of the metabotype overtime, because we obtain the same results at 3 and 6 months old.

Statistical models	Discrimination	A	N	R^2	Q^2	*p*-value
Thra$^{S1/+}$ vs. WT	Yes	1+2	52	0.695	0.347	0.003
Thra$^{S2/+}$ vs. WT	No	0	51	-	-	-
Thra$^{L1/+}$ vs. WT	No	0	50	-	-	-
Thra$^{L2/+}$ vs. WT	No	1+1	52	0.425	0.134	0.14
N359Y vs. WT	No	0	48	-	-	-

Table 5.1: **Discrimination between each mutant group and wild-type group in 3-month-old mice urine.**

Statistical models	Discrimination	A	N	R^2	Q^2	*p*-value
Thra$^{S1/+}$ vs. WT	Yes	1+2	51	0.697	0.368	0.0018
Thra$^{S2/+}$ vs. WT	No	0	51	-	-	-
Thra$^{L1/+}$ vs. WT	No	0	50	-	-	-
Thra$^{L2/+}$ vs. WT	No	0	52	-	-	-
N359Y vs. WT	No	0	48	-	-	-

Table 5.2: **Discrimination between each mutant group and wild-type group in 6-month-old mice urine.**

In plasma, both *Thra*$^{S1/+}$ and *Thra*$^{S2/+}$groups can be discriminated from wild-type group (Table 5.3). We notice also that the discrimination is slightly better in the blood plasma, and here an additional group can be discriminated from wild-type group.

Statistical models	A	N	R^2	Q^2	*p*-value
Thra$^{S1/+}$ vs. WT	1+6	55	0.832	0.422	0.034
Thra$^{S2/+}$ vs. WT	1+4	54	0.745	0.44	0.002
Thra$^{L1/+}$ vs. WT	0	53	-	-	-
Thra$^{L2/+}$ vs. WT	0	54	-	-	-
N359Y vs. WT	0	51	-	-	-

Table 3.4: **Discrimination between each mutant group and wild-type group in 6-month-old mice plasma.**

These results suggest that we cannot consider the set of mutants group as a homogenous group, theses mutations do not impact the metabolism with the same manner. *Thra*$^{S1/+}$ and probably *Thra*$^{S2/+}$ have a bigger effect than the other mutations. Our results are in line with the findings of Markossian et al[117]. They noticed that *Thra*$^{S1/+}$ and *Thra*$^{S2/+}$ display very similar phenotypes, reproducing several developmental traits present in RTHα patients, while *Thra*$^{L1/+}$ and *Thra*$^{L2/+}$ mice have an almost normal phenotype[117]. Discrimination between N359Y group and wild-type group were not possible. It was reported that the patient carrying this mutation has also other mutations in her genome (Appendix 1), and the biological study done by Markossian et al[117] show that N359Y mice do not have the same features that the N359Y patient. We decided to focus only on the four frameshift mutations for the next sections.

5.3.4 Metabolomic analysis segregates two types of frameshift mutations

We addressed whether metabolic profiling could differentiate *Thra*$^{S1/+}$, *Thra*$^{S2/+}$, *Thra*$^{L1/+}$ and *Thra*$^{L2/+}$ mice. A four-classes orthogonal partial least square discriminant analysis (OPLS-DA) of the metabolic profiles was performed to evaluate the impact of the different *Thra* mutations on urine metabolome. Although the 4 groups were not separated, we noted that mutants with short receptors (*Thra*$^{S1/+}$ and *Thra*$^{S2/+}$) were clustered in this statistical model as are mutants with long receptors (*Thra*$^{L1/+}$ and *Thra*$^{L2/+}$), and that the two groups tend to separate (Figure 5.3.3). Within each group, a new OPLS-DA analysis was unable to discriminate between the two mutations (*Thra*$^{L1/+}$ from *Thra*$^{L2/+}$ mice, and *Thra*$^{S1/+}$ from *Thra*$^{S2/+}$ mice, in both urine and plasma; data not shown).

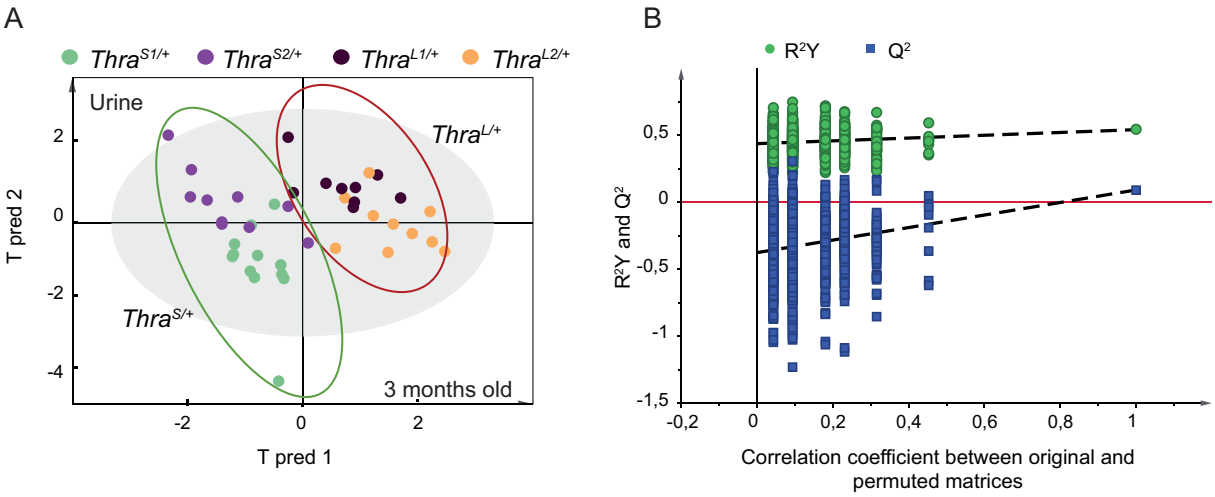

Figure 5.3.3: **Discrimination between *Thra*$^{S1/+}$, *Thra*$^{S2/+}$, *Thra*$^{L1/+}$ and *Thra*$^{L2/+}$.**
(A) OPLS-DA score plot for 3 months old mice urine, discriminating Thra$^{S1/+}$*, Thra*$^{S2/+}$*, Thra*$^{L1/+}$ *and Thra*$^{L2/+}$ *(N = 40, 3+2 components, R^2Y = 0.661, Q^2 = 0.355, ANOVA of the cross-validated residuals (CV-ANOVA) p-value = 0.005). (B) The OPLS-DA model validation by resampling 1000 times under the null hypothesis.*

As no clear discrimination was observed, we pooled the mutant mice according to the type of frameshift mutation that they carry (*Thra*$^{L/+}$ group and *Thra*$^{S/+}$ group), and repeated OPLS-DA analysis. This improved the statistical power of the analysis and led to a clear distinction between these two groups. Statistical significance of these models was assessed by high values of goodness-of-fit parameters R^2 and Q^2 (which explain the variance and predictive power of the model, respectively) and CV-ANOVA *p*-values < 0.05 and model resampling under the null hypothesis. Altogether, these results show a clear distinction between *Thra*$^{L/+}$ and *Thra*$^{S/+}$ mice, as expected from previous phenotyping.

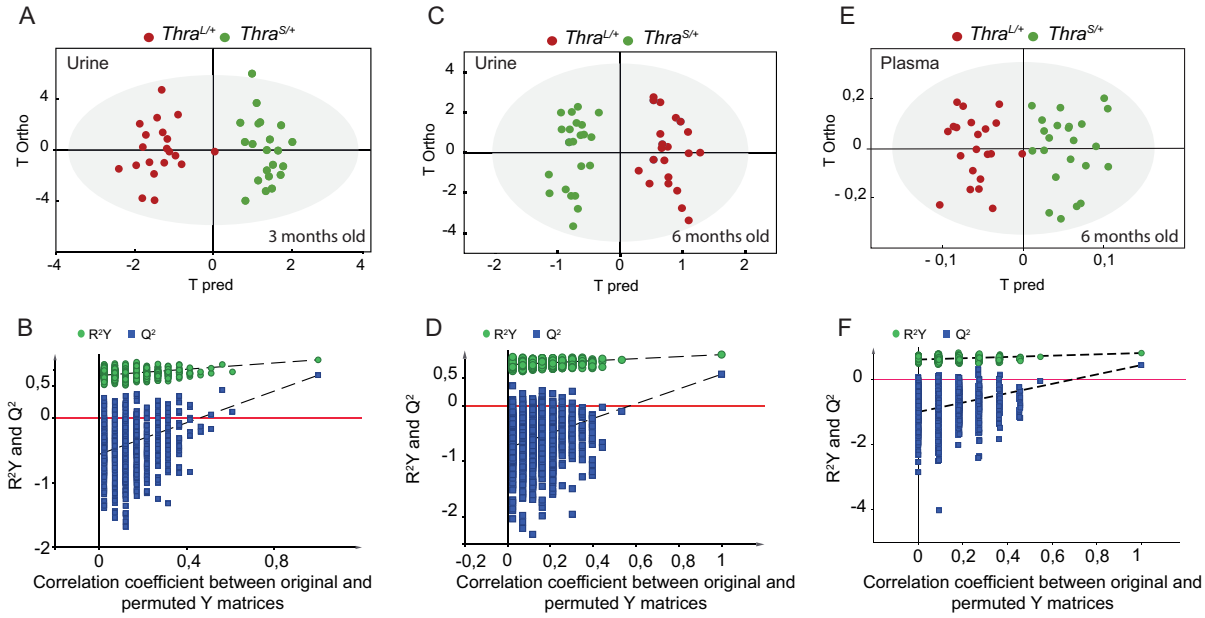

Figure 5.3.4: **Discrimination between the two type of frameshift mutations: *Thra*$^{S/+}$ and *Thra*$^{L/+}$.** *(A) OPLS-DA model for 3 months old mice urine (N = 41, 1+3 components, R^2Y = 0.908, Q^2 = 0.669, CV-ANOVA p-value = 6.6.10^{-6}). (B) Corresponding OPLS-DA model validation by resampling 1000 times under the null hypothesis. (C) OPLS-DA model for 6 months old mice urine (N = 43, 1+4 components, R^2Y = 0.924, Q^2 = 0.57, CV-ANOVA p-value = 8.10^{-5}). (D) Corresponding OPLS-DA model validation by resampling 1000 times under the null hypothesis. (E) OPLS-DA model for 6 months old mice blood plasma (N = 44, 1+5 components, R^2Y = 0.829, Q^2 = 0.458, CV-ANOVA p-value = 0.04). (F) Corresponding OPLS-DA model validation by resampling 1000 times under the null hypothesis.*

5.3.5 Discrimination between Thra$^{S/+}$ mice with human-like mutations and wild-type mice

We then asked whether the group of *Thra*$^{S/+}$ mice, which carry mutations relevant to human cases, could be recognized from a group of wild-type littermates. We performed three comparisons, using either urine (3 or 6 months) or plasma. OPLS-DA of the metabolic profiles was performed to drive robust statistical models based on the discrimination between *Thra*$^{S/+}$ and wild-type mice. We observed a significant discrimination between *Thra*$^{S/+}$ samples and their associated wild-type controls in all three comparisons (Figure 5.3.5). By

contrast similar comparisons were unable to discriminate the group of *Thra*$^{L/+}$ mice from the wild-type group, as expected from the very limited consequences of these mutations on phenotype (data not shown).

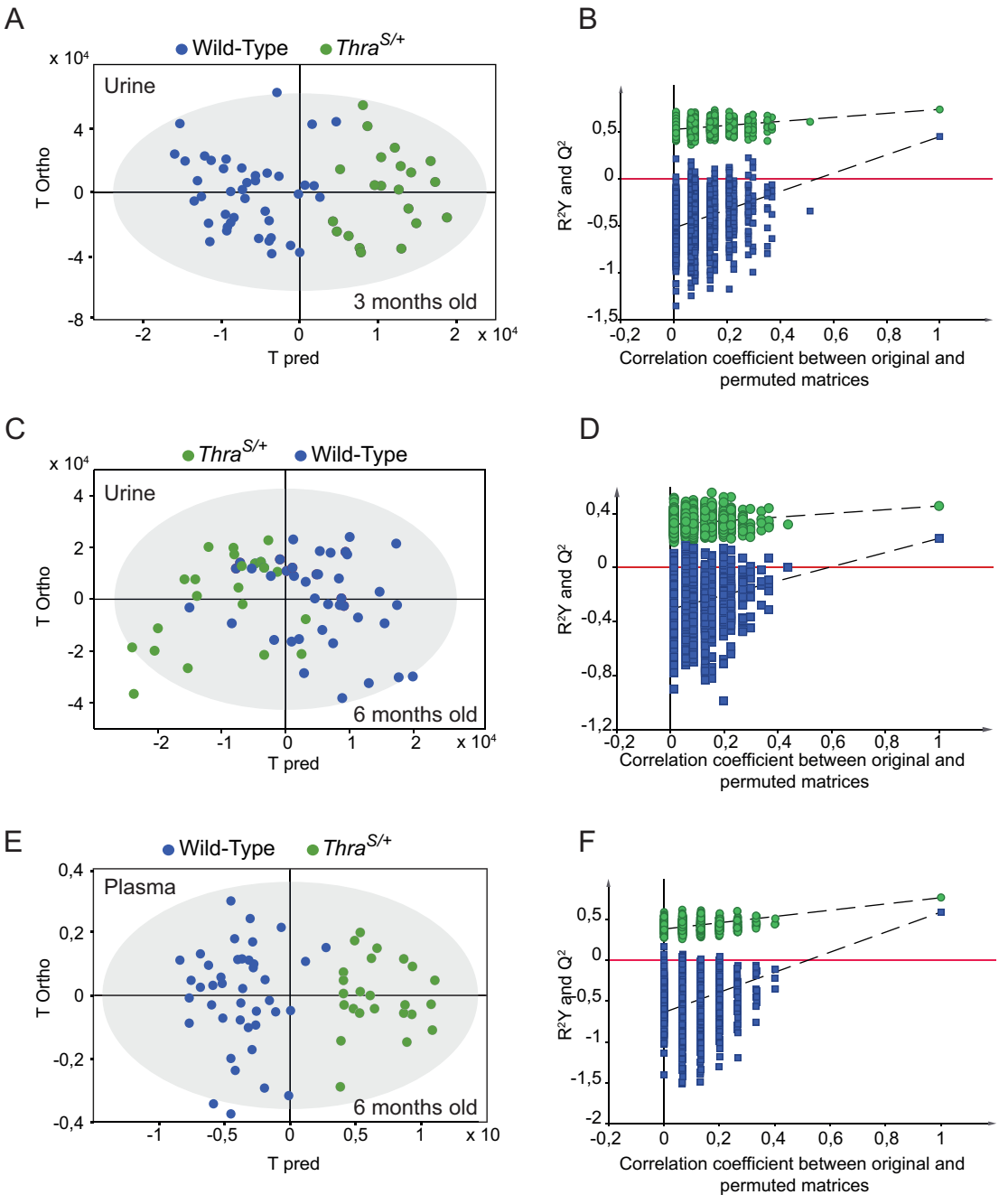

Figure 5.3.5: **Significant discrimination between human-like mutations *Thra*$^{S/+}$ and wild-type groups.**

(A) OPLS-DA model for 3 months old mice urine, discriminating Thra$^{S/+}$ *and wild-type (N = 62, 1+3 components, R^2Y = 0.744, Q^2 = 0.453, CV-ANOVA p-value = 4.5.10^{-5}). (B) The OPLS-DA model validation by resampling 1000 times under the null hypothesis. (C) OPLS-DA model for 6 months old*

mice urine, discriminating Thra$^{S/+}$ and wild-type (N = 62, 1+1 components, R^2Y = 0.457, Q^2 = 0.217, CV-ANOVA p-value = 7.10^{-3}). (D) Corresponding OPLS-DA model validation by resampling 1000 times under the null hypothesis. (E) OPLS-DA model for 6 months old mice plasma, discriminating Thra$^{S/+}$ and wild-type (N = 66, 1+4 components, R^2Y = 0.768, Q^2 = 0.591, CV-ANOVA p-value = 9.24.10^{-8}). (F) Corresponding OPLS-DA model validation by resampling 1000 times under the null hypothesis.

5.3.6 Determination of metabolic signature of Thra mutation in urine and blood plasma

The most significant variations of individual metabolites discriminating the *Thra*$^{S/+}$ group from wild-type were identified with univariate analysis of spectral variables from urine and plasma NMR profiles. Urine metabolic signatures of *Thra*$^{S/+}$ mice were characterized by increased levels of hippurate, formate, fumarate, and decreased levels of Krebs cycle metabolites (acetate, succinate, citrate and cis-aconitate), urea, allantoin, creatine, creatinine, isovalerylglycine, trimethylamine, dimethylamine, taurine and oxoglutarate with respect to wild-type animals (Figure 5.3.6 A-B). Meanwhile, plasma metabolic signature was characterized by higher levels of formate, phenylalanine, valine, isoleucine, allantoin and lactate, and lower levels of Krebs cycle metabolites (acetate, succinate, ketobutyrate), lipids, lipoproteins (VLDL, LDL), phosphocholine, glucose, creatine, threonine, glutamine and pyruvate when compared to wild-type mice (Figure 5.3.6 C). The metabolic signatures of *Thra*$^{S/+}$ obtained from urine and plasma metabolic profiles share similarities in the composition and variations of 4 metabolites: formate, creatinine, acetate and citrate.

Concentrations of dimethylamine, trimethylamine, isovalerylglycine, choline and N-acetylglucosamine were shown to be significantly lower in urine of *Thra*$^{S/+}$ mice, while polyunsaturated lipids were lower in the blood. Overall, this study provides metabolic signatures associated with RTHα in urine and plasma that present common and complementary information.

Comparison between the metabolic signatures of urine of 3 and 6 months old mice provides useful information on the temporal stability of the observed metabolic changes. Overall, a large similarity in metabolites composition and variations was observed, 13

metabolites varying in the same way at both ages (Figure 5.3.6). Few differences were noticed, notably for formate and fumarate, which differential concentration only appear in 6 months old mice. Variation in oxoglutarate content was also amplified in 6 months old mice. Dimethylamine, trimethylamine and choline remained present in both signatures but became statistically significant, in univariate analysis, only after 6 months. This shows that the urine metabolic signature associated with RTHα is globally stable over time, while variations become more visible with age for some metabolites.

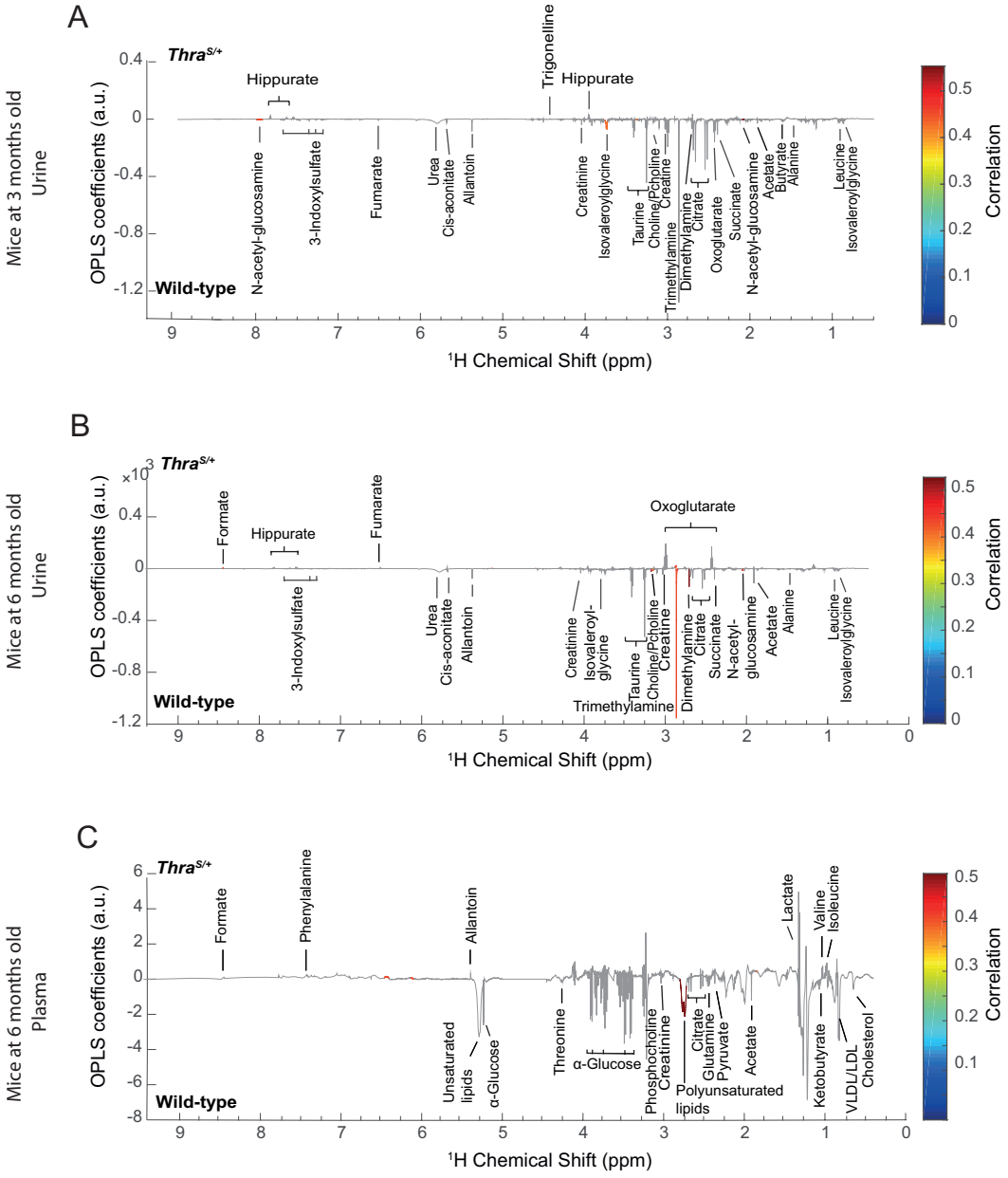

Figure 5.3.6: **Determination of a metabolic signature of *Thra*$^{S/+}$ mutation in urine and blood plasma.**

(A) OPLS-DA loading plot for 3 months old mice urine, discriminating Thra$^{S/+}$ and wild-type, after significance to ANOVA tests followed by Benjamini-Hochberg multiple correction. The coloured spectral regions correspond to the statistically significant signals. Non-significant NMR variables are colored in grey. (B) OPLS-DA loading plot for 6 months old mice urine, discriminating Thra$^{S/+}$ and wild-type. (C) OPLS-DA loading plot for 6 months old mice plasma, discriminating Thra$^{S/+}$ and wild-type.

5.3.7 RTHα signature is different from hypothyroidism signature

RTHα patients share symptoms with hypothyroid patients. We thus investigated whether the metabolic signatures found for *Thra* mutations can be distinguished from a signature of hypothyroidism. We compared thus these results with the results detailed in the chapter 2, where wild-type mice were made hypothyroid with propyl-thio-uracyl treatment, and ^{1}H-NMR analysis was performed to obtain a signature related to hypothyroidism in urine and plasma. We noticed that there is a strong discrimination was observed between hypothyroid and control groups. We noticed also that 24 and 17 metabolites vary in hypothyroid condition with respect to the non-treated group.

When the *Thra*$^{S/+}$ and hypothyroidism metabolic signatures were compared, clear differences were obvious. Only 6 common metabolites variations were found in urine: increased level of hippurate, and decreased levels of acetate, citrate, succinate, dimethylamine and trimethylamine (Figure 5.3.7 A). In plasma, only 7 metabolites were shared between RTHα and hypothyroidism metabolic signatures. Both were characterized by a decrease in low density lipoprotein (LDL), very low density lipoprotein (VLDL), acetate, citrate, pyruvate, choline, phosphocholine and glucose (Figure 5.3.7 B).

These results show that RTHα and hypothyroidism metabolic signatures present few similarities. The metabolic profiles recorded in urine and plasma could therefore potentially contribute to the specific diagnosis of RTHα, which is a rare disease, much less frequent than hypothyroidism.

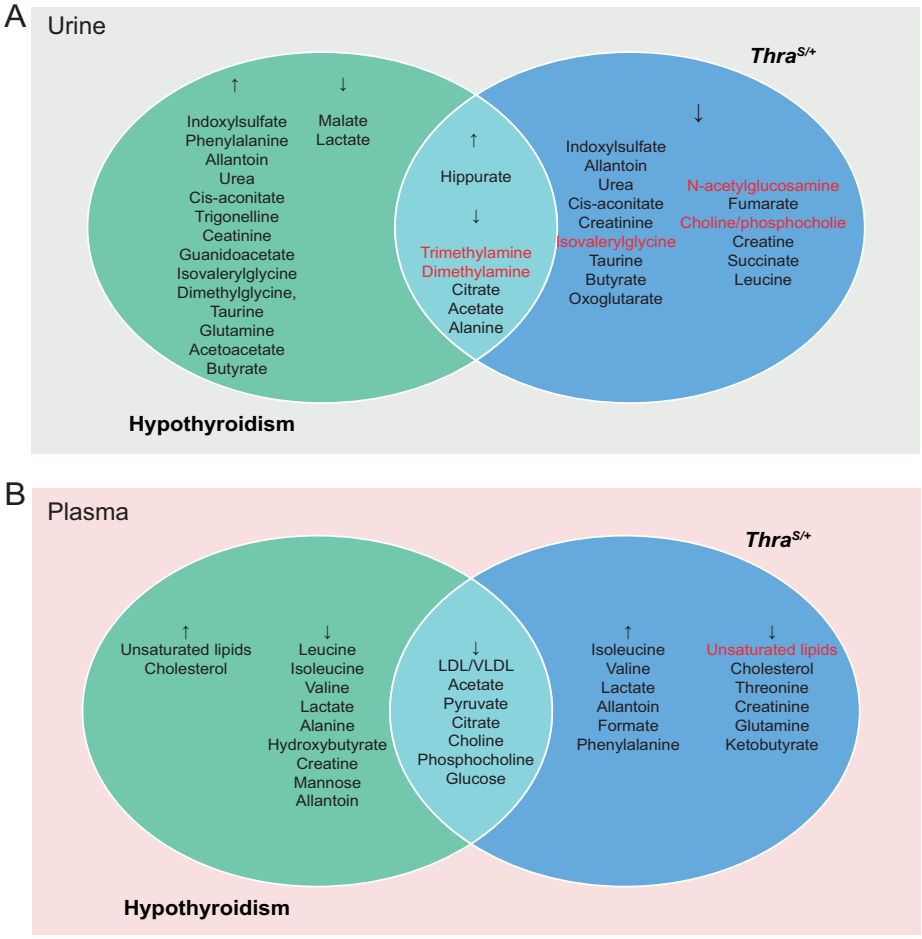

Figure 5.3.7: **Summary of key metabolites associated with *Thra*$^{S/+}$ and hypothyroid phenotypes.**
↑ : present in higher level compared to control group. ↓: lower ever compared to control group. Metabolites in red vary significantly in Thra$^{S/+}$ *condition.*

5.4 Discussion

The main objective of our study was to establish that metabolomic fingerprinting can be used as a diagnostic tool for a rare genetic disease, RTHα. Multivariate analysis of urine

spectra provides a metabolic fingerprint that enables to recognize mice carrying a pathological mutation in the *Thra* gene, relevant to the human genetic disease. By contrast, the method did not identify the presence of a weak allele, which has little consequences on the development and physiology, and has never been reported in humans. Also the method did not identify a single metabolite, which presence in urine or plasma would be the hallmark of RTHα. Its statistical power rather relies on the capacity to evaluate the concentrations of a large number of metabolites simultaneously.

Considering that mouse *Thra* and human *THRA* genes display extensive sequence similarities, mouse lines with *Thra* mutations are highly relevant animal models for RTHα. We thus expect that ^{1}H NMR can be used for RTHα diagnostic in humans. However, clinical implementation of this method would imply to address additional issues: first, the environment and genetic background of lab animals is highly controlled, and the body fluid composition is certainly more variable in human populations. Therefore, the predictive capacity of the method remains to be tested on a human cohort. Second, the interpretation of the metabolic signatures is not straightforward, and we thus cannot ascertain at this point that the underlying biochemical mechanisms are conserved in humans. In the following, we thus attempt to give hypothetical interpretations of the observed changes.

One encouraging observation is that, although ^{1}H NMR is instrumental to recognize hypothyroidism, privation of thyroid hormone provides a very different signature than *Thra* mutations. Our analyses show that, while *Thra* mutations and hypothyroidism may have a similar impact on glucose metabolism, they impact differently the plasma content in lipids and cholesterol. In particular, variations in the plasma content in fatty acids are in opposite direction. This is expected if one considers that liver, which secretes a large fraction of the lipids found in serum and urine, expresses *Thrb* at much higher level than *Thra*. Liver is thus expected to be more sensitive to changes in TH status than to *Thra* mutations. Studying both urine and plasma is also useful because they provide common and complementary information. For example, coordinated variations suggest that changes in urine reflect variations initially present in plasma, for creatinine, citrate and acetate and not an alteration of the renal function.

Additional features of the metabolic signature can be tentatively interpreted in biochemical terms. Isovalerylglycine is a product of leucine degradation to acetyl-CoA, which

is an important feeder into the Krebs cycle[165]. A significant decrease in urinary level of isovalerylglycine, and the decrease in the levels of citrate, succinate and acetate may thus indicate a change in the degradation of leucine.

Finally, the lower concentration of dimethylamine, trimethylamine, choline and hippurate observed in the urine of mutant mice and hypothyroid mice may reflect intestinal alterations. Gut microbial metabolism of choline, present in diet, leads to the production of trimethylamine, which, once absorbed, is metabolized to generate dimethylamine. Hippurate, is also synthesized by the gut microbiota and its decreased concentration in urine is a marker of bowel inflammation[166]. It is tempting to speculate that changes for these metabolites are direct or indirect consequences of the defect in the intestinal epithelium, reported in hypothyroid[167] and *Thra* mutant mice[117,168]. Also providing a snapshot of only a fraction of metabolome, ^{1}H NMR analysis of *Thra* mutant mice may thus be revealing changes in metabolic pathways and physiology, which are expected to be conserved in humans.

6. Functional genomics by metabonomics to study the thyroid hormone receptor β

The previous chapters were dedicated to the application of metabolomics for biofluids analysis in order to discover biomarkers related to hormonal diseases (hypothyroidism, hyperthyroidism and RTHα). In this chapter, we propose to use metabolomics to address a specific biological question. Metabolomics has the potential to get insight into molecular mechanisms and metabolic pathways and can be used by biological studies as a strategy to read-out metabolism. Among model organisms, genetically modified organisms using *knocking-in* or *knocking-out* (KO) technologies can be viewed as functional genomic tools for which the study of the resulting altered phenotype can serve to elucidate the role of the protein products of the targeted genes. In this chapter, we provide a description of the impact of the regulation by thyroid hormone of liver metabolism using a mouse model that is characterized by a specific deletion of the gene encoding the thyroid hormone receptor β (TRβ) in hepatocytes, i.e. LTRβ-KO mice[169].

This project was started few years ago with another PhD student (A. Fages). The obtained results were very interesting, but a supplementary experiment done by another student from the laboratory then challenged one of the results. My work, in this project, was to repeat the same experiment to validate it, and extend the analysis to extract deeper information. This chapter contains a combination of the previous results and the new analysis. To improve the statistical analysis, larger groups for the liquid NMR analysis were used. This chapter describes in details results that were submitted recently for publication[170]. HR-MAS NMR experiments and their analysis were done exclusively by A. Fages.

6.1 Introduction

TH regulates metabolism in a global manner, acting in the brain, white fat, brown fat, skeletal muscle, pancreas and liver. In the liver, the major TH receptor is TRβ1. Individual organs also respond to TH in an indirect manner, as TH can trigger various humoral responses, change the sensitivity of an organ to exogenous signals, and exert an important influence on the autonomous nervous system[88,157]. *In vivo* analysis of the metabolic function of TH is thus challenging, due to the intricate combination of multiple levels of regulation.

Here we used metabolomics analyses of the hepatic metabolome by nuclear magnetic resonance (NMR) to gain a deeper understanding of the effect of TH on the mouse liver metabolism. This method proved to be well suited to analyze the hydrophilic fraction of the metabolome and identified novel liver metabolites sensitive to hypothyroidism and/or subsequent TH replacement. We also determined the metabolome modifications induced by the elimination of TRβ1 receptors selectively in mice hepatocytes using a Cre/loxP recombination strategy. Both intact tissues and hydrophilic fraction were investigated by NMR to characterize metabolic fingerprints for these TRβ1 KO mice with respect to wild-type. By selectively eliminating TRβ1 from hepatocytes we were able to identify a subset of metabolites that are related to the direct influence of TH on this cell type.

6.2 Study design

Thrβlox/lox mice[171] were crossed to AflpCre mice[172] to selectively eliminate TRβ1 from hepatocytes. The resulting mice are designated in the following as HepTRβ-KO mice. Littermates without Cre were kept as control. All mice were fed ad libitum and housed under recommended standard conditions for 3 to 5 months. TH deficiency in adult animals was induced by 14 days of propyl-thio-uracyl (PTU) treatment as described [173]. For TH replacement, T3 treatment was performed for the last 4 days of PTU treatment using daily intraperitoneal injections (Figure 6.2.1). Liver biopsies were immediately flash-frozen after dissection in liquid nitrogen and subsequently stored at -80°C. Biopsies of the right lobe were used for metabolomics studies.

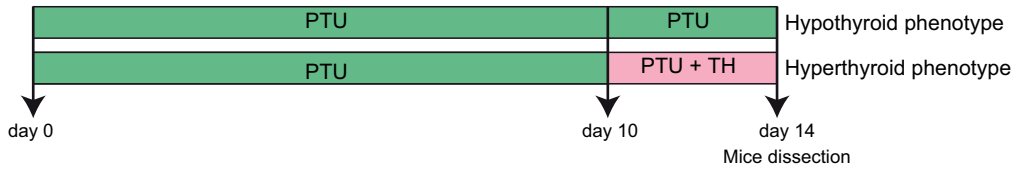

Figure 6.2.1: **Representation of the protocol.**
Wild-type mice and LTRβ-KO mice underwent ten days of PTU treatment prior to four days of PTU+TH or PTU only in order to induce hyperthyroid phenotype (PTU-TH) and hypothyroid treatment (PTU), respectively.

6.3 Results

6.3.1 Untargeted NMR Metabolomics analysis of the liver response to thyroid hormone

We attempted to gain a broad view of the liver metabolome for the four groups of mice (WT-PTU, WT-PTU+TH, TRβ-KO-PTU, and TRβ-KO-PTU+TH) by using ^{1}H NMR spectroscopy by following two distinct experimental approaches. We used HR-MAS analysis

of intact tissues, a direct method associated with minimal sample processing, as well as solution NMR investigation of aqueous liver extracts. HR-MAS NMR analysis enabled us to detect a range of lipophilic and hydrophilic low molecular weight metabolites, while the solution NMR data provided a high-resolution, though more indirect, picture of water-soluble metabolite extracted from liver tissues, allowing us to detect up to 40 hydrophilic metabolites. The extraction process has removed proteins and lipids. Representative metabolic profiles obtained using the two techniques are illustrated in figure 6.3.1.

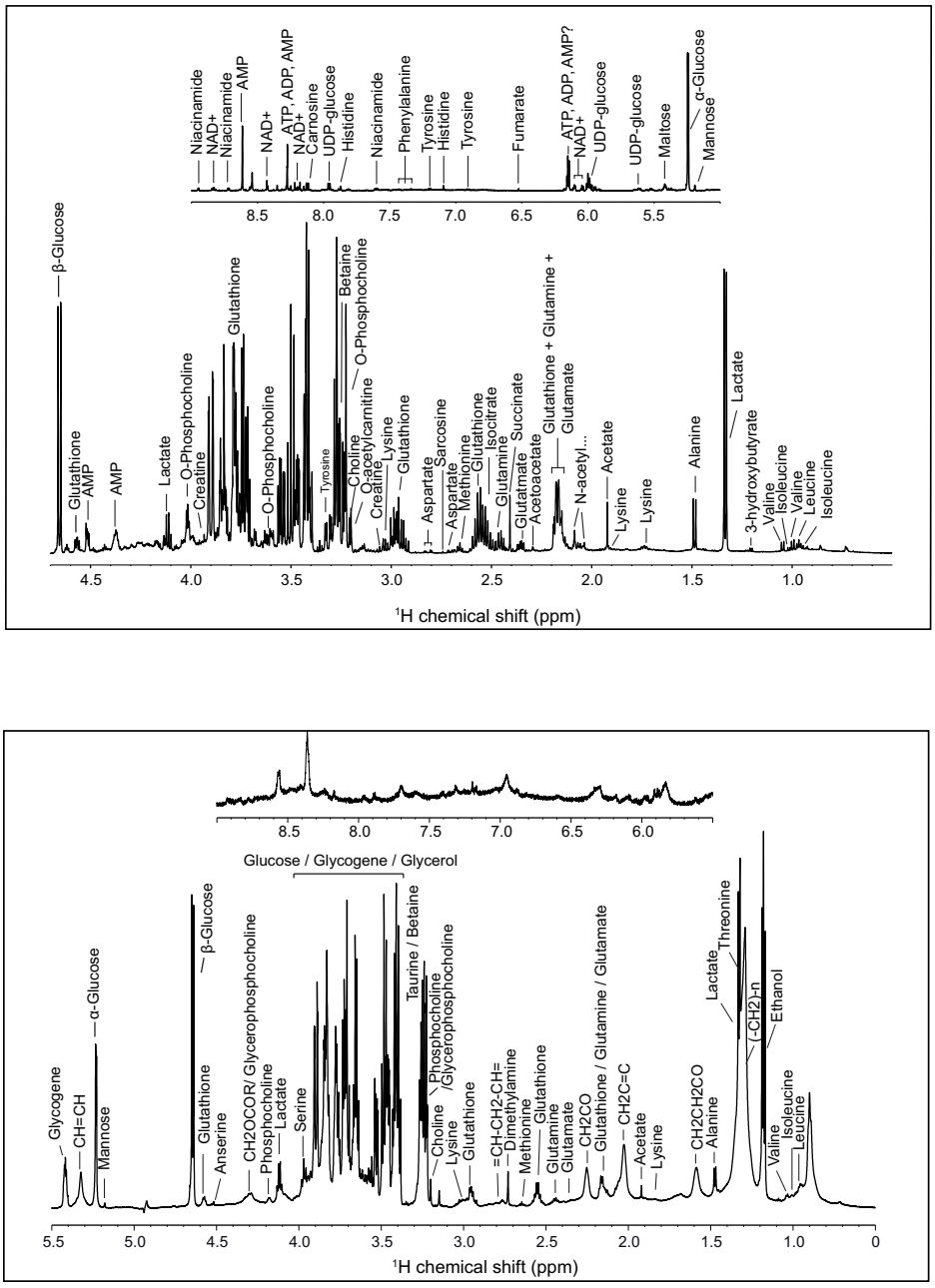

Figure 6.3.1: **Metabolites assignment**

(A) 600 MHz ^{1}H NOESY NMR spectrum of aqueous liver extract with metabolites assignment. The spectrum has been divided into two parts (from 0.5 to 4.7 ppm and from 5 to 9 ppm). (B) Typical 700 MHz ^{1}H NOESY HR-MAS NMR spectrum of mouse liver tissue with metabolites assignment. The spectrum has been divided into two parts (from 0.5 to 5.5 ppm and from 5.5 to 9 ppm).

6.3.2 Impact of TH nuclear receptor on liver metabolism

TRβ represents about 70 to 80% of thyroid hormone receptors in the liver, studying wild-type liver, and comparing PTU group to PTU+TH group provide information on the direct and indirect impact of TH on liver metabolism. Here we performed NMR analysis on aqueous liver extracts (^{1}H liquid NMR) and intact liver (^{1}H HR-MAS NMR).

The O-PLS supervised model based on the ^{1}H HR-MAS NMR spectra of liver tissue of the wild type mice shows a good discrimination between PTU and PTU+TH groups (Figure 6.3.2.A). The predictivity of the model is 0.58 and the explained variance is 0.76. The model is also well validated after resampling (data not shown). The metabolic signature associated with hyperthyroidism is represented by a relative decrease of the lipid content, phosphocholine, along with an increase of glucose in the liver (Figure 6.3.2.B).

The analysis of the aqueous liver extracts gives further details of the systematic difference due to small hydrophilic metabolites. In agreement to what was observed by the analysis of the ^{1}H HR-MAS NMR spectra of liver biopsies, we could discriminate PTU from PTU+TH treatment within wild type mice based on the analysis of metabolic profiles (Figure 6.3.2.C-D). Based on the explained variance (89%) and the predictive variance (61%), the O-PLS model obtained from liver extracts seems to discriminate better the two treatments. But the information obtained from the two techniques are highly complementary.

From these results, we were able to discriminate hypothyroid phenotype from hyperthyroid phenotype. Metabolic fingerprints associated to this condition, which reflects the impact of TH on the liver metabolism, were identified in both aqueous liver extracts and intact liver tissue.

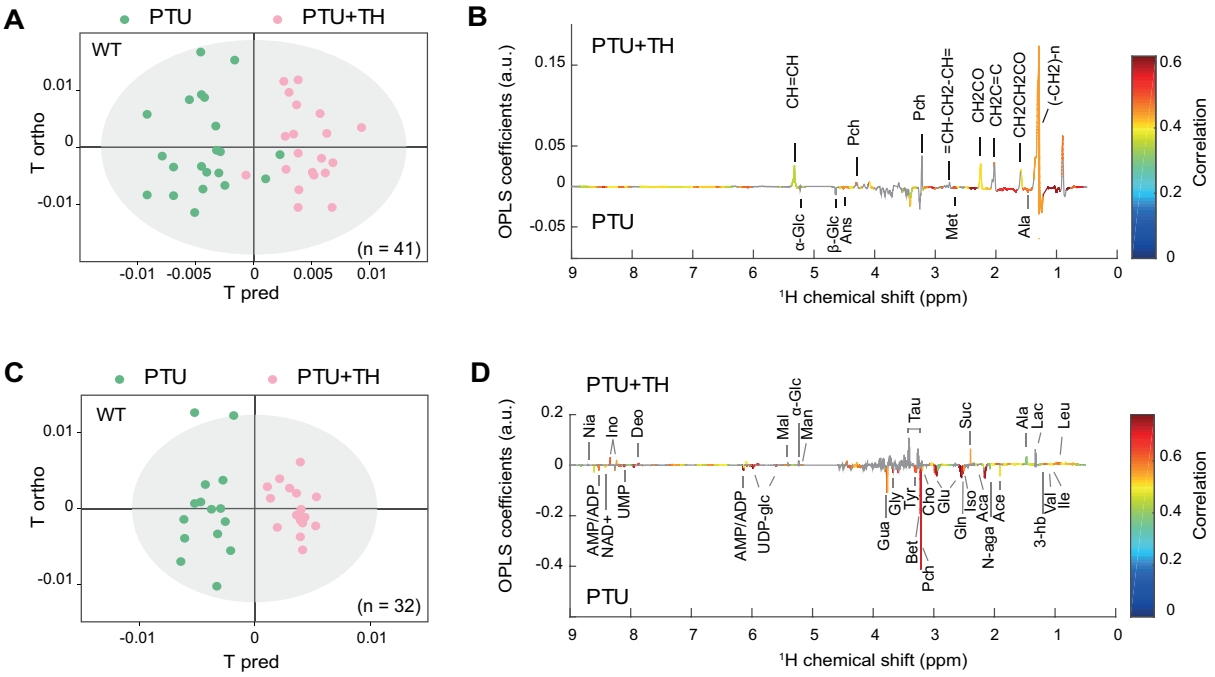

Figure 6.3.2: **Discrimination between PTU and PTU+TH groups in aqueous liver extracts and intact liver.**

(A) ^{1}H HR-MAS spectra of liver tissue from wild-type mice. O-PLS-DA model discriminating PTU treatment from PTU-TH treatment with (N = 41, R^2Y = 0.76, Q^2 = 0.58). (B) The O-OPLS loading plot after SRV analysis and Benjamini-Hochberg multiple testing correction. The coloured spectral regions correspond to the statistically significant signals. (C) OPLS-DA model of the liver extracts of wild-type mice, discriminating PTU treatment from PTU-TH treatment with (N = 32, 1+4 components, R^2Y = 0.89, Q^2 = 0.61, CV-ANOVA p-value = 0.01). (D) The corresponding OPLS-DA loading plot. Acetate (Ace), acetoacetate (Aca), alanine (Ala), anserine (Ans), choline (Cho), deoxyuridine (Deo), glutamate (Glu), glutamine (Gln), glycine (Gly), guanidoacetate (Gua), inosine (Ino), isocitrate (Iso), isoleucine (Ile), lactate (Lac), leucine (Leu), maltose (Mal), mannose (Man), methionine (Met), niacinamide (Nia), succinate (Suc), taurine (Tau), tyrosine (Tyr), UDP-glucose (UDP-Glc), valine (Val), α-glucose (α-Glc), β-glucose (β-Glc), N-acetylglucosamine (N-aga), 3-hydroxybutyrate (3-hb).

6.3.3 Impact of TRβ on liver metabolism

To understand the metabolic function of TRβ in the liver, we studied the impact of TH on mice having a specific KO of TRβ in the liver (LTRβ-KO mice). This leads also to identify the indirect effect of TH on the liver metabolism.

The supervised statistical analysis of the ^{1}H HR-MAS NMR spectra highlighted systematic variation between PTU and PTU-TH mice (Figure 6.3.3.A). While no significant variation identified from multiple univariate testing (after Benjamini-Hochberg correction), the global metabolic signature shows that TH treatment is associated with a relative decrease of glucose content and an increase of lipid content in the liver (Figure 6.3.3.B).

These results are in agreement with the results obtained from the analysis of the aqueous extracts that also display a relative decrease of glucose in the PTU-TH group. Figure 6.3.3.C presents the O-PLS analysis of the liver extract. The explained variance and the predicted variance of the model are enhanced to 0.77 and 0.65, respectively. The metabolic signature also shows a relative increase of choline and AMP and a relative decrease of phosphocholine for mice that had undergone TH treatment compared to PTU treatment (Figure 6.3.3.D).

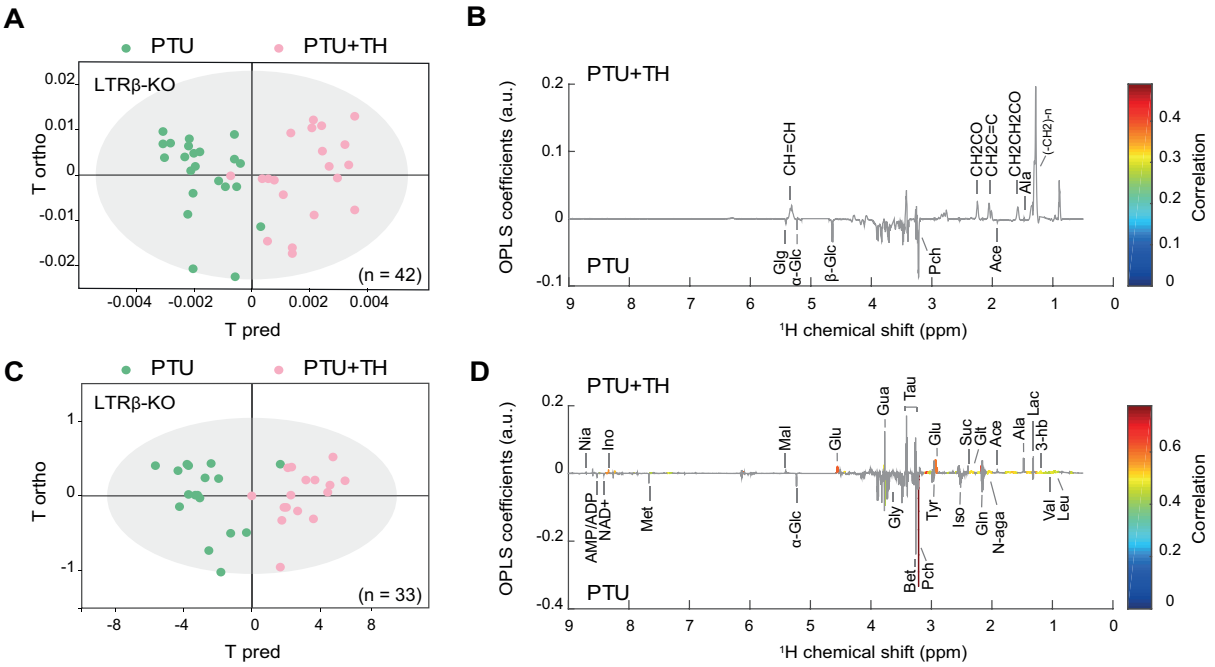

Figure 4.4.3: **The indirect effect of thyroid hormones on the liver metabolism.**

(A) ^{1}H HR-MAS spectra of liver tissue from LTRβ-KO mice. O-PLS-DA model discriminating PTU treatment from PTU-TH treatment with (N = 42, R^2Y = 0.74, Q^2 = 0.5). (B) The corresponding OPLS-DA loading plot. (C) OPLS-DA model of the liver extracts of LTRβ-KO mice, discriminating PTU treatment from PTU-TH treatment with (N = 33, 1+1 components, R^2Y = 0.773, Q^2 = 0.651, CV-ANOVA p-value = $4.07.10^{-6}$). (D) The corresponding OPLS-DA loading plot. All these models are validated by resampling 1000 times. Acetate (Ace), acetoacetate (Aca), alanine (Ala), anserine (Ans), choline (Cho), deoxyuridine (Deo), glutamate (Glu), glutamine (Gln), glycine (Gly), guanidoacetate (Gua), inosine (Ino), isocitrate (Iso), isoleucine (Ile), lactate (Lac), leucine (Leu), maltose (Mal),

mannose (Man), methionine (Met), niacinamide (Nia), succinate (Suc), taurine (Tau), tyrosine (Tyr), UDP-glucose (UDP-Glc), valine (Val), α-glucose (α-Glc), β-glucose (β-Glc), N-acetylglucosamine (N-aga), 3-hydroxybutyrate (3-hb).

6.3.4 Summary

If we compare the composition of the TH signature obtained from aqueous liver extracts in both wild type and LTRβ-KO mice, we notice that there are 20 common metabolites that vary in the same way (Table 6.1). This suggests that the activity of TH is maintained despite the absence of TRβ. So, there is an indirect effect of TH on liver metabolism.

We notice a relative increase of the lipid content within hyperthyroid mice compared to hypothyroid mice. Besides the increase of energy expenditure associated with hyperthyroidism, liver of LTRβ-KO mice is no longer able to provide fuel through lipolysis or cholesterol release. This result strengthens the idea that in normal condition, the effect of lipolysis is stronger than the effect of lipogenesis. We also notice a relative decrease of glucose content within hyperthyroid mice. The action of TH on glucose metabolism in the liver is complex and includes stimulation by a direct action of TH on the liver but also probably by an indirect effect of TH through the sympathetic nervous system.

	^{1}H liquid NMR of liver extracts		^{1}H HR-MAS of intact liver tissue	
Metabolites	T3 response wild-type	T3 response LTRβ-KO	T3 response wild-type	T3 response LTRβ-KO
Niacinamide	↑	↑		
Inosine	↑	↑		
Deoxyuridine	↑	/		
Glucose	↑	↓	↓	↓
Taurine	↑	↑		
Succinate	↑	↑		
Alanine	↑	↑	↓	↑
Lactate	↑	↑		
Leucine	↑	↓		
AMP	↓	↓		
ADP	↓	↓		
NAD/NADP+	↓	↓		
UDP-Galactose/UDP-Glucose	↓	/		
Glutathione	↓	↑		
Phosphocholine, choline	↓	↓	↑	↓
Isocitrate	↓	↓		
Hydroxybutyrate	↓	↑		
Isoleucine	↓	↓		
Valine	↓	↓		
Acetate	↓	↑		↓
Guanidoacetate	↓	↑		
Methylhistidine	↓	↓		
Glutamine	↓	↓		
Glycine	↓	↓		
N-acetylglucosamine	↓	↓		
Tyrosine	↓	↓		
Maltose	↑	↑		
Betaine	↓	↓		
Mannose	↑	/		
Acetoacetate	↓			
Glutamate	/	↑		
Anserine			↓	
Glycogen				↓
Methionine			↓	
Lipids			↑	↑

Table 6.1: Summary of metabolite variation in the different condition.

6.4 Conclusion

In the present study we used ^{1}H HR-MAS of unprocessed liver biopsies and NMR of liver aqueous extracts for a global and unbiased analysis of the metabolomic consequences of eliminating TRβ1 from hepatocytes.

We expected that the elimination of TRβ1 from the hepatocytes would abrogate the liver response to T3. Surprisingly, although the metabolic signature to T3 was modified and the changes induced by T3 of generally of lesser amplitude as compared to controls, the response remained significant. The residual response of HepTRβ-KO mice could have different sources. The first possible explanation would be that it reflects the response of non-hepatocyte cell types, which represent 20% of the liver cell mass, and in which both TRα1 and TRβ1 could be present. The second possibility would be that hepatocytes have enough TRα1 to mediate a significant response. Thra gene expression is very low in adult mice liver, and previous transcriptome analyses concluded that Thrb knock-out, but not Thra knock-out, alters the liver response to T3[96,174,175]. More targeted approaches also concluded that only TRβ1 is required for the T3 response of hepatocytes[176,177]. However, the combination of both Thra and Thrb mutations seems to aggravate the liver phenotype, leaving open the possibility that TRα1 can partially compensate for the absence of TRβ1 after Thrb knock-out[96]. While these mutations are not restricted to hepatocytes, and might thus affect liver function in a very indirect manner, Cre/loxP recombination has already been used to restrict to hepatocytes the expression of a Thra mutant encoding the dominant-negative TRα1L400R receptor. This selective alteration appeared sufficient to reduce the expression of the genes encoding pyruvate kinase and phosphoenolpyruvate carboxykinase, which should notably impact hepatic neoglucogenesis[178]. Overall, the possibility exists that TRα1 fulfills a specific function in hepatocytes. Finally the residual metabolomics response of the HepTRβ-KO liver might reflect a T3 response-taking place outside of the liver. One important pathway has been identified, which involves a T3-dependent sympathetic stimulation of the liver while stimulates hepatic glucose production[75]. It can be hypothesized that this pathway is important to control blood glucose and triglyceride concentration. As TH normally controls several aspects of glucose and glycogen metabolism, a combination of cell-autonomous and distant regulations could explain why the glucose content of liver is decreased by hypothyroidism in control mice and paradoxically increased in HepTRβ-KO mice.

Our metabolomic analysis provides a static view of liver metabolism. Therefore interpreting our data in terms of metabolism should thus be made with caution. It also provides a partial of the metabolome, as lipids, which metabolism is highly sensitive to T3 cannot be precisely analyzed. For example, we observed significant changes in acetate and hydroxybutyrate content, two molecules that are key elements of fatty acids metabolism, and these changes should probably correlate with changes in fatty acid composition. Only few of the changes in liver metabolites content caused by the thyroid hormone status are clearly altered in HepTRβ-KO mice and thus reflect the cell-autonomous influence of TRβ1. This allows to distinguish two categories of metabolites: for choline, glutamine, glutathione, glycine, guanidoacetate the liver content differ between HepTRβ-KO and control liver only when mice are made hypothyroid. By contrast for in leucine, isoleucine, succinate and valine, only the TH response of hypothyroid HepTRβ-KO mice is clearly blunted. This distinction between metabolites parallels the conclusion of transcriptome studies, which showed that some metabolic genes are more sensitive to the negative regulation exerted by the unliganded TRβ1, while others are not sensitive to hypothyroidism but quickly upregulated after T3 treatment[96].

The decrease of glutathione observed in response to T3 has been reported before[179]. It is likely to reflect a T3-induced oxidative stress {Mancini, 2016 #11488}, and increased glutathione consumption[180]. The presence of AMP and succinate in the metabolic signature of T3 response is also compatible with an increase in metabolic rate, succinate and ATP consumption reported before[181]. The presence of branched chain amino acids (leucine, isoleucine, valine) among these metabolites is a novel information which interpretation will require deeper investigation. It is noticeable that a recent metabolomic study in which an excess of TH was given to healthy subjects also identified an increase of leucine and isoleucine content in the serum[158]. A urine metabolome analysis also found a positive correlation between the circulating level of T4 and the urinary content in glycine and alanine in euthyroid subjects[182]. A unifying hypothesis would be that the release of branched amino-acids reflects an increase in protein catabolism.

Conclusion and perspectives

Metabolomic is a comprehensive technique that allows capturing an instant metabolic picture of an organism, reflecting molecular and pathophysiological states. Metabolic profiles are sensitive to environmental factors, genetic, diseases lifestyle and pathophysiological stimuli, making metabolomics as a promising tool to identify disease biomarkers and to get insight into metabolism to address specific fundamental biological questions.

In this thesis, untargeted ^{1}H NMR-based metabolomics was applied to study the emerging genetic disease RTHα, for which absence of biochemical markers and specific symptoms make it hard to diagnose. RTHα features present common features with hypothyroidism. By studying both urine and plasma collected from dedicated mice models for RTHα and hypothyroidism, we were able to identify metabolic fingerprint related to hypothyroidism and RTHα, and differentiate them. Our results suggest that ^{1}H NMR of body fluids might be able to recognize a metabolic signature of RTHα in humans. These findings could be the starting point for further investigations aimed at translating these results into clinical practice with carefully designed and controlled prospective studies. Metabolomics could be used in the near future as a systematic, cheap, and automatic analysis of the urinary metabolome at birth, which would detect many common or rare diseases including RTHα.

Studying both urine and blood plasma is highly useful because they provide common and complementary information. The difference between the two biofluids is that blood analysis provides information about lipids, lipoproteins and glucose metabolisms. While, urine analysis gives an idea about kidney function and gut microbial state, for example. A number of issues should be addressed before clinical implementation of ^{1}H NMR for RTHα diagnostic: first of all, the plasma and urine metabolome are downstream readouts of complex physiological processes, which are different in humans and rodents. Second, the environment and genetic background of lab animals is highly controlled, and the body fluid metabolomes are certainly more variable in human populations. Performing this study on patients is primordial to complete and validate our findings. However, the majority of RTHα patients are treated with thyroid hormone, which improve their condition, and this can skew the study.

These different factors must be taken into account for the further and additional studies in humans. Pr. K. Chatterjee, director of Cambridge clinical centres, who discovered the first RTHα case, owns urine samples of RTHα patients. Collaboration between the two laboratories is foreseen in the near future to carry out new investigations on RTHα human samples.

We also used NMR-based metabolomics to investigate mouse model to gain a deeper understanding of impact of thyroid hormones and TRβ nuclear receptor loss of function on the liver metabolism. Both intact liver tissues and hydrophilic liver fraction were investigated. We were able here to identify a subset of metabolites that are related to the influence of TH on the liver metabolism. We would have liked to perform a lipidomic study to understand the roles of lipids in our biological question, but our technical tools limited us because it needs specific methodologies. The new advances in analytical technologies, in particular, the development of new MS, chromatographic and of course NMR tools[183] for the characterization and quantification of the wide array of diverse lipid species in the cellular lipidome[45,184] are nowadays very interesting.

Metabolomics is certainly a promising tool to understand biological processes, and identify diseases biomarkers, but bias can be easily inserted in the different steps (study design, sample collection and preparation, statistical analysis, data interpretation, etc.). On the other hand, metabolites assignment is a very delicate step because we need to be sure that a specific peak is referred to a specific metabolite. The situation is further complicated by peak shifts and overlaps typical in the spectra. Identification is time consuming because it requires the use of 1D and 2D spectra and different reference databases to assign peaks. In addition, in reference databases, many NMR peaks are not assigned to metabolites. This is an active research area, where improvements in metabolite identification, in particular its automation, are underway, and they will considerably reduce the needed time for this fastidious task.

Most of the untargeted studies show the ability of metabolomics to distinguish between disease and healthy control cohorts. However, only few studies follow up to replicate and validate their discoveries in accordance with clinical performance standards. Biomarker identification represents only the starting point in the translation from discovery phase to clinical diagnostics. The interpretation of the obtained metabolic signature is a very delicate

step. Combination of genomics, transcriptomics, proteomics and metabolomics and other disciplines can be a formidable technological resource to further expand our knowledge of the complexities of human diseases.

This thesis allows a deeper understanding of three different diseases (hypothyroidism, hyperthyroidism and RTHα) and the impact of thyroid hormone on the global system and on liver metabolism. It also contributes to identify a specific metabolic signature of the emerging genetic disease resistance to thyroid hormone receptor RTHα, which is a first step to facilitate its diagnosis in humans.

References

1. Nicholson, J. K. & Lindon, J. C. Metabonomics. *Nature* **455,** 1–3 (2008).
2. Mamas, M., Dunn, W. B., Neyses, L. & Goodacre, R. The role of metabolites and metabolomics in clinically applicable biomarkers of disease. *Arch Toxicol* **85,** 5–17 (2010).
3. Holmes, E., Wilson, I. D. & Nicholson, J. K. Metabolic phenotyping in health and disease. *Cell* **134,** 714–717 (2008).
4. Jacob, M. *et al.* A targeted metabolomics approach for clinical diagnosis of inborn errors of metabolism. *Anal. Chim. Acta* **1025,** 141–153 (2018).
5. Coene, K. L. M. *et al.* Next-generation metabolic screening: targeted and untargeted metabolomics for the diagnosis of inborn errors of metabolism in individual patients. 1–17 (2018).
6. Ikegami, R., Shimizu, I., Yoshida, Y. & Minamino, T. Metabolomic analysis in heart failure. *Circ J* **82,** 10–16 (2018).
7. Ruiz Canela, M. *et al.* Comprehensive metabolomic profiling and incident cardiovascular disease: A Systematic Review. *J Am Heart Assoc* **6,** 1–22 (2017).
8. Markley, J. L. *et al.* The future of NMR-based metabolomics. *Current Opinion in Biotechnology* **43,** 34–40 (2017).
9. Sethi, S. *et al.* in *Metabolomics: From Fundamentals to Clinical Applications* (ed. Sussulini, A.) **965,** 265–290 (Springer International Publishing, 2017).
10. Newgard, C. B. Metabolomics and Metabolic Diseases: Where Do We Stand? *Cell Metab* **25,** 43–56 (2017).
11. Jobard, E. *et al.* A serum metabolomic fingerprint of bevacizumab and temsirolimus combination as first-line treatment of metastatic renal cell carcinoma. *Br. J. Cancer* **113,** 1148–1157 (2015).
12. Wang, N., Zhu, F., Chen, L. & Chen, K. Proteomics, metabolomics and metagenomics for type 2 diabetes and its complications. *Life Sciences* **212,** 194–202 (2018).
13. Oresic, M. Metabolomics, a novel tool for studies of nutrition, metabolism and lipid dysfunction. *Nutr Metab Cardiovasc Dis* **19,** 816–824 (2009).
14. Struja, T. *et al.* Metabolomics for Prediction of Relapse in Graves' Disease: Observational Pilot Study. *Front. Endocrinol* **9,** 2594–6 (2018).
15. Armitage, E. G. & Barbas, C. Metabolomics in cancer biomarker discovery: Current trends and future perspectives. *J Pharm Biomed Anal* **87,** 1–11 (2014).
16. Bino, R. J. *et al.* Potential of metabolomics as a functional genomics tool. *Trends Plant Sci* **9,** 418–425 (2004).
17. Psychogios, N. *et al.* The Human serum metabolome. *PLoS ONE* **6,** e16957 (2011).
18. Bouatra, S. *et al.* The human urine metabolome. *PLoS ONE* **8,** 1–28 (2013).
19. Fiehn, O. Combining genomics, metabolome analysis, and biochemical modelling to understand metabolic networks. *Comp Funct Genomics* **2,** 155–168 (2001).
20. Wilkins, J. M. & Trushina, E. Application of metabolomics in Alzheimer's disease. *Front. Neurol.* **8,** 59–20 (2018).
21. Nicholson, J. K., Holmes, E. & Lindon, J. C. 'Metabonomics': understanding the metabolic responses of living systems to pathophysiological stimuli via

multivariate statistical analysis of biological NMR spectroscopic data. *Xenobiotica* **29,** 1181–1189 (1999).
22. Wishart, D. S. Metabolomics: applications to food science and nutrition research. *Trends Food Sci Technol* **19,** 482–493 (2008).
23. Madsen, R., Lundstedt, T. & Trygg, J. Chemometrics in metabolomics—A review in human disease diagnosis. *Anal. Chim. Acta* **659,** 23–33 (2010).
24. Dunn, W. B., Broadhurst, D. I., Atherton, H. J., Goodacre, R. & Griffin, J. L. Systems level studies of mammalian metabolomes: the roles of mass spectrometry and nuclear magnetic resonance spectroscopy. *Chem. Soc. Rev.* **40,** 387–426 (2011).
25. Kell, D. B. *et al.* Metabolic footprinting and systems biology: the medium is the message. *Nat Rev Micro* **3,** 557–565 (2005).
26. Heude, C., Nath, J., Carrigan, J. B. & Ludwig, C. in *Metabolomics: From Fundamentals to Clinical Applications* (ed. Sussulini, A.) **965,** 45–76 (Springer International Publishing, 2017).
27. Bollard, M. E., Stanley, E. G., Lindon, J. C., Nicholson, J. K. & Holmes, E. NMR-based metabonomic approaches for evaluating physiological influences on biofluid composition. *NMR Biomed.* **18,** 143–162 (2005).
28. Woo, H. M. *et al.* Mass spectrometry based metabolomic approaches in urinary biomarker study of women's cancers. *Clinica Chimica Acta* **400,** 63–69 (2009).
29. Zhang, S., Nagana Gowda, G. A., Ye, T. & Raftery, D. Advances in NMR-based biofluid analysis and metabolite profiling. *Analyst* **135,** 1490–9 (2010).
30. Izquierdo-GarcÃ, J. A., Villa, P., Kyriazis, A., Del Puerto-Nevado, L., Pérez-Rial, S., Ruiz-Cabello, J . Descriptive review of current NMR-based metabolomic data analysis packages. *Prog. Nucl. Magn. Reson. Spectrosc.* **59,** 263–270 (2011).
31. Dettmer, K., Aronov, P. A. & Hammock, B. D. Mass spectrometry-based metabolomics. *Mass Spectrom. Rev.* **26,** 51–78 (2006).
32. Lindon, J. C., Nicholson, J. K. & Holmes, E. *The handbook of metabonomics and metabolomics*. (2007).
33. Rabi, I., Zacharias, S., Millman, S. & kush, P. A new method of measuring nuclear magnetic moment. *American Physical Society* **53,** (1938).
34. Brown, F. F., Campbell, I. D. & Kuchel, P. W. Human erythrocyte metabolism studies by 1H spin echo NMR. *FEBS lett* **82,** 12–16 (1977).
35. Haukaas, T., Euceda, L., Giskeødegård, G. & Bathen, T. Metabolic portraits of breast cancer by HR MAS MR spectroscopy of Intact tissue samples. *Metabolites* **7,** 18–16 (2017).
36. Kumar, V., Dwivedi, D. K. & Jagannathan, N. R. High-resolution NMR spectroscopy of human body fluids and tissues in relation to prostate cancer. *NMR Biomed.* **27,** 80–89 (2013).
37. Moestue, S., Sitter, B., Bathen, T., Tessem, M., Gribbestad, I. HR MAS MR spectroscopy in metabolic characterization of cancer. *Curr Top Med Chem*. 1–25 (2011).
38. Sitter, B., Bathen, T. F., Tessem, M.-B. & Gribbestad, I. S. High-resolution magic angle spinning (HR MAS) MR spectroscopy in metabolic characterization of human cancer. *Prog Nucl Magn Reson Spectrosc* **54,** 239–254 (2009).
39. McDonald, I. R. Free-induction decays in a rotating solid. *Physica* **5,** 273–276 (1971).
40. Braunschweiler, L. & Rietzschel, E. R. Coherence transfer by isotopic mixing: application to proton correlation spectroscopy. *J. Magn. Reson.* **53,** 521–528

(1983).
41. Rodriguez-Martinez, A. *et al.* J-Resolved 1H NMR 1D-projections for large-scale metabolic phenotyping studies: application to blood plasma analysis. *Anal. Chem.* **89,** 11405–11412 (2017).
42. Saude, E. J., Adamko, D., Rowe, B. H., Marrie, T. & Sykes, B. D. Variation of metabolites in normal human urine. *Metabolomics* **3,** 439–451 (2007).
43. Chetwynd, A. J., Dunn, W. B. & Rodriguez-Blanco, G. in *Metabolomics: From fundamentals to clinical applications* (ed. Sussulini, A.) **965,** 19–44 (Springer International Publishing, 2017).
44. Lubes, G. & Goodarzi, M. GC–MS based metabolomics used for the identification of cancer volatile organic compounds as biomarkers. *J Pharm Biomed Anal* **147,** 313–322 (2018).
45. Griffiths, W. J. & Wang, Y. Mass spectrometry: from proteomics to metabolomics and lipidomics. *Chem. Soc. Rev.* **38,** 1882–15 (2009).
46. Beckonert, O. *et al.* Metabolic profiling, metabolomic and metabonomic procedures for NMR spectroscopy of urine, plasma, serum and tissue extracts. *Nat Protoc* **2,** 2692–2703 (2007).
47. Spratlin, J. L., Serkova, N. J. & Eckhardt, S. G. Clinical applications of metabolomics in oncology: A review. *Clin Cancer Res* **15,** 431–440 (2009).
48. Srivastava, S. *et al.* Taurine – a possible fingerprint biomarker in non-muscle invasive bladder cancer: A pilot study by ^{1}H NMR spectroscopy. *CBM* **6,** 11–20 (2010).
49. Assi, N. *et al.* A statistical framework to model the meeting-in-the-middle principle using metabolomic data: application to hepatocellular carcinoma in the EPIC study. *Mutagenesis* **30,** 743–753 (2015).
50. Sreekumar, A. *et al.* Metabolomic profiles delineate potential role for sarcosine in prostate cancer progression. *Nature* **457,** 910–914 (2009).
51. Monleón, D. *et al.* Metabolite profiling of faecal water extracts from human colorectal cancer. *NMR Biomed.* **22,** 342–348 (2009).
52. Tan, C., Chen, H. & Xia, C. Early prediction of lung cancer based on the combination of trace element analysis in urine and an Adaboost algorithm. *Journal of Pharmaceutical and Biomedical Analysis* **49,** 746–752 (2009).
53. Hirayama, A. *et al.* Quantitative metabolome profiling of colon and stomach cancer microenvironment by capillary electrophoresis time-of-flight mass spectrometry. *Cancer Res* **69,** 4918–4925 (2009).
54. Wen, H. *et al.* A new NMR-based metabolomics approach for the diagnosis of biliary tract cancer. *Journal of Hepatology* **52,** 228–233 (2010).
55. Navas-Carrillo, D., Manuel, R. J., Silvia, M.-G. & Esteban, O.-P. High-resolution proteomics and metabolomics in thyroid cancer: Deciphering novel biomarkers. *Critic Rev Clin Lab Sciences* **0,** 1–12 (2016).
56. Monleón, D. *et al.* Benign and atypical meningioma metabolic signatures by high-resolution magic-angle spinning molecular profiling. *J. Proteome Res.* **7,** 2882–2888 (2008).
57. Wang, Z. *et al.* Gut flora metabolism of phosphatidylcholine promotes cardiovascular disease. *Nature* **472,** 57–63 (2011).
58. Cai, H.-L. *et al.* Metabolomic analysis of biochemical changes in the plasma and urine of first-episode neuroleptic-naïve schizophrenia patients after treatment with risperidone. *J. Proteome Res.* **11,** 4338–4350 (2012).
59. Koriem, K. M. M. A lipidomic concept in infectious diseases. *Asian Pac J Trop Biomed* **7,** 265–274 (2017).

60. Eoh, H. Metabolomics: A window into the adaptive physiology of Mycobacterium tuberculosis. *Tuberculosis* **94,** 538–543 (2014).
61. Kettunen, J. *et al.* Genome-wide association study identifies multiple loci influencing human serum metabolite levels. *Nat Genet* **44,** 269–276 (2012).
62. Gieger, C. *et al.* Genetics meets metabolomics: A genome-wide association study of metabolite profiles in human serum. *PLoS Genet* **4,** e1000282–12 (2008).
63. Shin, S.-Y. *et al.* An atlas of genetic influences on human blood metabolites. *Nat Genet* **46,** 543–550 (2014).
64. Illig, T. *et al.* A genome-wide perspective of genetic variation in human metabolism. *Nat Genet* **42,** 137–141 (2009).
65. Raffler, J. *et al.* Genome-wide association study with targeted and non-targeted NMR metabolomics identifies 15 novel loci of urinary human metabolic individuality. *PLoS Genet* **11,** e1005487–28 (2015).
66. Tsepilov, Y. A. *et al.* Nonadditive effects of genes in human metabolomics. *Genetics* **200,** 707–718 (2015).
67. Sandlers, Y. The future perspective: metabolomics in laboratory medicine for inborn errors of metabolism. *Translational Research* **189,** 65–75 (2017).
68. Legault, J. T. *et al.* A Metabolic signature of mitochondrial dysfunction revealed through a monogenic form of leigh syndrome. *CELREP* **13,** 981–989 (2015).
69. Brent, G. A. Mechanisms of thyroid hormone action. *J. Clin. Invest.* **122,** 3035–3043 (2012).
70. Cheng, S.-Y., Leonard, J. L. & Davis, P. J. Molecular aspects of thyroid hormone actions. *Endocr Rev* **31,** 139–170 (2010).
71. Yen, P. M. Physiological and molecular basis of thyroid hormone action. *Physiol. Rev* **81,** 1097–1142 (2001).
72. Louzada, R. A. & Carvalho, D. P. Similarities and differences in the peripheral actions of thyroid hormones and their metabolites. *Front. Endocrinol.* **9,** 898–14 (2018).
73. van der Spek, A. H. *et al.* Increased circulating interleukin-8 in patients with resistance to thyroid hormone receptor α. *Endocr Connect* **6,** 731–740 (2017).
74. Cokkinos, D. V. & Chryssanthopoulos, S. Thyroid hormones and cardiac remodeling. *Heart Fail Rev* **21,** 365–372 (2016).
75. Martínez-Sánchez, N. *et al.* Thyroid hormones induce browning of white fat. *J Endocrinol* **232,** 351–362 (2017).
76. Silva, J. E. Thyroid hormone and the energetic cost of keeping body temperature. *Biosci Rep* **25,** 129–148 (2005).
77. Williams, G. R. & Bassett, J. H. D. Thyroid diseases and bone health. *J Endocrinol Invest* **41,** 99–109 (2017).
78. Bjergved, L. *et al.* Thyroid Function and Body Weight: A community-based longitudinal study. *PLoS ONE* **9,** 3–7 (2014).
79. Visser, W. E. *et al.* Physiological Thyroid Hormone Levels Regulate Numerous Skeletal Muscle Transcripts. *J. Clin. Endocrinol. Metab.* **94,** 3487–3496 (2009).
80. Flamant, F. & Gauthier, K. Thyroid hormone receptors: the challenge of elucidating isotype-specific functions and cell-specific response. *Biochim. Biophys. Acta* **1830,** 3900–3907 (2013).
81. Zhang, J. & Lazar, M. A. The mechanism of action of thyroid hormones. *Annu Rev Physiol* **62,** 439–466 (2000).
82. Gauthier, K. *et al.* Different functions for the thyroid hormone receptors TRα and TRβ in the control of thyroid hormone production and post-natal development. *EMBO J.* **18,** 623–631 (1999).

83. Evans, R. M. & Mangelsdorf, D. J. Nuclear receptors, RXR, and the big bang. *Cell* **157,** 255–266 (2014).
84. Leonard, J. Non-genomic actions of thyroid hormone in brain development. *Steroids* **73,** 1008–1012 (2008).
85. Visser, W. E., Friesema, E. C. H. & Visser, T. J. Minireview: Thyroid hormone transporters: the knowns and the unknowns. *Mol. Endocrinol* **25,** 1–14 (2011).
86. Stanya, K. J. & Kao, H.-Y. New insights into the functions and regulation of the transcriptional corepressors SMRT and N-CoR. *Cell Div* **4,** 7–9 (2009).
87. Dasgupta, S., Lonard, D. M. & O'Malley, B. W. Nuclear receptor coactivators: master regulators of human health and disease. *Annu. Rev. Med.* **65,** 279–292 (2014).
88. Muller, R., Liu, Y.-Y. & Brent, G. A. Thyroid hormone regulation of metabolism. *Physiol. Rev* **94,** 355–382 (2014).
89. López, M., Alvarez, C. V., Nogueiras, R. & Diéguez, C. Energy balance regulation by thyroid hormones at central level. *Trends Mol Med* **19,** 418–427 (2013).
90. Hannoush, Z. C. & Weiss, R. E. Defects of thyroid hormone synthesis and action. *Endocrinol Metab Clin North Am* **46,** 375–388 (2017).
91. Oetting, A. & Yen, P. M. New insights into thyroid hormone action. *Best Pract Res Clin Endocrinol Metab* **21,** 193–208 (2007).
92. Taylor, P. N. *et al.* Global epidemiology of hyperthyroidism and hypothyroidism. *Nature.* 1–17 (2018).
93. Fu, J., Fujisawa, H., Follman, B., Liao, X.-H. & Dumitrescu, A. M. Thyroid hormone metabolism defects in a mouse model of SBP2 deficiency. *Endocrinology* **158,** 4317–4330 (2017).
94. Dumitrescu, A. M. & Refetoff, S. The syndromes of reduced sensitivity to thyroid hormone. *Biochimica et Biophysica Acta (BBA) - Gen Subjects* **1830,** 3987–4003 (2013).
95. Refetoff, S., DEWIND, L. T. & DEGROOT, L. J. Familial syndrome combining deaf-mutism, stippled epiphyses, goiter and abnormally high PBI: possible target organ refractoriness to thyroid hormone. *J Clin Endocrinol Metab* **27,** 279–294 (2008).
96. Yen, P. M. *et al.* Effects of ligand and thyroid hormone receptor isoforms on hepatic gene expression profiles of thyroid hormone receptor knockout mice. *EMBO reports* **4,** 581–587 (2003).
97. Refetoff, S. & Dumitrescu, A. M. Syndromes of reduced sensitivity to thyroid hormone: genetic defects in hormone receptors, cell transporters and deiodination. *Best Pract Res Clin Endocrinol Metab* **21,** 277–305 (2007).
98. Brucker-Davis, F. *et al.* genetic and clinical features of 42 kindreds with resistance to thyroid-hormone - the national-institutes-of-health prospective-study. *Ann Intern Med* **123,** 572–583 (1995).
99. LaFranchi, S. H. *et al.* Follow-up of newborns with elevated screening T4 concentrations. *J Pediatri* **143,** 296–301 (2003).
100. Moran, C. & Chatterjee, K. Resistance to thyroid hormone α-emerging definition of a disorder of thyroid hormone action. *J. Clin. Endocrinol. Metab.* **101,** 2636–2639 (2016).
101. Weiss, R. E., Dumitrescu, A. & Refetoff, S. Approach to the Patient with Resistance to thyroid hormone and pregnancy. *J. Clin. Endocrinol. Metab.* **95,** 3094–3102 (2010).
102. Bochukova, E. *et al.* A Mutation in the Thyroid Hormone Receptor Alpha Gene.

N. Engl. J. Med. 243–249 (2012).
103. van Mullem, A. A. *et al.* Clinical phenotype and mutant TRα1. *N. Engl. J. Med.* **366,** 1451–1453 (2012).
104. Van Mullem, A. A. *et al.* Clinical phenotype of a new type of thyroid hormone resistance caused by a mutation of the TRα1 receptor: consequences of LT4 treatment. *J. Clin. Endocrinol. Metab.* **98,** 3029–3038 (2013).
105. Moran, C. *et al.* Resistance to thyroid hormone caused by a mutation in thyroid hormone receptor (TR)α1 and TRα2: clinical, biochemical, and genetic analyses of three related patients. *Lancet Diabetes Endocrinol* **2,** 619–626 (2014).
106. Yuen, R. K. C. *et al.* Whole-genome sequencing of quartet families with autism spectrum disorder. *Nat Med* **21,** 185–191 (2015).
107. Demir, K. *et al.* Diverse genotypes and phenotypes of three novel thyroid hormone receptor-α mutations. *J. Clin. Endocrinol. Metab.* **101,** 2945–2954 (2016).
108. Moran, C. *et al.* Contrasting phenotypes in resistance to thyroid hormone alpha correlate with divergent properties of thyroid hormone receptor α1 mutant proteins. *Thyroid* **27,** 973–982 (2017).
109. van Gucht, A. L. M. *et al.* Resistance to thyroid hormone alpha in an 18 months old girl; clinical, therapeutic and molecular characteristics. *Thyroid* **26,** 338–346 (2016).
110. Espiard, S. *et al.* A novel mutation in thra gene associated with an atypical phenotype of resistance to thyroid hormone. *J. Clin. Endocrinol. Metab.* **100,** 2841–2848 (2015).
111. Zavacki, A. M. & Larsen, P. R. RTHα, a newly recognized phenotype of the resistance to thyroid hormone (rth) syndrome in patients with thra gene mutations. *J. Clin. Endocrinol. Metab.* **98,** 2684–2686 (2013).
112. Schoenmakers, N. *et al.* Resistance to thyroid hormone mediated by defective thyroid hormone receptor alpha. *BBA-Gen subjects* **1830,** 4004–4008 (2013).
113. van Gucht, A. L. M. *et al.* Anemia in patients with resistance to thyroid hormone α: a role for thyroid hormone receptor α in human erythropoiesis. *J. Clin. Endocrinol. Metab.* **102,** 3517–3525 (2017).
114. Moran, C. *et al.* An adult female with resistance to thyroid hormone mediated by defective thyroid hormone receptor α. *J. Clin. Endocrinol. Metab.* **98,** 4254–4261 (2013).
115. Liu, Y.-Y., Schultz, J. J. & Brent, G. A. A Thyroid hormone receptor α gene mutation (p398h) is associated with visceral adiposity and impaired catecholamine-stimulated lipolysis in mice. *J. Biol. Chem.* **278,** 38913–38920 (2003).
116. Venero, C. Anxiety, memory impairment, and locomotor dysfunction caused by a mutant thyroid hormone receptor α 1 can be ameliorated by T3 treatment. *Genes Dev* **19,** 2152–2163 (2005).
117. Markossian, S. *et al.* CRISPR/Cas9 editing of the mouse thragene produces models with variable resistance to thyroid hormone. *Thyroid* **28,** 139–150 (2018).
118. Tylki-Szymańska, A. *et al.* Thyroid hormone resistance syndrome due to mutations in the thyroid hormone receptor α gene (THRA). *J Med Genet* **52,** 312–316 (2015).
119. Quignodon, L., Vincent, S., Winter, H., Samarut, J. & Flamant, F. A point mutation in the activation function 2 domain of thyroid hormone receptor α1 expressed after cre-mediated recombination partially recapitulates hypothyroidism. *Mol. Endocrinol* **21,** 2350–2360 (2007).

120. O'Shea, P. J. *et al.* Contrasting skeletal phenotypes in mice with an identical mutation targeted to thyroid hormone receptor α1 or β. *Mol. Endocrinol* **19,** 3045–3059 (2005).
121. Tinnikov, A. *et al.* Retardation of post-natal development caused by a negatively acting thyroid hormone receptor 1. *EMBO J.* **21,** 5079–5087 (2002).
122. Kanashige, M. *et al.* A targeted dominant negative mutation of the thyroid hormone 1 receptor causes increased mortality, infertility, and dwarfism in mice. *Proc. Natl. Acad. Sci.* **98,** 15095–15100 (2001).
123. Wikström, L. *et al.* Abnormal heart rate and body temperature in mice lacking thyroid hormone receptor. *EMBO J.* **17,** 455–461 (1998).
124. Fraichard, A. *et al.* The T3Rα gene encoding a thyroid hormone receptor is essential for post-natal development and thyroid hormone production. *EMBO J.* **16,** 4412–4420 (1997).
125. Seo, J. W. *et al.* Application of metabolomics in prediction of lymph node metastasis in papillary thyroid carcinoma. *PLoS ONE* **13,** e0193883–11 (2018).
126. Chi, Y. *et al.* Metabonomic phenotyping reveals an embryotoxicity of deca-brominated diphenyl ether in mice. *Chem. Res. Toxicol.* **24,** 1976–1983 (2011).
127. Zbucka-Kretowska, M. *et al.* Evaluation of bisphenol a influence on endocannabinoid system in pregnant women. *Chemosphere* **203,** 387–392 (2018).
128. Wu, S. *et al.* Serum metabonomics coupled with ingenuity pathway analysis characterizes metabolic perturbations in response to hypothyroidism induced by propylthiouracil in rats. *J Pharm Biom Anal* **72,** 109–114 (2013).
129. Piras, C. *et al.* Metabolomic profile in hyperthyroid patients before and after antithyroid drug treatment_ Correlation with thyroid hormone and TSH concentration. *Intern J Biochem Cell Biol* **93,** 119–128 (2017).
130. Constantinou, C., Chrysanthopoulos, P. K., Margarity, M. & Klapa, M. I. GC−MS Metabolomic analysis reveals significant alterations in cerebellar metabolic physiology in a mouse model of adult onset hypothyroidism. *J. Proteome Res.* **10,** 869–879 (2011).
131. Anwar, M. A. *et al.* Optimization of metabolite extraction of human vein tissue for ultra performance liquid chromatography-mass spectrometry and nuclear magnetic resonance-based untargeted metabolic profiling. *Analyst* **140,** 7586–7597 (2015).
132. Savorani, F., Tomasi, G. & Engelsen, S. B. Icoshift: A versatile tool for the rapid alignment of 1D NMR spectra. *J. Magn. Reson.* **202,** 190–202 (2010).
133. Craig, A., Cloarec, O., Holmes, E., Nicholson, J. K. & Lindon, J. C. Scaling and normalization effects in NMR spectroscopic metabonomic data sets. *Anal. Chem.* **78,** 2262–2267 (2006).
134. Dieterle, F., Ross, A., Schlotterbeck, G. & Senn, H. Probabilistic quotient normalization as robust method to account for dilution of complex biological mixtures. application in ^{1}H NMR metabonomics. *Anal. Chem.* **78,** 4281–4290 (2006).
135. van den Berg, R. A., Hoefsloot, H. C. J., Westerhuis, J. A., Smilde, A. K. & van der Werf, M. J. Centering, scaling, and transformations: improving the biological information content of metabolomics data. *BMC Genomics* **7,** 142 (2006).
136. Massart, D. L., Deming, S. N., Michotte, Y., Kaufman, L. & Vandeginste, B. G. M. *Chemometrics: a text book*. 348–349 (2002).
137. Wold, S., Esbensen, K. & Geladi, P. Principal component analysis. *Chemom. Intell. Lab. Syst* **2,** 37–52 (1987).
138. Caesar, L. K., Kvalheim, O. M. & Cech, N. B. Hierarchical cluster analysis of

technical replicates to identify interferents in untargeted mass spectrometry metabolomics. *Anal. Chim. Acta* **1021,** 69–77 (2018).
139. Mehmood, T., Liland, K. H., Snipen, L. & Sæbø, S. A review of variable selection methods in Partial Least Squares Regression. *Chemom. Intell. Lab. Syst* **118,** 62–69 (2012).
140. Godoy, J. L., Vega, J. R. & Marchetti, J. L. Chemometrics and intelligent laboratory systems. *Chemom. Intell. Lab. Syst* **130,** 182–191 (2014).
141. Gromski, P. S. *et al.* A tutorial review: Metabolomics and partial least squares-discriminant analysis – a marriage of convenience or a shotgun wedding. *Anal. Chim. Acta* **879,** 10–23 (2015).
142. Bylesjö, M. *et al.* OPLS discriminant analysis: combining the strengths of PLS-DA and SIMCA classification. *J. Chemometrics* **20,** 341–351 (2007).
143. Eriksson, L., Trygg, J. & Wold, S. CV-ANOVA for significance testing of PLS and OPLS® models. *J. Chemometrics* **22,** 594–600 (2008).
144. Worley, B. & Powers, R. Multivariate analysis in metabolomics. *Curr Metabolomics* **1,** 92–107 (2012).
145. Wishart, D. S. *et al.* HMDB 4.0: the human metabolome database for 2018. *Nucleic Acids Res* **46,** D608–D617 (2017).
146. Sugimoto, M. *et al.* MMMDB: Mouse Multiple Tissue Metabolome Database. *Nucleic Acids Res* **40,** D809–D814 (2012).
147. Sugimoto, M. *et al.* MMMDB: Mouse Multiple Tissue Metabolome Database. *Nucleic Acids Res* **40,** D809–D814 (2011).
148. Peters, C., van Trotsenburg, A. S. P. & Schoenmakers, N. diagnosis of endocrine disease: congenital hypothyroidism: update and perspectives. *Eur J Endocrinol* **179,** R297–R317 (2018).
149. Jonklaas, J. *et al.* Guidelines for the treatment of hypothyroidism: prepared by the american thyroid association task force on thyroid hormone replacement. *Thyroid* **24,** 1670–1751 (2014).
150. Macchia, P. E. Recent advances in understanding the molecular basis of primary congenital hypothyroidism. *Mol Med Today* **6,** 36–42 (2000).
151. Gomez-Peralta, F., Velasco-Martínez, P., Abreu, C., Cepeda, M. & Fernández-Puente, M. Hepatotoxicity in hyperthyroid patient after consecutive methimazole and propylthiouracil therapies. *Endocrinol Diab Metab Case Rep* **13,** 1397–4 (2018).
152. Wu, S. *et al.* Metabolic profiling provides a system understanding of hypothyroidism in rats and its application. *PLoS ONE* **8,** e55599–15 (2013).
153. Heidari, R., Niknahad, H., Jamshidzadeh, A. & Abdoli, N. Factors affecting drug-induced liver injury: antithyroid drugs as instances. *Clin Mol Hepatol* **20,** 237–12 (2014).
154. weiss, S. R. & Burns, J. M. The effect of acute treatment with two goitrogens on plasma thyroid hormones, testosterone and testicular morphology in adult male rats. *Comp. biochem. physiol* **90A,** 449–452 (1988).
155. Hodge, J. V., Melmon, K. L. & Sjoerdsma, A. Hormone-induced modifications of free tyrosine in the rat thyroid gland. *J. Physiol* **203,** 1–12 (1969).
156. OBrien, T. *et al.* The effect of the treatment of hypothyroidism and hyperthyroidism on plasma lipids and apolipoproteins AI, AII and E. *Clin Endocrinol* 17–20 (1997).
157. Martinez, B. *et al.* Hypothyroidism decreases the biogenesis in free mitochondria and neuronal oxygen consumption in the cerebral cortex of developing rats. *Endocrinology* **150,** 3953–3959 (2009).

158. Pietzner, M. *et al.* Plasma proteome and metabolome characterization of an experimental human thyrotoxicosis model. *BMC Medicine* **15,** 1–18 (2017).
159. Huang, M.-J. & Liaw, Y.-F. Clinical associations between thyroid and liver diseases. *J Gastroenterold Hepatol* 344–350 (1995).
160. Cicatiello, A. G., Di Girolamo, D. & Dentice, M. Metabolic effects of the intracellular regulation of thyroid hormone: old players, new concepts. *front. Endocrinol.* **9,** 355–7 (2018).
161. Mitrou, P., Raptis, S. A. & Dimitriadis, G. Insulin action in hyperthyroidism: a focus on muscle and adipose tissue. *Endocr Rev* **31,** 663–679 (2010).
162. Asatoor, A. M. Aromatisation of quinic acid and shikimic acid by bacteria and the production of urinary hippurate. *Biochim. Biophys. Acta* 290–292 (1965).
163. Moran, C., Chatterjee, K. Resistance to thyroid hormone due to defective thyroid receptor alpha. *Best Pract Res Clin Endocrinol Metab* **29,** 647–657 (2015).
164. Boumaza, H. *et al.* Metabolomic profiling of body fluids in mouse models demonstrates that NMR is a putative diagnostic tool for the presence of thyroid hormone receptor α1 mutations. *Submitted for publication* (2018).
165. Goudarzi, M. *et al.* Development of urinary biomarkers for internal exposure by cesium-137 using a metabolomics approach in mice. *RADIAT RES* **181,** 54–64 (2014).
166. Williams, H. R. *et al.* Differences in gut microbial metabolism are responsible for reduced hippurate synthesis in Crohn's disease. *BMC Gastroenterol* **10,** 1–8 (2010).
167. Flamant, F. *et al.* Congenital hypothyroid pax8-/- mutant mice can be rescued by inactivating the tralpha gene. *Mol. Endocrinol* **16,** 24–32 (2002).
168. Sirakov, M. *et al.* The thyroid hormone nuclear receptor TRα1 controls the Notch signaling pathway and cell fate in murine intestine. *Development* **142,** 2764–2774 (2015).
169. Fages, A. High-field NMR metabolomics for investigation of cancer in human populations and metabolic perturbations in model systems. Thesis (2013).
170. Fages, A., Boumaza, H. *et al.* A metabolomics investigation of the influence of thyroid hormone receptor trβ1 on the liver metabolome. *In preparation for publication* (2018).
171. Winter, H. *et al.* Deafness in TRbeta mutants is caused by malformation of the tectorial membrane. *J. Neurosci.* **29,** 2581–2587 (2009).
172. Parviz, F. *et al.* Hepatocyte nuclear factor 4a controls the development of a hepatic epithelium and live morphogenesis. *Nat Genet* **34,** 292–296 (2003).
173. Weiss, R. *et al.* Thyroid hormone action on liver, heart, and energy expenditure in thyroid hormone receptor. *Endocrinology* **139,** 4945–4952 (1998).
174. Ramadoss, P. *et al.* Novel mechanism of positive versus negative regulation by thyroid hormone receptor β1 (TRβ1) identified by genome-wide profiling of binding sites in mouse liver. *J. Biol. Chem.* **289,** 1313–1328 (2014).
175. Hönes, G. S. *et al.* Noncanonical thyroid hormone signaling mediates cardiometabolic effects in vivo. *Proc Natl Acad Sci USA* **114,** E11323–E11332 (2017).
176. Zhang, A. *et al.* Thyroid hormone receptor regulates most genes independently of fibroblast growth factor 21 in liver. *J Endocrinol* **224,** 289–301 (2015).
177. Finan, B. *et al.* Chemical hybridization of glucagon and thyroid hormone optimizes therapeutic impact for metabolic disease. *Cell* **167,** 843–850 (2016).
178. Vujovic, M. *et al.* Interference of a mutant thyroid hormone receptor α1 with hepatic glucose metabolism. *Endocrinology* **150,** 2940–2947 (2009).

179. Das, K. & Chainy, G. B. N. Modulation of rat liver mitochondrial antioxidant defence system by thyroid hormone. *Biochim. Biophys. Acta* 1–13 (2001).
180. Venditti, P., Napolitano, G., Barone, D., Coppola, I. & Di Meo, S. Effect of thyroid state on enzymatic and non-enzymatic processes in H2O2 removal by liver mitochondria of male rats. *Mol Cell Endocrinol* **403,** 57–63 (2015).
181. Venditti, P. *et al.* T3 and the thyroid hormone -receptor agonist GC-1 differentially affect metabolic capacity and oxidative damage in rat tissues. *J Experim Biol* **212,** 986–993 (2009).
182. Friedrich, N. *et al.* Urinary metabolomics reveals glycemic and coffee associated signatures of thyroid function in two population-based cohorts. *PLoS ONE* **12,** e0173078–17 (2017).
183. Ala-Korpela, M. Potential role of body fluid 1H NMR metabonomics as a prognostic and diagnostic tool. *Expert Rev Mol Diagn* **7,** 761–773 (2014).
184. Lam, S. M. & Shui, G. Lipidomics as a principal tool for advancing biomedical research. *J Genet Genomics* **40,** 375–390 (2013).

Appendices

Appendix 1

Clinical features of RTHα identified patients.

TRα mutation position	Patient	Symptoms	Remarks	References
E403X	Female child, age 6 years	• Growth retardation • Developmental retardation • Delayed bone development • Severe constipation. • Low heart rate • Low blood pressure • Borderline-abnormal thyroid hormone levels	Thyroxine treatment was commenced at the age 6 years	[102]
E397fs406X	Female child, 11 years	In the first 3 years: • Macroglossia • Omphalocele Congenital hip dislocation • No hip ossification centers • Delayed closure of skull sutures • Delayed tooth eruption • Delayed motor development • Low serum levels of free T4 • High levels of T3 Normal levels of TSH At the age of 11: • Delayed bone development • Macrocephaly • Delayed motor development • Short stature • Dry skin and hair • Slow deep tendon reflexes • Slow reactions and drowsiness • Severe constipation	Her father (47 years of age) has the same mutation and similar phenotype (short stature, thyroid function tests and constipation, mild cognitive deficit) and high cholesterol level Thyroxine treatment had improved her condition and the condition of her father	[103]
A263V	A 60-year-old woman	• Large head circumference • Normal stature (mild parental height) • Skin tags • Dysarthric speech • Low ratio of T3 • Anemia	Two sons (30 and 26 year-old) with the same features. The third son is unaffected The same mutation is found in TRα2. She was treated with thyroxine	[105]
R384C			Detected after whole genome sequencing in human autism spectrum	[106]

			This amino acid change is almost certainly pathogenic Mice model were investigated	
N359Y	A 27-year-old female	• Congenital macrocytic anemia • Severe bone malformation • Growth retardation • Dwarfism • Clavicular agenesis • Abnormalities of the fingers and toes • Elbow joints • Chronic motor diarrhea • Hypercalcemia • Lower TSH • Higher FT3 levels	TR1 and the non-receptor isoform TRα2 affected This case differs from previous reported cases of RTHα. This phenotype is not only the result of TRα mutation. Other mutations were found in her genome.	[110]
C380fs387X	Female child	**First evaluation at the age of 16 months**: • Can not control her head until the age of 8 months (normal < 2 months) • Not able to sit at 16 months (normal < 8 months) • No teeth eruption (normal at 13months) • Constipation • Horse sounding cry • Coarse facies • Macroglossia • Umbilical hernia • Normocytic anemia • Normal TSH • Low FT4 • High T3 • Normal TSH response to TRH **At the age of 2 years**: • Treatment with thyroxine • Sitting occurred at 26 months • Resolution of umbilical hernia at 3 years **At the age of 12, 7 years** • Severely handicapped • Not able to walk	Her parents are not affected	[107]

		• Mild scoliosis • Severe defects in growth, mental, and motor development		
A263S	7 patients from the same family	**First evaluation at the age of 13 months** • Because of frequent infections. • Low FT4 • Normal FT3 and TSH • Delay in tooth eruption • Constipation **Second examination at the age of 2 years and 7 months** • Mild growth retardation • Mild clinical features • Mildly increased head circumference • TSH levels were normal • Serum free T3 ranged from high-normal to high and serum free T4 and rT3 from normal to low	One of his two older sisters is affected (mild growth retardation) Two of his three cousins are affected Constipation is the common feature between these family members. Low/borderline low hemoglobin level in six of the seven affected subjects but in none of the unaffected relatives	
R384H	Male child	**At birth** • Macroglossia **First evaluated at the age of 8 months** • High FT3, low FT4, and a normocytic normochromic anemia were detected • High head circumference • Bone age corresponded to 6 months • Cognitive ability moderately impaired • Motor development severely impaired • Serum free T3 ranged from high-normal to high and serum free T4 and rT3 from normal to low	The child and his mother are affected	
	35-year-old mother	**In adulthood** • Constipation • Slow speech • Borderline intellectual functioning • Impaired executive	Her parents were not affected A mice model were developed (Results: impairment of postnatal development	

		functioning • Mild deficits in memory • Elevated serum T3 and T3 to rT3 ratio • Mild anemia	and growth)	
A263V	17 year-old male	**In infancy** • Small umbilical hernia • Slow movements • Walked at 24 months (< 12 months) **In childhood** • Problems with coordination: inability to use stairs, hop, use a ball, tie shoelaces (until 11 years of age) • Delayed dentition • Delayed puberty at 16 years of age • Neurodevelopmental delay Skeletal dysplasia • Growth retarded **In the age of 17** • Macrocephaly • Delayed dentition • Constipation, • Subnormal T4/triiodothyronine (T3) ratio and low reverse T3 levels • Mild anemia • Increased head circumference • Mild neurocognitive impairment	Both TRα1 and TRα2 proteins are affected Healthy parents	
L274P	15-year-old male	• Umbilical hernia • Sat at 12 months • Walked at two and a half years Significant speech delay Dysmorphic facies • Truncal hypotonia • Delayed dentition • Myopic astigmatism • Genu valgum • Ankyloglossia • Skeletal dysplasia • Macroglossia • Skin tags	TRα1 and α2 proteins	[108]

		• Increased head circumference • Constipation. • Persistent learning disability • Short stature • Subnormal T4/triiodothyronine (T3) ratio, low reverse T3 levels, • Mild anemia		
Hypothyroidism		• Patent cranial sutures • Delayed dentition • Femoral epiphyseal digenesis (disordered, endochondral ossification) • Wormian bones (disordered, intramembranous ossification) • Flattened nasal bridge • Slow-transit constipation with colonic dilatation • Ileus • Delayed bone age in childhood Adult short stature		[148]

Appendix 2

Metabolites identified from 1D and 2D NMR profiles of mice urine.

ID	Metabolite	^{1}H [ppm]	^{13}C [ppm]	Multiplicity
1	1-Methylhistidine	3,03	30,85	
		3,18	31,01	m
		3,69	36,24	s
		3,94	56,58	dd
		7,00	122,70	s
		7,67	144,85	
2	1-methylicotinamide	4,47	51,48	s
		8,18	131,27	m
		8,96	150,37	m
		9,27	148,13	m
3	2-oxoglutarate	2,44	33,67	t
		3,00	38,54	t
4	3-Indoxyl sulfate	7,19		m
		7,27	125,04	m
		7,35	119,26	s
		7,54	114,82	d
		7,69	120,44	d
5	3-hydroxybutyrate	1,18	24,60	d
		2,30		dd
		2,39		dd
		4,14	68,54	m
6	3-hydroxyisovalerate	1,26	30,83	s
		2,35	52,28	s
7	Acetate	1,91	26,19	s
8	Acetoacetate	2,28	32,20	s
		3,46	55,91	s
9	Alanine	1,48	19,05	d
		3,78	53,61	q
10	Allantoin	5,38	66,28	s
		6,05		s
11	Betaine	3,25	56,17	s
		3,89		s
12	Butyrate	0,90		t
		1,55		m
		2,14		t
13	Choline	3,19		s
		3,51	70,57	
		4,06	58,89	m
14	Cis-aconitate	3,10	46,36	s
		5,68	126,82	d

15	Citrate	2,51	48,39	d
		2,67	48,30	d
16	Creatine	3,03	39,93	s
		3,92	56,83	s
17	Creatinine	3,03	33,16	s
		4,04	59,26	s
18	Dimethylamine	2,71	37,59	s
19	Dimethylglycine	2,91	46,51	s
		3,71	62,81	s
20	Formate	8,45	151,19	s
21	Fumarate	6,51	138,00	s
22	Glutamine	2,12		m
		2,46		m
		3,76		t
23	Glycine	3,55	44,57	s
24	Glycolate	3,95	63,27	s
25	Guanidoacetate	3,79	47,58	s
26	Hippurate	3,96	46,67	d
		7,54	131,87	m
		7,63	135,22	m
		7,82	130,02	dd
		8,55		s
27	Isovalerylglycine	0,92	23,51	d
		2,03	28,76	m
		2,17	47,72	d
		3,75	46,27	d
		7,96		s
28	Lactate	1,32	22,80	d
		4,10	71,64	q
29	Leucine	0,92	23,51	d
		0,94	23,99	d
		1,66	27,24	m
30	Malate	2,36		dd
		2,66		dd
		4,29		dd
31	Methylamine	2,59		s
32	Methylguanidine	2,82	30,17	s
33	N-acetylcholine	2,14		s
		3,21		s
34	N-acetylglucosamine	2,05	25,05	s
		2,06		s
		8,08		d
		8,18		d
35	N-acetylglycine	2,03	24,95	
		3,77	46,07	

36	Phenylalanine	3,10	39,62	q
		3,25	38,45	dd
		7,34	132,04	d
		7,35	130,33	m
		7,42	131,81	m
37	Phosphocholine	3,21	56,94	s
		3,60	68,43	m
		4,14	60,05	m
38	Succinate	2,39	37,05	s
39	Taurine	3,25	50,57	t
		3,41	38,38	t
40	Trigonelline	8,89	146,93	
		9,11		s
41	Trimethylamine	2,85	45,66	s
42	Tryptophan	3,48	31,73	dd
		4,04	57,14	dd
		7,49	115,04	d
		7,19	122,56	m
		7,26	125,31	m
43	Tyrosine	3,05	38,01	dd
		3,19		dd
		3,94	59,65	q
		6,88	118,79	d
		7,18	133,70	d
44	Urea	5,8		s
45	Valine	0,98	19,5	d
		1,03	20,76	d
		2,26	31,9	m
		3,6	63,34	d

Appendix 3

Metabolites identified from 1D and 2D NMR profiles of mice blood plasma.

ID	Metabolite	^{1}H [ppm]	^{13}C [ppm]	Multiplicity
1	3-Hydroxybutyrate	1,19	24,3	d
		2,29		q
		2,4		q
		4,15		m
2	Acetate	1,91	26,1	s
3	Acetoacetate	2,27	32,2	s
		3,43	56,2	s
4	Alanine	1,47	18,89	d
		3,78	53,1	q
5	Allantoin	5,39	66,27	s
6	Betaine	3,25	56,29	s
		3,89		s
7	Choline	3,19	42	
		4,4	56,5	
8	Citrate	2,53	48,7	d
		2,68	48,71	d
9	Creatine	3,03		s
		3,92		s
10	Creatinine	3,04		s
		4,05		s
11	Formate	8,45		s
12	Fumarate	6,51	138	s
13	β-glucose	3,24	76,78	dd
		3,4	72,2	dd
		3,46	78,37	m
		3,49	78,4	t
		3,9	63,3	dd
		4,64	98,5	d
14	α-glucose	3,4	72,2	q
		3,54	74	dd
		3,71	75,3	t
		3,72	63,4	dd
		3,76		m
		3,82	74	ddd
		3,85	63,1	m
		5,23	94,5	d
15	Glutamine	2,11	29,5	m
		2,43	33,5	m
		2,46		m
		3,77	57	t
16	Glycine	3,54	44,5	s
17	Histidine	7,05		s

		7,87		s
18	Isoleucine	0,92		t
		1		d
19	Lactate	1,32	22,7	d
		4,1	71	q
20	Leucine	0,94		d
		0,96		d
		1,71		m
21	Lipids (mainly LDL)	0,84	16,4	m
22	Lipids (mainly VLDL)	0,86	23,4	m
		1,25	34,3	m
		1,55	27,35	m
23	Lipids	0,93	27,3	m
		1,26	25	m
		1,7	29	m
		2,22	36,3	m
		2,7	27,8	m
24	Methionine	2,12		s
25	O-Phosphocholine	3,19		s
26	Phenylalanine	3,12		q
		7,32		m
		7,37		m
		7,42		m
27	Pyruvate	2,37		s
28	Succinate	2,39		s
29	Threonine	1,325		d
		3,61		d
		4,24		m
30	Trimethylamine	2,88		s
31	Tyrosine	6,89		m
		7,19		m
32	Urea	5,73		
33	Valine	0,98	19,2	d
		1,035	20,5	d
		3,6	63,2	d

Appendix 4

Metabolites identified from 1D and 2D NMR profiles of mice liver aqueous extracts.

ID	Metabolite	^{1}H [ppm]	^{13}C [ppm]	Multiplicity
1	3-Hydroxybutyrate	1,2	24,45	d
		2,314	49,23	m
		2,414	49,23	m
		4,16	65,5	m
2	Acetate	1,91	25,97	s
3	Acetoacetate	2,27	32,26	s
		3,43	56	s
4	ADP	4,15	83	m
		4,16	65,4	m
		4,57	73,7	m
		5,94	87	m
		8,29	148,38	s
		8,54	140,4	s
5	L-Alanine	1,48	19	d
		3,76	53,5	q
6	AMP	4,01	66,2	dd
		4,36	87,14	dd
		4,5	73,3	dd
		6,12		d
		8,23	155	s
		8,58	142,6	s
7	Aspartate	2,66	39	dd
		2,8	39,5	dd
		3,89	55	dd
8	ATP	4,21	67,7	m
		4,28	67,78	m
		4,39	86,6	m
		4,5	73	m
		4,619	76,9	t
		6,14	89,27	d
		8,239	155,36	s
		8,528	142,5	s
9	Carnosine	2,68	34,8	dt
		3,03	30,8	dd
		3,19	30,8	dd
		3,24	38,57	dt
		4,48	57,57	m
		7,09	119,87	s

		8,1	137,4	s
10	Choline	3,19	56,7	s
		3,5	70,15	dd
		4	58,5	ddd
11	Creatine	3,02	56,43	s
		3,92	39,5	s
12	Glucose	3,23	77	dd
		3,39	72,34	m
		3,45	78,57	m
		3,53	74,2	dd
		3,72	75,63	m
		3,82	74,14	m
		3,89	63,47	dd
		4,63	98,7	d
		5,22	94,93	d
13	Glutamate	2,04	29,8	m
		2,12		m
		2,34	36,35	m
		3,75	57,64	dd
14	Glutamine	2,12	29,28	m
		2,44	33,9	m
		3,76	57,23	t
15	Glutathione	4,2	58	q
		3,78	57/46	m
		2,97	28,32	dd
		2,54	34	m
		2,15	29	m
16	Histidine	3,16	30	dd
		3,23	30	dd
		3,98		dd
		7,09		d
		7,9		d
17	Isoleucine	0,93	13,9	t
		0,99	17,36	d
		1,24	27	m
		1,45	27	m
		1,98	38,68	m
		3,66	62,5	d
18	Lactate	1,32	22,9	d
		4,1	71,3	q
19	Leucine	0,95	24	t
		1,7	42.5/26.7	m
		3,72	56,2	m
20	Lysine	1,46	24	m

		1,71	29	m
		1,89	32,6	m
		3,02	42	t
		3,74	57,45	t
21	Methionine	2,16	32,7	m
		2,63	31,58	t
		3,85	56,8	dd
22	N-Acetylcysteine			
23	N-Acetylglutamate	4,1	58,14	m
		2,22	36,8	t
		2,05		m
		2,02	24,75	s
		1,87	31,2	m
24	NAD+			
25	Niacinamide	7,58	126,8	dd
		8,24	139,3	dd
		8,7	154,5	dd
		8,92	150,4	s
26	O-Acetylcarnitine	2,13	23,2	s
		2,48	42,8	dd
		2,61	42,8	dd
		3,18	56,4	s
		3,61		d
		3,82	70,7	dd
		5,57	69,5	q
27	O-Phosphocholine	3,21		s
28	O-Phosphoethanolamine	3,24	43,35	td
		4,01	63	t
29	Phenylalanine	3,19		m
		3,98	59	dd
		7,32	132,12	d
		7,36	130,42	m
		7,42	132,8	m
30	Sarcosine	2,73	35,6	s
		3,6	53,5	s
31	Succinate	2,39	36,8	s
32	Taurine	3,25	50,37	t
		3,42	38,3	t
33	Trimethylamine N-oxide	3,25	62,2	s
34	Tyrosine	3,02	38,27	dd
		3,17	38,27	dd
		3,92	59	dd
		6,87	118,9	m
		7,17	133,5	m

35	Valine	0,98	19,4	d
		1,03	20,75	d
		2,26	31,9	m
		3,6	63,35	d
36	N-Methylhistidine	7,92	141,14	s
		7,05	127,2	s
		3,93	56,2	dd
		3,7	34,5	s
		3,24	27,6	m